

Alma Mater Studiorum – Università di Bologna

DOTTORATO DI RICERCA

Science for Conservation

Ciclo XXII

Settore/i scientifico disciplinari di afferenza: CHIM/12

TITOLO TESI

**STUDY OF MATERIALS AND TECHNOLOGY OF
ANCIENT FLOOR MOSAICS' SUBSTRATE**

Presentata da: Vincenzo Starinieri

Coordinatore Dottorato

Relatore

Prof. Rocco Mazzeo

Prof. Ioanna Papayianni

Esame finale anno 2009

Table of Contents

1. Introduction	1
1.1. Definition and relevance of the topic	1
1.2. Objectives of the research.....	2
2. Theory	3
2.1. The mosaics' substrate in the ancient treatises	3
2.2. Modern studies on mosaics' substrate	5
2.3. Mosaic conservation: an overview of the modern practice	10
2.4. Definition of mortar.....	12
2.5. Components of a mortar	13
2.5.1. Types of binder.....	13
2.5.1.1. Air lime	13
2.5.1.1.1. Calcitic lime	14
2.5.1.2. Natural hydraulic lime.....	14
2.5.1.3. Air lime and pozzolanic materials.....	15
2.5.2. Aggregates	15
2.5.3. Water	17
2.5.4. Additives.....	17
2.6. Types of mortar	18
2.6.1. Air mortars.....	18
2.6.2. Hydraulic mortars	19
2.6.3. Natural and artificial pozzolanic mortars	19
3. The Case Studies	20
3.1. Introduction	20
3.2. The ancient city of Dion	20
3.2.1. Geographical position.....	20
3.2.2. History	20
3.2.3. Geological and geomorphological features	21
3.3. The “Villa Romana delle Muracche” in Tortoreto	22
3.3.1. Geographical position.....	22
3.3.2. History	22
3.3.3. Geological and geomorphological features	23
3.4. The archaeological area of St. Severo, Classe.....	23

3.4.1.	Geographical position.....	23
3.4.2.	History	23
3.4.3.	Geological and geomorphological features	23
3.5.	The “Cortile Romano” in the Archaeological Museum of Florence.....	24
3.5.1.	Geographical position.....	24
3.5.2.	History	24
3.5.3.	Geological and geomorphological features	24
3.6.	The Palace of Aegae in Vergina.....	25
3.6.1.	Geographical position.....	25
3.6.2.	History	25
3.6.3.	Geological and geomorphological features	25
4.	Materials and Methods.....	27
4.1.	<i>In situ</i> analyses and sampling	27
4.2.	Laboratory analyses.....	27
4.2.1.	Preparation of samples.....	27
4.2.2.	Optical microscopy.....	28
4.2.3.	Mortars disaggregation	28
4.2.4.	Mechanical sieving.....	29
4.2.5.	Chemical analyses	29
4.2.5.1.	Loss on Ignition.....	29
4.2.5.2.	Atomic Absorption Spectrometry	30
4.2.5.3.	Ion Chromatography	31
4.2.5.4.	Pyrolysis Gas Chromatography Mass Spectrometry.....	31
4.2.6.	Water absorption under vacuum.....	32
4.2.7.	Compression test	32
5.	Results and Discussion.....	34
5.1.	Results of the analyses.....	34
5.1.1.	The ancient city of Dion	34
5.1.2.	The “Villa Romana delle Muracche” in Tortoreto	62
5.1.3.	The archaeological area of St. Severo, Classe.....	73
5.1.4.	The “Cortile Romano” in the Archaeological Museum of Florence.....	78
5.1.5.	The Palace of Aegae in Vergina.....	94
5.2.	Discussion.....	104
5.3.	Practical application of the results.....	112
5.3.1.	Suggestions for the design of repair mortars for pavements	112
5.3.2.	A model for the documentation of ancient pavements in the conservation practice	113

5.3.3. Suggestions for the presentation of ancient pavements <i>in situ</i> and in museums	113
6. Conclusions	117
6.1. Results of the research.....	117
6.2. Suggestions for further work	119
References	120
Appendix	128
Abstract	140
Acknowledgements	141
Publications	143

Chapter 1

Introduction

1.1. Definition and relevance of the topic

Ancient pavements are composed of a variety of preparatory or foundation layers constituting the substrate, and of a layer of *tesserae*, pebbles or marble slabs, forming the surface of the floor. In other cases, the surface consists of a mortar layer beaten and polished. The term mosaic is associated with the presence of *tesserae* or pebbles, while the more general term pavement is used in all the cases [Vit62, Pli71, Alb65]. The use of mosaic as floor decoration dates back to the Hellenistic period, when the *opus tessellatum* (surface made of stone *tesserae*), the *opus signinum* (surface made of a mortar layer with stone *tesserae* inserted into it, either scattered or disposed to form geometrical patterns) and the *opus vermiculatum* (surface made of very small irregularly shaped stone *tesserae*), were the commonly used mosaic styles [Fio02]. It is then in the 1st century A.D. that there was the best development of floor mosaics, with the advent of the *opus sectile* (surface made of marble elements with various geometric shapes), which substituted the *opus vermiculatum* [Lav88].

While a wide documentation of the different floor mosaic styles exists, much less has been done about the invisible part of the structure of a pavement, which is its substrate. Ancient pavements were complex artefacts with both aesthetic and functional duties [Fio02]. Their structure is the result of the development of construction criteria that were spread throughout a large geographic area and include a careful selection of a wide range of raw materials like limestones, aggregates and pozzolans. As past and modern archaeological excavations demonstrated, all pavements do not necessarily display the stratigraphy of the substrate described in the ancient treatises by Vitruvius [Vit62], Pliny [Pli71] and Leon Battista Alberti [Alb65] [Mos03]. In fact, the number and thickness of the preparatory layers, as well as the nature and the properties of their constituent materials, are often varying in pavements which are placed either in different sites or in different buildings within a same site or even in a same building. For such a reason it is evident how important is an investigation that takes account of the whole structure of the pavement, when studying the archaeological context of

the site where it is placed, when designing materials to be used for its maintenance and restoration [Pap03, Fio02], when documenting it and when presenting it to public.

1.2. Objectives of the research

The objectives of this research, which has focused on the study of the materials, the function and the technology of ancient pavements' substrate, are:

- to contribute to the characterization of the constituent materials of ancient pavements;
- to contribute to the understanding of the function and the technology of ancient pavements' substrate;
- to contribute to the development of criteria for designing the materials to be used in the maintenance and restoration of ancient pavements;
- to develop a model for the documentation of ancient pavements in the conservation practice;
- to suggest solutions for the presentation to public *in situ* and in museums of ancient pavements.

To reach these objectives, five case studies represented by archaeological sites containing floor mosaics and other kind of pavements, dated to the Hellenistic and the Roman period, have been investigated by means of *in situ* and laboratory analyses. The theoretical section included a review of the literature on ancient pavements' study, an overview of the modern practice in mosaic conservation, and a description of the general characteristics of the different types of mortars that were commonly used in the construction of ancient pavements.

Chapter 2

Theory

2.1. The mosaics' substrate in the ancient treatises

In the 1st century B.C., Vitruvius in his *De Architectura* [Vit62], and in the 1st century A.D., Pliny in his *Naturalis Historia* [Pli71], described in detail the methods of construction of pavements. Vitruvius distinguishes between pavements to be built on ground level and on upper floors. According to the Latin author, when building on ground level the soil was rammed and leveled and then three foundation layers were spread on top of it. The first layer, called *statumen*, was made of large stones “each of which is not less than a handful”, laid on the ground. The second layer, called *rudus*, was spread over the *statumen* and consisted of stones mixed with lime in proportion of three to one. This layer was rammed by means of wooden stamps and its thickness was no less than about 23 cm. The third layer, called *nucleus*, was made of powdered pottery and lime in proportion of three to one and it was about 15 cm thick. On top of the *nucleus* a “pavement of marble slabs or of mosaic” was laid and rubbed down. After the rubbing down, when the pavement was “completely smoothed and finished”, marble dust was sprinkled over it, and over that coats of lime and sand were applied. In case of pavements to be built on upper floors, Vitruvius recommends that no wall from the rooms of the level below have to be built right up to the pavement. In fact, this would cause the formation of cracks in the pavement as it dries or sags in contact with the solid structure of the wall [Vit62]. Pliny [Pli71] describes a kind of pavement that he defines “terrace-roof pavement”, which according to the Latin author were invented by the Greeks, who were used to cover their houses with them. In making these pavements the first step was to lay down two layers of boards running different ways and nailed at the extremities. Upon this planking, “fresh rubble” mixed with “a third of its weight in pounded potsherds” was laid. On top of this layer, another layer of rubble two fifths composed of lime and rammed down to a thickness of about 30 cm, was laid. The *nucleus* was then laid down with a thickness of about 12 cm, and upon that, large square stones not less than about 4 cm thick were laid. An inclination of about 4 cm to about every 3 m was maintained and, finally, the

surface of the pavement was carefully polished with grindstones [Pli71]. Pliny describes also another kind of pavement called graecanic. When building it the ground was well rammed down and a layer of rubble or of pounded potsherds was laid on it. On the top of this layer, a layer of charcoal was spread, “*well trodden down with a mixture of sand, lime and ashes*”, to a thickness of about 15 cm. The surface of this layer was then smoothed with a grindstone until it had the appearance of a black stone floor [Pli71]. In the 15th century A.D., in his *Ten Books on Architecture* [Alb65], Leon Battista Alberti treated of pavements referring to Pliny and Vitruvius and to the “*Works of the Ancients*”. In particular, Alberti describes the way to convey into cisterns or sinks the water from the surface of outdoor pavements. Then, after describing the construction of pavements according to Pliny and Vitruvius, the author reports what he says he discovered about pavements from the actual work of the ancients. He begins with a description of the “*outward shell*”, which he writes it is very difficult to make, so it shall not rot or crack. This outer layer was made either of tiles or of stone, often of very large slabs of marble, some other time of smaller pieces, and little square [Alb65]. There are other ancient pavements, continues Alberti, which were “*made all of one piece*”, composed by a “*mixture of lime, sand and pounded brick, of each a third part*”. This mixture, according to the author, could be made even more strong and lasting by the addition of a fourth part of “*Tyber-Stone, beat to powder*”, or of the sand of “*Pozzuolo*”, called “*Rapillo*”. This “*plaster*” designed for pavements was subjected to continual beating, which made it “*daily acquire greater stiffness and hardness*” and, if “*sprinkled with lime-water and linseed oil*”, it grew “*almost as hard as glass, and defied all manner of weather*” [Alb65]. Before going on with the description of the inner layers, Alberti mentions again the use of linseed oil as organic additives in flooring mortars: “*Mortar worked up with oil, is said in pavements to keep out everything that is noxious*”. Under the outer layer, it was made a layer of mortar, 8 – 5 cm thick, containing “*small pieces of broken brick*”. Next to this layer it was made a layer composed of brick and stone fragments, about 30 cm thick. The author refers that in some cases, between these two layers, it was interposed a layer made of “*baked tile, or brick*”. Finally, the bottom layer was composed of “*stones, none bigger than a man’s fist*”. These stones, writes Alberti, are those “*found in rivers, as for instance, those round ones which partake of the nature of flint*”, which “*dry immediately when they are taken out of water*”. For this reason, continues the author, “*many affirm that the damp which arise out of the earth will never be able to penetrate to the shell of the pavement, if it is underlaid with those stones*”. Alberti also describes the case of pavements built in Baths, which have the same structure of those above described but were laid upon a series of “*pilasters a foot and half*

high next to the ground, standing about two foot distance one from the other, upon which they laid baked tiles". Finally, the author points out which are the most suitable conditions for the building of a pavement: "Pavements delight in damp, and wet air, while they are making, and endure best and longest in moist and shady places; and their chief enemies are the looseness of the earth, and sudden droughts". Furthermore, he stresses out the importance of keeping the pavement wet, so it acquires good mechanical properties: "For as repeated rains make the ground close and firm, so pavements being heartily wetted, grow compact, and hard as iron". As a conclusion of this paragraph about the mosaics' substrate in the ancient treatises, in Figure 1 is reported a graphic reproduction of a floor mosaic stratigraphy adapted from ancient literary sources by The Getty Conservation Institute and the Israel Antiquities Authorities, in the frame of the *Mosaics In Situ Project* [Mos03].

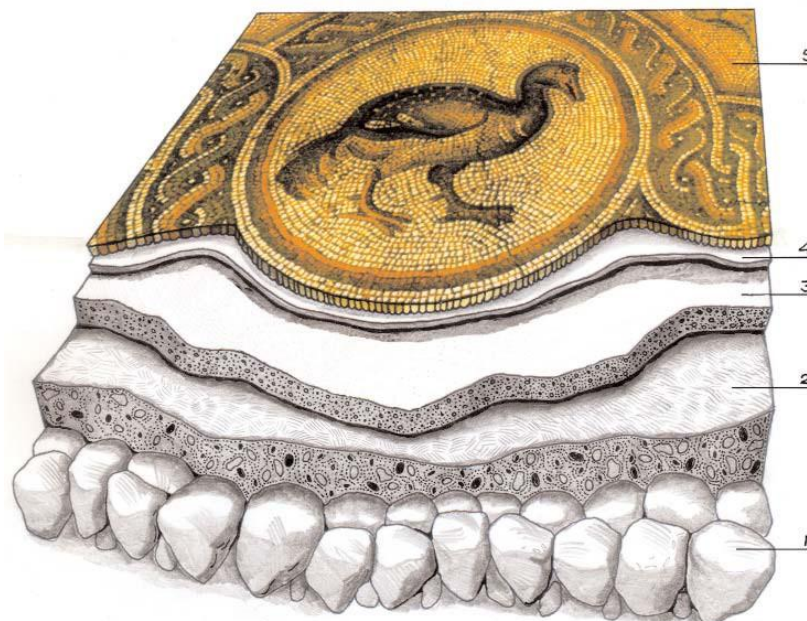


Figure 1 Graphic reproduction of mosaic stratigraphy: 1 – *Statumen* - First preparatory layer which is made of large stones laid on the ground, previously leveled and rammed. This layer only exists if the mosaic has been constructed on a natural soil. 2 – *Rudus* - Second preparatory layer which is spread over the *statumen*. This layer is made of a lime mortar with large aggregates. 3 – *Nucleus* - Third preparatory layer which is spread over the *rudus* in a thinner layer. The nucleus is made of a mortar with fine aggregates. 4 – *Bedding layer* - Fourth preparatory layer of mortar which is very rich in lime, and thinly applied in small sections over the *nucleus*. Tesserae are inserted in this layer before the mortar sets. 5 – *Tessellatum* - Layer which constitutes the mosaic surface and is composed of tesserae and mortar filling the interstices between them [Mos03].

2.2. Modern studies on mosaics' substrate

Nowadays mosaics' substrate is studied in case of restoration interventions, when information about the original mortars constituting the preparatory layers of the pavement is needed for the design of compatible repair mortars. In this section, some of the published works including a documentation of the whole substrate structure are listed in chronological order.

Todua [Tod75] describes the restoration of a 4th century A.D. floor mosaic discovered in a temple of the ancient town of Pitiunt, today Bichvinta, Abkhazia. The work included the recording of the mosaic's stratigraphy, which according to the author starts with a "*water proof layer of well mixed clay*", 40 cm thick, built by the ancient craftsmen "*to protect the temple from ground water vapors*". Above this layer, the author reports the presence of a 20 – 30 cm thick layer consisting of "*cobbles mixed with mortar*" followed by a "*strong lime concrete 15 cm thick*" whose "*flattened surface*" is covered with "*three layers of mortar mixed with fine sand, broken ceramic pieces and charcoal*", respectively 5 cm, 3 cm and 1 cm thick. Finally, the bedding layer, on which *tesserae* are set, is composed of "*pure mortar*" [Tod75]. Idil [Idi82] describes an intervention of restoration and conservation carried out on a 4th century A.D. floor mosaic from the Episcopal Palace at Aphrodisias, in Turkey, which included a study of the mortar foundation layers. According to the description of the mosaic's substrate given by the author, "*the rudus is made up of a first layer of aggregate composed of 5 - 15 mm gravel laid on the natural soil and a second layer of aggregate of 2 - 4 mm gravel mixed with lime mortar. The nucleus above the rudus is made up of river sand with particles measuring 1 mm or less, crushed brick and lime. The tesserae themselves are set in a layer of pure lime*" [Idi82]. Fiori *et alii* [Fio87] describe structure and materials composition of two floor mosaic fragments coming from S. Severo's Church and the archaeological area of Classe, in Ravenna, Italy. According to the authors, the two mosaic fragments have substrates composed of three layers of mortar each: a bedding layer 8-10 mm thick on which tesserae are set, containing a fine aggregate; an intermediate layer 6 - 7 cm thick with an aggregate composed exclusively of brick fragments having max diameter of 1.5 – 2 cm; a last layer 13 - 15 cm thick containing an aggregate composed of brick fragments with diameter up to 4 cm. Furthermore, the authors report the results of laboratory analyses performed on the mortars of each single preparatory layer and make some hypothesis about their production technology. In particular, the authors suggest that the presence of macro-crystalline calcite grains in the mortars, not related to the carbonation of lime, could be due to an incomplete calcination of the limestone used for the lime production. In this case, the transformation of calcium carbonate into calcium oxide is incomplete and fragments of the original limestone are present in the lime used to make the mortars [Fio87]. Authors also point out that the above-mentioned macro-crystalline calcite grains are not present in the layer on which tesserae are set, indicating that only the finer lime was selected to be used for the mortar of this layer. Always the same authors make the hypothesis that the brick fragments used as aggregate in the mortars of the intermediate and the lowest layer could be recycled material once used for the

internal walls of ceramic kilns. In fact, some of these brick fragments show to be over baked or to have undergone repeated baking cycles [Fio87]. Puertas *et alii* [Pue94a, Pue94b] characterized the preparatory layers of a number of 2nd century A.D. floor mosaics from the Roman city of Italica, in Spain. The analytical methodology included chemical, physical, mineralogical and mechanical analyses of the mortar layers as well as schematic reproductions of the substrates' stratigraphy (Figure 2).

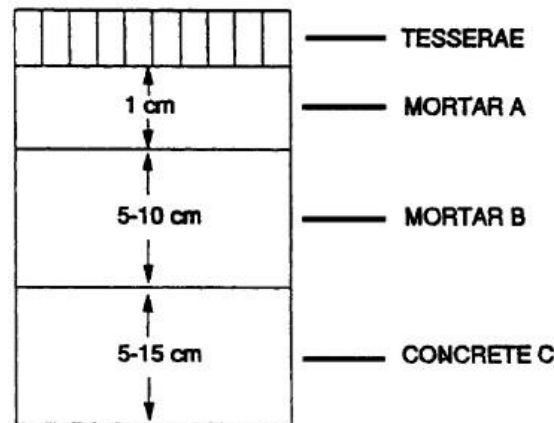


Figure 2 Schematic reproduction of the stratigraphy of the Mosaic of Tellus from the Roman city of Italica [Pue94a].

In the case of the Tellus mosaic, located in the so-called House of the Birds in the Roman city of Italica, the authors describe a substrate composed of three mortar layers whose characteristics are showed in Figure 3.

Layer	Binder	Aggregate	Dosage	Aggregate (ϕ Maximum mm)	Compressive strength (MP _a)	Density (g/cm ³)	Porosity (% vol.)
1	Lime	Siliceous	1/2	< 0.5	ND	ND	ND
2	Lime	Siliceous	3/1	2	ND	1.7	28.5
3	Lime	Siliceous	3/1	> 20	16	2.07	12.2

Figure 3 Characteristics of the mortars from Tellus mosaic [Pue94a].

Layers number 1, 2 and 3 in the table correspond to mortars A, B and C respectively, in Figure 2. The authors also report the results of analyses performed on the mortar foundation layers of mosaic fragments for which the house of provenance within the city was unknown (Figure 4).

Layer	Binder	Aggregate	Dosage	Aggregate (ϕ maximum mm)	Compressive strength (MP _a)
A	Lime + pozzolana	Siliceous	1/10	< 0.5	ND
B	Lime + pozzolana	Siliceous	2/1	2	6-7
C	Lime + pozzolana	Siliceous	ND	> 30	ND

Figure 4 Characteristics of the mortars from mosaics fragments [Pue94a].

Authors point out that while the substrate stratigraphy of these mosaic fragments is very similar to that of the Tellus mosaic, although with differences in layers thickness, the binder composition of the mortars is different. In fact, while the binder of the mortars of the Tellus mosaic is composed of the only calcium carbonate, the one of the mortars of the mosaic fragments contains also calcium silicates hydrates due to the addition of natural pozzolanic materials to lime. The same authors also make some consideration about the function of each mortar layer in the mosaic structure. Specifically, they define the deepest layer as “*a material of considerable thickness that acts as a base upon which mortar 2, being more porous and less compact, is laid*” [Pue94a]. Furthermore, they also mention a hypothetical leveling function of mortar layer 2 [Pue94b]. Roby [Rob95] describes the conservation treatments carried out on the architectural remains of a Byzantine basilica in Petra, Jordan, that include two mosaic pavements. According to the description given by the author, “*the tesserae were set in a lime bedding mortar on which the preparatory design was painted using red pigment. Underneath the bedding mortar is a preparatory mortar, or nucleus, made of lime and sand with the addition of charcoal. This layer was placed over a foundation or statumen of small stone slabs set in mortar*” [Rob95]. Montanaro *et alii* [Mon98] describe the restoration intervention carried out on a 2nd century A.D. floor mosaic from the archaeological area of *Histonium* in Vasto, Italy. The restoration was supported by the study of the constituent materials of the mosaic, included those of the foundation layers. The authors reproduced schematically the stratigraphy of the mosaic’s substrate (Figure 5), which according to their description is composed of six layers. The bedding mortar on which tesserae are set is composed of air lime and a small quantity of aggregate. The *nucleus* is made of air lime, silicatic sand and brick fragments, which gave hydraulic properties to the mortar. The binder/aggregate ratio in this mortar is approximately equal to 1/2, the average size of the sandy aggregate is around half millimeter, while that of the brick fragments is smaller. Authors also point out the presence in this mortar layer of calcite fragments that could be due to incomplete calcination of the stone used for the production of lime. The *rudus* contains coarser brick fragments, stone and vitreous tesserae fragments up to few centimeters in size, mixed with air lime and sand. Authors attribute low hydraulicity to this mortar, for which they estimate a binder/aggregate ratio equal to 1/1.5 and report, as in the previous one, the presence of unbaked fragments of the stone used for calcination. Below the *rudus* the authors found two layers made of air lime, silicatic sand and brick dust. For both the layers they estimated a binder/aggregate ratio close to 1/1, an average size of aggregate around one third of millimeter and low hydraulic properties. Also for these two layers the authors confirm the presence of unbaked limestone

fragments. The last layer, namely the *statumen*, is reported in the schematic reproduction of the substrate but, as specified by the authors, was not analyzed.

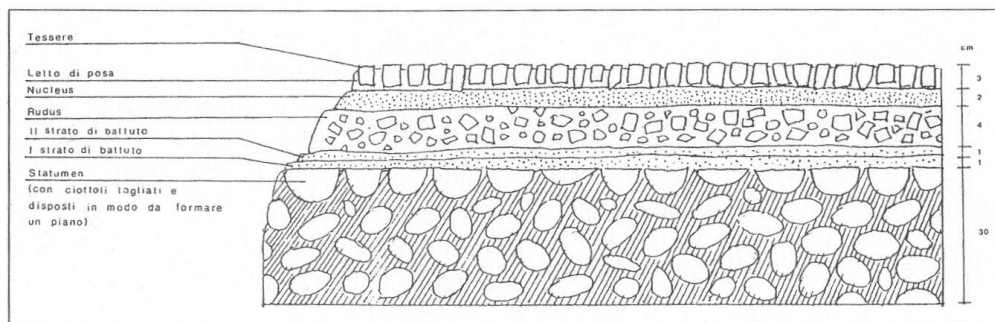


Figure 5 Schematic reproduction of the stratigraphy of a 2nd century A.D. floor mosaic from Histonium, Vasto, Italy [Mon98].

Lopreato *et alii* [Lop03], describe a conservation and restoration intervention of a 6th century A.D. floor mosaics from Santa Eufemia's Cathedral in Grado, Italy, that included a study of its constituent materials. According to the description given by the authors the mosaic's substrate is composed of three mortar layers: a bedding layer on which tesserae are set, composed almost exclusively by air lime; a *nucleus* composed of air lime and mostly carbonatic aggregate in ratio close to 1.5/1; a third layer composed of air lime and mostly carbonatic aggregate with maximum grain size of two millimeters and half, in ratio close to 1.5/1. Chlouveraki and Politis [Chl03], report the documentation and conservation of the Early Byzantine nave mosaic in the basilica of Agios Lot, Jordan. The work included the recording of the substrate stratigraphy and the characterization of the construction materials used for the pavement. According to the description given by the authors, the following layers were distinguished (Figure 6) [Chl03]:

- A. *Tesselatum*, 1.5 – 2 cm thick;
- B. Fine white lime mortar, 2 cm thick with a small amount of fine aggregates in which the *tesselatum* is set;
- C. Grey lime-based mortar with coarse aggregates consisting of sand and ceramic sherds mixed gravel with charcoal inclusions. Debitage from tesserae-cutting have also been used instead of 3 cm sized gravel. This second layer is 2.5 – 3 cm thick;
- D. Grey lime mortar with finer aggregates and the same gravel, 2.5 – 3 cm thick;
- E. Rubble hard core made up of fist-sized rounded cobbles, 7 – 8 cm thick;
- F. Red silt, 10 – 11 cm thick;
- G. Parallel rows of stones and wooden beam remnants existed under the mosaic floor.

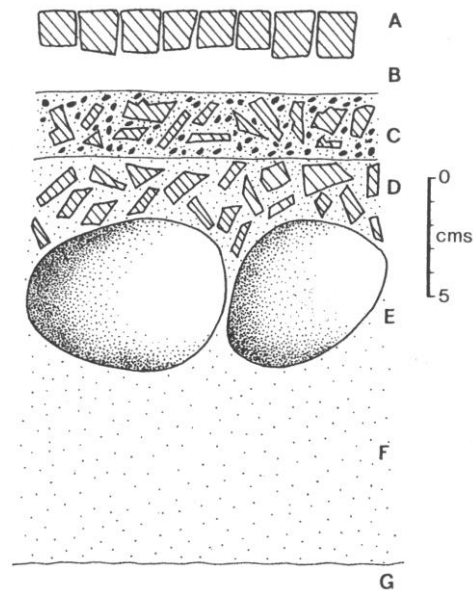


Figure 6 Schematic reproduction of the stratigraphy of the nave mosaic in the basilica of Agios Lot, Jordan [Chl03].

Papayianni and Pacht [Pap03], studied the mortar layers of the substrate of a number of floor mosaics located in eight archaeological sites in Greece, dated to the Classic, Hellenistic, Roman and Early Christian period. The authors describe and compare the stratigraphies of the studied mosaics, and the mineralogical, chemical, physical and mechanical characteristics of their mortar layers, underlining which properties seemed to be peculiar of each layer. Furthermore, the authors stress the importance of the examination of the whole structure of a mosaic before any kind of conservation intervention. Finally, two still unpublished works on floor mosaics in which a special attention is focused on the importance of substrate are those presented by Wootton [Woo08] and Chlouveraki *et alii* [Chl08] at the last conference of the ICCM (International Committee for the conservation of Mosaics) that has been held in Palermo, Italy, on the 20th - 26th of October 2008. Wootton stresses out how case studies highlight the quality and the quantity of technical data that can be gleaned from *in situ* recording and the examination of fragmentary mosaics. Chlouveraki *et alii* further illustrate the conservation project carried out at the monastic complex of Saint Lot, Jordan, pointing out how the variation in the bedding stratigraphy, together with other characteristics of the mosaics, contribute to the study of the archaeological context and especially in understanding the succession of the renovation and modification phases of the building.

2.3. Mosaic conservation: an overview of the modern practice

This section summarizes the history of mosaic conservation focusing on conservation activities like documentation, treatment and presentation to public. One can say that mosaic

conservation is a practice as old as the making of mosaics themselves, in the sense that already when the floors were still in use they were undergoing maintenance performed by the ancient craftsmen when needed [deG06]. During the postwar period discoveries of mosaics occurred very frequently throughout Europe. At that time strategies for mosaic conservation were very limited, detachment was the primary option available, materials used were exclusively cement, gypsum and glues and, furthermore, documentation was lacking [deG06]. The original context of mosaics was destroyed and mosaics were valued only by the image created by a fine layer of tesserae. These early approaches evolved when the interest on all the components of archaeological sites increased and the attention shifted from the single object, the mosaic, to its context, represented by the room, the building and the site. This new view led to a trend to keep *in situ* all those elements, mosaics included, which qualify and identify the site [Nar03]. The shift from mosaics removal to *in situ* conservation recognized the historic and scientific value of context, represented by the architectural ensemble for which they were made, and technology, meaning the information that resides in the mosaic stratigraphy [Ste06]. This approach fostered knowledge about mosaics, since the constituent materials, the building techniques and the traces that time had left started to be studied and documented [Nar03]. The increasing attention paid to mosaics and especially to archaeological sites generated a growing number of projects and initiatives. In 1977, in occasion of a first meeting on mosaic conservation was founded in Rome the International Committee for the Conservation of Mosaics (ICCM). Since then the ICCM organized a series of regular conferences, whose themes were pointing out the importance of *in situ* conservation, the rejection of the use of cement in the restoration of mosaics, the issues of public presentation of mosaics. Materials and techniques used in the treatment of mosaics were modified according to new principles and methods, aimed at reproducing the original recipes for mortars and at respecting the signs that time has left on mosaics [Nar03]. In 1980, the Italian conservation scientist Giorgio Torraca launched research to replace cement with one of the oldest construction materials known, lime-based mortar, which use has allowed the development of *in situ* consolidation [deG06]. Both conservators and archaeologists have always recognized the fundamental importance of documentation. Corfield [Cor03], in his framework for the documentation of *in situ* mosaic conservation projects, suggests that all the elements of documentation like iconography, materials, condition, treatments, should be brought together into a single integrated archive. In this way, the best conservation could be applied in relation to the mosaic's condition, its situation, the factors affecting its condition and the mosaic's relationship to the site and its interpretation [Cor03]. Furthermore, the

author stresses out the importance of considering the reason for collecting the data and the purpose to which it will be put. One of the most complex subjects in the field of presentation and interpretation of heritage is the presentation of mosaics to the public [Ren03]. It is recognized in the mosaic conservation field that an objective of the conservation profession is to present and to interpret for the public the cultural properties that need to be conserved [deG06]. Renée [Ren03], points out the differing problems to face for mosaics presented *in situ* and in a museum. While in the case of mosaics exhibited *in situ* one has to contend with the problem of protecting them from the ravages of nature and man, in the case of museum exhibition the problem relates more to the character of the display and the aim of the exhibition [Ren03]. Once the mosaic is removed from its natural surroundings, it loses much of its intrinsic value and becomes more of an object, which can be moved to the most suitable place for display, chosen taking into account, for example, the angles of lighting or how people will move around the mosaic. On the other hand, a mosaic *in situ* is not an isolated object but part of an architectural context [Ren03]. One of the most discussed topics about *in situ* presentation of mosaics is the role of the shelter to be constructed over them, whether it should be to resemble the original architectural structure or to fulfil a purely functional purpose. In the first case, the shelter would be part of the presentation itself, while in the second case exclusively a protective device [Ren03]. Renée considers several other aspects of mosaics presentation, stressing out how in presenting and interpreting a mosaic is necessary to deal with different levels of information, that together evoke the cultural significance of the mosaic and the site. Illustrating two case studies, both in the ancient city of Sepphoris, Lower Galilee, he describes how the displaying of a reproduction of the original building can make the public understand the structure and function of the site. Always through a case study, Renée illustrates the use of interactive computerized material through which visitors can find information about the discovery of the sites and the restoration of the mosaics, as well as about how the mosaics were made.

2.4. Definition of mortar

A mortar can be defined as a mixture of inorganic or organic binders, mostly fine aggregates, water and eventual organic and/or inorganic additives (or a mixture of just binder and water) in the proportions necessary to give to the mixture proper workability in the fresh state and adequate physical (porosity, permeability to water etc) and mechanical (resistance, deformability, adhesion etc) properties, outward aspect, durability etc, in the hardened state [UNI01]. Mortars are classified according to several factors. They are distinguished in

mortars for use in interior environment and mortars for use in exterior environment. According to their function, they are divided in mortars for bedding, pointing, rendering, plastering and for decorations (stuccoes) [Gro04]. Furthermore mortars are classified according to their composition. The nature of the mortar components and their combination and proportion in the mix determine the properties of the mortar itself. Following are briefly described the various types of the main components of mortars.

2.5. Components of a mortar

According to the UNI 10924 standard [UNI01], the components of a mortar are:

- inorganic or organic binders;
- aggregates;
- water;
- eventual organic and/or inorganic additives;

Furthermore, several added materials can be present such as straw, animal hair, charcoal etc.

2.5.1. Types of binder

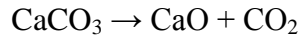
Binders are materials that mixed with water generate plastic masses that harden resulting in a compact mass resistant to mechanical stresses and to atmospheric agents [Got78]. Binders are classified according to their capability of setting and curing in air or under water. In the first case they are defined as air binders (air lime and gypsum), in the second case as hydraulic binders (hydraulic lime, air lime with the addition of pozzolanic materials, cement). Other types of binder like the organic and the argillaceous ones are less used [Pec08]. In the next pages, the types of binders related to the experimental work done in this research are treated theoretically.

2.5.1.1. Air lime

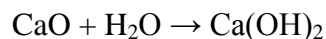
Air lime is a binder produced by burning in a kiln, at a temperature of 850-900 °C, carbonatic rocks containing no less than 95% of calcium and/or calcium magnesium carbonate [Pec08]. When in the burning process, called calcination, limestones containing the only calcium carbonate (CaCO_3) are used, calcitic lime is produced. When the rocks used for calcination are magnesian limestones, dolomitic limestones or dolomites, that are limestones containing up to 10%, 50% and 100% respectively of calcium magnesium carbonate ($\text{CaMg}(\text{CO}_3)_2$), magnesian lime is produced [Pec08].

2.5.1.1.1. *Calcitic lime*

During the calcination process, the calcium carbonate contained in the limestones is converted in to calcium oxide, the so-called quicklime, according to the following endothermic reaction:



The production of CaO takes place with the elimination of CO₂ in an amount equal to the 44% in mass of the initial quantity of CaCO₃. Several factors control the thermal decomposition of CaCO₃. One of these is the dimension of the stone fragments burned in the kiln. Because of the low thermal conductivity of limestones, the bigger fragments the longer time is necessary before all the CaCO₃ converts in to CaO [Pec08]. Once the calcination is completed, the quicklime is added to water in a process called slaking. During the slaking calcium oxide reacts with water to produce calcium hydroxide according to the following exothermic reaction:



If the amount of water used in the slaking process is calculated stoichiometrically, hydrated lime is produced. If the quicklime is slaked with water in excess, the final product is called lime putty. Both hydrated lime and lime putty have the same chemical composition but while hydrated lime is in form of a very fine white powder, lime putty consists of a white unctuous paste with plastic consistency. Lime putty is the traditional pre-industrial era material used, whose preparation was already described by Plinius and Vitruvius in the ancient treatises [Pli71, Vit62]. Hydrated lime or lime putty is a binder that sets and cures with air reacting with the CO₂ in a process called carbonation:



This reaction develops slowly in time due to the low concentration of CO₂ in the air and leads to a more or less complete transformation of calcium hydroxide in to calcium carbonate [Pec08].

2.5.1.2. *Natural hydraulic lime*

Natural hydraulic lime is a binder produced by burning at a temperature of 900-1100 °C a limestone with clay content percentage ranging from 6% to 20% [Pec08]. During the calcination of such a limestone, the clay minerals (hydrous aluminum silicates) dehydrate forming free silica, alumina and iron oxides that combine with calcium oxide forming calcium

silicates, aluminates and ferrites. Once the calcination is complete, the uncombined calcium oxide is slaked with water to produce calcium hydroxide. The final product is calcium hydroxide together with calcium silicates, aluminates and ferrites. The more or less hydraulic character of the obtained binder is directly related to the percentage of calcium silicates, aluminates and ferrites formed during burning. In fact, these compounds react with mixing water to form calcium silicates and aluminates hydrates, which contribute to the setting and hardening of the mortar. For this reason, a special care has to be taken for the amount of water to use in the slaking process. Water should be in the quantity necessary to combine with all the calcium oxide. An excess of water would cause the hydration the calcium silicate, aluminates and ferrites resulting in an early hardening of the binder [Mar76]. On the other hand, too little water would be responsible of the presence of un-slaked calcium oxide in the final product, which would later on react with the mixing water forming the so-called lime lumps. Lime lumps are among the most common technological defects of historic mortars. They cause swelling phenomena in the mixture and are associated with the presence of fractures in the hardened mortar.

2.5.1.3. Air lime and pozzolanic materials

Hydraulic binders can be produced also adding pozzolanic materials to air lime. Pozzolanic materials are materials rich in reactive silica, or alumina plus silica, that react with lime and water in the mortar mixture forming calcium silicate and aluminate hydrates with hydraulic properties. Pozzolanic materials can be natural or artificial. The former are products of volcanic origin, specifically volcanic ash or artificially crushed volcanic tuff. Ancient Greeks were using pumice and other volcanic materials from the island of Thera, today Santorini, while Romans used volcanic materials from Colli Albani and Pozzuoli. In Pozzuoli it was extracted the so-called Pozzolana (from the Latin *pulvis puteolana*), a grey-dark trachytic tuff with low cohesion and pumice-like structure [Pec08]. Artificial pozzolans are brick, tile and other ceramic fragments, also used in the ancient times by both Greeks and Romans. Another type of artificial pozzolanic material already used in the past (13th – 15th century A.D.) [Pec08] is metakaoline, produced by burning kaoline, a rock composed of the clay mineral kaolinite.

2.5.2. Aggregates

According to the UNI 10924 standard [UNI01], aggregates can be divided, depending on their origin, in:

- sand (fluvial, quarry, marine);

- artificially crushed rocks;
- natural pozzolanic materials;
- artificial pozzolanic materials;
- hardened mortar fragments.

In the past, sand used as aggregate in mortars was extracted from rivers bed or lacustrine shorelines. The use of marine sand was not recommended already in the ancient treatises because of the presence of salt that affects negatively the setting process. Artificially crushed rocks were used where sand was not available or in cases when mortars with special colors were needed. For example to obtain a white mortar, artificially crushed marble or calcite dusts were used [Men92]. The aggregate represents the fraction of the mortar mixture that has the function to avoid the formation of cracks and fissures during the mortar setting and curing. In fact, the aggregate, if homogeneously distributed in the mixture can contrast the process of shrinking of the binder due to the evaporation of the water used in the mix and to the creation of a new crystalline structure. However, there exist some kinds of aggregates, such as natural and artificial pozzolanic materials, that have also the capability to react chemically with the binder giving it hydraulic properties (see section 2.5.1.3). The characteristics of aggregates that affect mortar properties are mechanical resistance, porosity, granulometric distribution, morphology, superficial texture and composition. Since the aggregate represents a sort of skeleton of the mortar, its mechanical characteristics influence those of the mortar itself. For this reason, aggregates should have higher mechanical resistance than that of the binder of the mortar [Cag00]. Porosity of aggregates depends on porosity of rocks and minerals constituting them, which varies from 2% in plutonic rocks such as granite to 10-40% in limestones or volcanic rocks. Porosity of aggregates influences physical, chemical, mechanical properties and durability of mortars [Pec08]. The granulometric distribution of the aggregate affects mortar properties such as mechanical strength and porosity [Ste05]. Aggregates characterized by a wide range of grain sizes (poorly sorted) need a minor quantity of binder in the mortar mixture. This happens because the smaller aggregate grains fit into the spaces left among the bigger ones. This way the shrinking phenomena are reduced and the resulting mortar has a relatively low porosity [Pec08]. Morphology includes sphericity and roundness of the aggregate grains, which influence the workability of the mortar in the fresh state [Pec08]. Superficial texture of the aggregate grains affects their adhesion to the binder and the amount of water that is necessary to add to the mixture. The aggregate/binder adhesion then, influences the mortar resistance to traction, while the quantity of water its porosity. Finally, the composition of the aggregate plays an important role in the durability of

a mortar. In fact, the aggregate should not contain a number of substances that would affect negatively the mortar durability. The presence of sulfates in general is responsible of the formation of expansive compounds like gypsum in air lime mortars, which causes their disaggregation. Chloride salts in the aggregate are also harmful not only because of the mechanical action due to their crystallization but also because their presence is altering the mortar setting. Clay minerals adsorb water in their crystalline structure, causing an extra need of water in the mixture that result in a less durable mortar [Pec08].

2.5.3. Water

The characteristics of mixing water that influence mortar properties after its application on the masonry are quality, quantity and temperature. The water used in the mortar mixture should not contain, either in solution or in suspension, impurities that could interfere with the adhesion between binder and aggregate. The content of salts like sulfates, chlorides, nitrates is to be low, since they can slow down the drying of the mortar causing the formation of superficial efflorescence and stains and can weaken its mechanical resistance after the setting and curing [Pec08]. The quantity of water in the mixture should be such as to produce a plastic homogeneous mortar. An excess of water increases mortar workability but slows down the setting of the binder and decreases the mechanical resistance of the final product. In general, the higher is the amount of aggregate and the finer is the binder, the higher is the volume of water necessary in the mixture [Pec08]. Furthermore, the quantity of mixing water depends on the masonry units that the mortar bonds, on the weather conditions and on the porosity of the building stone in contact with the mortar. For example, mortar for heavier units needs less water in order to be denser, to prevent uneven settling and to keep excessive mortar from being squeezed out of the joints. On the other hand, on hot dry days mortar is subject to a higher water loss by evaporation that requires an extra addition of mixing water to compensate for evaporation [Bea00]. Building stones with high porosity absorb water from the mixture, which needs to be replaced to keep mortar workability [Pec08]. Finally, temperature of the mixing water affects setting time of the mortar. Hot water accelerates the setting process. In fact, in winter in areas where temperature drops below zero, mix water is heated to avoid the freezing of lime mortars before the setting, which would cause their disaggregation [Pec08].

2.5.4. Additives

An additive is a substance that added to the mortar mixture improves its properties and workability. The use of additives in mortars dates back to ancient times. A first differentiation

of additives used in the past separates additives of proteinic nature, polysaccharidic additives, oils and fats [Pec08]. The use of proteinaceous substances in mortar mixtures dates back to the 1st century B.C. [Sic81]. There are indications about the use of additives by the ancient Cretans (arabic gum, animal glue, blood, mixed with yolk) and Egyptians (egg white, keratin, casein) especially for stuccoes. Pliny the Elder in his *Naturalis Historia* [Pli71] refers that Romans produced highly resistant mortars using additives of animal and vegetal origin. In the Middle Ages and Renaissance additives of animal and vegetal origin like wax, egg white, beer, bitumen, urine, sugar, fruit juices, gluten, rice, blood were used [Ban08, Arc01]. The use of proteinic additives, according to an empirical practice handed down through centuries, makes mortars especially durable in time. The use of proteinic additives in the mortar mixture has the following effects:

- increases air entrainment in the mortar mixture enhancing its workability [Pec08, Bea00];
- increases the dispersion of the lime particles in the mixing water lowering water requirements and minimizing volume loss due to evaporation [Pec08];
- accelerates or retards carbonation and therefore the setting process [Arc01, Ber98];
- makes pores surface hydrophobic and therefore the mortar water repellent [Pec08].

Further indications on the use of organic additives by the ancient craftsmen come from Leon Battista Alberti [Alb65], who refers to the use of oil, specifically linseed oil, in the manufacture of mortars for pavements. According to Alberti the addition of linseed oil to a mortar increases its mechanical resistance and durability.

2.6. Types of mortar

Following are described the main characteristics of mortars made with the different types of binder that have been treated in the previous paragraphs.

2.6.1. Air mortars

An air mortar is produced mixing hydrated lime or lime putty with aggregates and water. Air mortars set and harden only with air by the reaction between lime and carbon dioxide, which produce calcium carbonate. The curing is initially faster close to the surface of the mortar, and then it gradually slows down toward the interior part of it. This is due to the formation of calcium carbonate around the aggregate grains, which decreases mortar porosity [Mar76]. In general, after two-three weeks the 60-70% of lime turned in to calcium carbonate, while the curing takes up to one year to be completed [Pec08]. As already explained in the previous paragraphs, factors affecting mortar properties are the amount of mixing water, the weather

conditions during the application and the characteristics of the aggregate. Aggregates with different composition and granulometric distribution are selected depending on mortar function. For example, coarser aggregates are chosen for mortars used in foundations, siliceous sands are preferred for walls, while artificially crushed colored stones are used for the mortar bedding tesserae in mosaics or in mortars for decorations [Men92, Pec08]. Also the binder/aggregate ratio depends on use and function of the mortar. In general, the quantity of lime should be such as to fill the spaces left among the aggregate grains. The most commonly used binder/aggregate ratios range from 1/2 to 1/3 [Mar76, Pec08].

2.6.2. Hydraulic mortars

A hydraulic mortar is produced mixing natural hydraulic lime with aggregates and water. Since natural hydraulic lime contains both calcium hydroxide and hydraulic compounds, hydraulic mortars set and harden both with air and under water. The aerial setting and curing is due to the reaction of calcium hydroxide with carbon dioxide to form calcium carbonate. The hydraulic setting and curing is due to the reaction of calcium silicates, aluminates and ferrites with mixing water to form calcium silicates and aluminates hydrates. As for air mortars, hydraulic mortars properties are influenced by the amount of mixing water, the weather conditions during the application and the characteristics of the aggregate [Pec08].

2.6.3. Natural and artificial pozzolanic mortars

A natural or artificial pozzolanic mortar is produced mixing air lime with natural or artificial pozzolanic materials respectively, other aggregates and water. Pozzolanic mortars set and harden both with air and under water. The aerial setting and curing is due to the reaction of calcium hydroxide with carbon dioxide to form calcium carbonate. The hydraulic setting and curing is due to the reaction between calcium hydroxide, free silica and alumina contained in the pozzolans, and mixing water, which produces calcium silicates and aluminates hydrates. Pozzolanic mortars were used especially in the ancient times for hydraulic works like aqueducts, cisterns, bridges etc. Furthermore, the Romans also used mortars made with pozzolana for external walls coating [Sca83, Fio80]. Finally, the use of mortars containing either pozzolana or brick fragments in the construction of pavements is described in the ancient treatises by Vitruvius [Vit62] and Pliny [Pli71], and later by Leon Battista Alberti [Alb65].

Chapter 3

The Case Studies

3.1. Introduction

Five archaeological sites characterized by the presence of floor mosaics and other kind of pavements have been investigated. Some of these sites were undergoing archaeological excavation at the time of the sampling operations, like the Palace of Aegae in Vergina, the House of Epigenes in the ancient city of Dion and the area of St. Severo's Church in Classe. Some others were recently restored, like the Roman Villa in Tortoreto, or were waiting for restoration intervention, like the pavements fragments stored in the courtyard of the Archaeological Museum of Florence. In this chapter, geographical position, history, geological and geomorphological features of the area of the investigated case studies are described. The information available about the sites varies from site to site, depending on factors like the state of archaeological excavations, the existence of published material, the policy of the institutions in charge of managing the site, etc.

3.2. The ancient city of Dion

3.2.1. Geographical position

Dion is located in the foothills of Mount Olympos, at the southern end of the Prefecture of Pieria, Greece, 425 km to the north of Athens and 65 km to the south-west of Thessaloniki. The archaeological site can be reached either directly from the Athens – Thessaloniki motorway or from Katerini via a local road.

3.2.2. History

The first mention of the city of Dion in history occurs in the description given by Thucydides of the advance of the Spartan general Brasidas from Thessaly to Macedonia. It was the first city that Brasidas came to after crossing the borders in the summer of 424 B.C. According to Diodoros, it was the king of Macedonia Archelaos who, at the end of the 5th century B.C.,

gave to the city its subsequent importance by instituting a nine-day festival that included athletic and dramatic competitions in honor of Zeus and the Muses. In 219 B.C., Dion was destroyed by Aetolian invaders but was immediately rebuilt by Philip V. Then, in 169 B.C., the Roman consul M. Philippus captured it. The city was given a new lease of life in 32/31 B.C., when Octavian founded a Roman colony there, the Colonia Julia Augusta Diensis. The city grew and prospered, flourishing particularly in the 2nd century A.D. and the early part of the 3rd, until the latter half of that century when barbarian invasions, earthquakes and floods drove it into decline. Dion knew a further period of prosperity in the 4th century A.D., when it became the seat of a bishopric. After the middle of the 5th century A.D., however, a combination of natural disasters and Gothic raiders forced the town's inhabitants to move up into the mountains. The last reference to Dion, which dates from the 10th century A.D., occurs in the work by Constantine Porphyrogenetos, *De Thematibus*. The ruins of the ancient Dion were discovered in 1806 by the English officer W.M. Leake, who identified the fortifications, theatre, stadium, a temple and a tumulus. Excavations began in 1928 and continued at different time intervals until today. They brought to light the enceinte of the fortified walls and an urban core laid on a grid plan including the remains of public buildings, shops, workshops, public latrines and luxurious dwellings. Furthermore, in 1983 Dion acquired an archaeological museum. [Pan97]

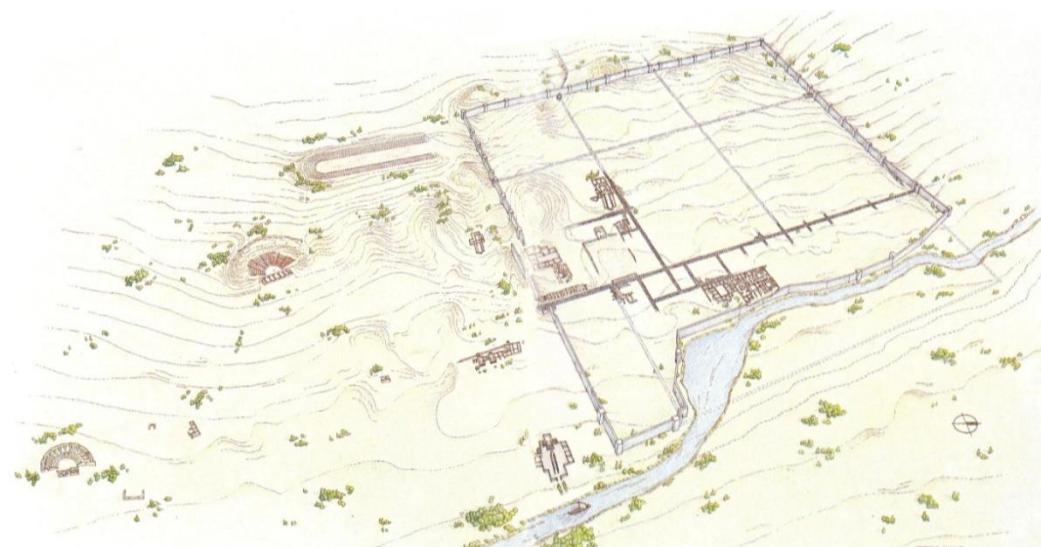


Figure 7 Dion: The sanctuaries and the city [Pan97].

3.2.3. Geological and geomorphological features

Dion, located in the plain in between the sea and the Mt. Olympos, lies on Pleistocenic scree and talus cones. These deposits are composed of calcareous breccio-conglomerates, with elements of various size, loose to cohesive, with clayey and carbonate cement. The rock

formations which outcrop west and south of the city consist of the Mt. Olympos autochthonous series. This is made of regular continuous carbonate bed sediments, mainly composed of crystalline limestones and dolomitic limestones, locally schistose, neritic and organogenic (Triassic – Cretaceous). South to Dion and west to the town of Litochoro, along the east flank of Mt. Olympos, overthrust rock formations of metamorphic and volcanic origin are present. These formations consist of metamorphic basic ophiolitic and volcano-sedimentary greenrocks mainly composed of amphibolites and amphibolite schists with serpentinite bodies tectonically placed into them. [Igm85]

3.3. The “Villa Romana delle Muracche” in Tortoreto

3.3.1. Geographical position

The “Villa Romana delle Muracche” is located in Tortoreto, a town in the province of Teramo, in the Abruzzo region of Italy. Tortoreto can be reached either by car, from the Bologna – Taranto highway, taking the exit to Val Vibrata, or by train, arriving at the station of Tortoreto Lido. The Villa, placed at about 10 m above the sea level and at a distance of about 25 km from the Statale Adriatica Road, can be found following the road that from Tortoreto Lido leads to Tortoreto Alto.

3.3.2. History

Starting from the half of the 19th century, a number of archaeological findings dated to the Roman period have been discovered in the area of Tortoreto. Considering these evidences, it can be stated that a series of *Villae rusticae* were built in the area of Tortoreto during the 2nd and 1st century B.C. One of these is the “Villa delle Muracche”, whose name is due to the presence of an ancient wall (in Italian *muro*) that still stands next to the *Villa*. The building underwent two archaeological excavations in 1988 and 1989 conducted by the Soprintendenza Archeologica dell’Abruzzo, which brought to light a number of rooms organized around a peristyle. The *Villa* is composed of a *pars rustica* and a *pars urbana*, the first occupying the area toward the hill, the second the area facing the sea. The building went through four construction phases. The first one, recognized in the structure of the *pars rustica*, dates to the Late Roman Republic period (end of 2nd century B.C. – first half of 1st century B.C.). To the second phase, which dates to the period of the Emperor Augustus (27 B.C. – 14 A.D.), can be referred the construction of the *pars urbana* of the *Villa*. In the third phase, the *pars rustica* underwent modifications aimed at the improvement of the wine production processes, and in the fourth phase the *pars urbana* was enlarged. The last evidences of the occupation of the

Villa date to the 4th century A.D. for the *pars urbana* and to the 5th century A.D. for the *pars rustica*. The *Villa* was then abandoned in the 5th – 6th century A.D. [Lap96]

3.3.3. Geological and geomorphological features

Tortoreto, located on the oriental edge of the hilly area that separates the Apennines from the Adriatic Sea, lies on sedimentary Pleistocene deposits of marine origin. These deposits are composed of conglomerates and, downward, of stratified sands and sandy clays. Moving toward the inland, first Miocene foredeep deposits composed of stratified sandstones alternated to sandy clays and marls, and then Cretacic limestones and Jurassic limestones and marly limestones, are outcropping. [Ser69]

3.4. The archaeological area of St. Severo, Classe

3.4.1. Geographical position

Classe is located 5 km to the south of the city of Ravenna, in the Emilia Romagna region of Italy. It can be reached either by car from the Bologna – Ancona highway, taking the exit to Cesena Nord and then following the road E45 to Ravenna, or by train, arriving at the station of Classe.

3.4.2. History

The ancient city of Classe was built in the 5th century A.D. as commercial port of Ravenna, when it became the capital of the occidental empire. The St. Severo's Basilica was discovered and partially excavated in the 1960s, and from 2006 is undergoing a new archaeological excavation campaign. The first evidences of the occupation of the area of the Basilica consist of the remains of a Roman *Villa*, dated to the 1st century A.D., which was composed of several rooms with mosaic pavements, and a bathhouse. Probably this building was inhabited until the 6th century A.D., when the St. Severo's Basilica was built. In the following centuries further structures were constructed close to the Basilica, like a bell tower dating to the 12th century A.D. After a long period of decline the Basilica was rebuilt a first time in the 15th century A.D. and a second time in the 18th century A.D., before being demolished in the 19th century A.D. [Aug03] [Mai91] [Ber83]

3.4.3. Geological and geomorphological features

Ravenna and Classe are located on the Romagna coastal plain, which is filled by late Quaternary deposits, composed of sandy clays and clayey sands. The area is characterized by

saltwater intrusion in the phreatic aquifer and by natural and anthropogenic land subsidence, which has dropped most of the territory below mean sea level, modifying the river and normal groundwater flow regimes. Toward the inland the outcropping geologic formations are mainly composed of Pliocene marly clays, Miocene gypsum, sands, sandstones and silty marls, Oligocene marls, Eocene and Paleocene marly limestones, Giurassic diabase, serpentine and vulcanite. [Gia07] [Ser56]

3.5. The “Cortile Romano” in the Archaeological Museum of Florence

3.5.1. Geographical position

The so called “Cortile Romano” is one of the internal courtyards of the “Palazzo della Crocetta”, a 17th century palace that from 1881 hosts the National Archaeological Museum of Florence, in the Tuscany region of Italy. The Museum has its main entrance in the “Piazza Santissima Annunziata”.

3.5.2. History

In the “Cortile Romano”, the remains of Roman monuments, which were brought to light during works of renovation of the city center executed at the end of the 19th century, are stored. These monuments belonged to the Roman city of Florentia, whose foundation, still uncertain, is likely to be dated to the end of the 1st century B.C. The archaeological finds come from the excavation of different areas of the city of Florence. In the area of the Baptistery of St. Giovanni, a Roman House dated to the 1st century B.C. was discovered below the sacred Christian building. The House, which underwent several construction phases until in the 3rd century A.D. it was transformed in a bathhouse, had its entrance on the south side of the building, which gave access to an *atrium* surrounded by several rooms. In the specific, the *impluvium* of the House and a number of floor mosaics fragments dated to the 2nd century A.D., also found in St. Giovanni’s square, are stored in the courtyard of the museum. The remains of further houses were found in the same period in other parts of the city. In the area between the “Via Strozzi”, the “Via de’ Vecchietti” and the “Via de’ Pescioni”, stood the *Thermae Capitoline* of the ancient Florentia, also partially reconstructed and stored in the “Cortile Romano”. [Peg62] [Sat00]

3.5.3. Geological and geomorphological features

Florence lies on an alluvial plain filled by fluvial and lacustrine quaternary sediments composed of sand and clay with gravel beds, and by actual fluvial deposits made of gravel

and sandy clays. The plain, which is extended from Florence to Pistoia, is located on the side of the Apennines facing the Tyrrhenian Sea, in between two ridges of pre-Pliocene sediments oriented from northwest to southeast. The southwest ridge is mostly composed of Oligocene sandstones alternated to schist, above which, on the northeast side, there are allochthonous deposits composed of Eocene and Cretaceous slates, limestones and marly limestones, sandstones. On the northeast ridge, higher of the previous one, autochthonous deposits made of Oligocene sandstones alternated to schist and allochthonous deposits made of Oligocene sandstones, marly limestones, slates, and the ophiolite series including serpentine, gabbro and diabase, are present. [Ser67] [Ser69]

3.6. The Palace of Aegae in Vergina

3.6.1. Geographical position

The Palace of Aegae is placed in Vergina, a small town in northern Greece located in the prefecture of Imathia, about 13 km southeast of the district centre of Veria, 80 km southwest of Thessaloniki and 515 km northwest of Athens. The Palace is built on the northern slope of the Pierian Mountains and occupies the higher among the terraces of the fortified city. Vergina can be reached by car following the Athens – Thessaloniki motorway and continuing through the E90 Egnatia road.

3.6.2. History

The modern village of Vergina, founded in 1922, knew worldwide renown in 1977, when the archaeologist Manolis Andronikos discovered in its vicinity the tomb of King Philip II of Macedon, father of Alexander the Great. The discovery confirmed that Vergina was the site of the city of Aegae, the ancient capital of the Macedonian kings, and its cemetery. Aegae flourished chiefly in the 2nd half of the 4th century B.C. To this period dates the Palace, which is considered the earliest royal residence in the late Classical Greece, destroyed by the Romans in the mid 2nd century B.C. The Palace, discovered in 1856 by the French archaeologist Leon Heuzev, is since 1938 the nucleus of the Aristotle University of Thessaloniki excavations. [Dro00]

3.6.3. Geological and geomorphological features

Vergina lies on the southwest end of the Thessaloniki plain, the largest deltaic area of Greece. The plain is filled with Pleistocene conglomerates and Holocene alluvial sandy deposits. To the west and south of Vergina the plain ends towards the Vermion Mountain, where Mesozoic

limestones and marbles, schists and ophiolites are outcropping. To the south and the east it is the hilly range of Pieria made of Neogene fluvial-lacustrine deposits. [Ghi08] [Igm82]

Chapter 4

Materials and Methods

4.1. *In situ* analyses and sampling

A first characterization of the studied pavements, including the description of number, thickness and mutual adhesion of the preparatory layers, the measurement of tesserae's size, and the investigation of the type of surface on which the pavements were built, has been carried out *in situ*. The layers constituting the substrate have been indicated with progressive numbers, from the deepest to the most superficial one. The stratigraphy of the substrates has been reproduced in a schematic graphic form, in order to compare its characteristics among the pavements under study. Furthermore, information about the sites have been collected, especially those regarding the ancient use of the rooms where the investigated pavements are located, and an effort to connect these information with substrates characteristics has been made. The sampling has been performed according to the Italian standard NORMAL 3/80 [Nor80]. The samples have been collected by means of hammer, chisel and scalpel and stored in sealed plastic cups or bags for the transfer to the laboratory. The quantity of the collected material varied according to several factors, in the specific the layer thickness, the size of the mortar's aggregate, the state of conservation of the artefact, and it was ranging from less than 10 g to up to 300 g. The location of the studied pavements within each site and of the sampling points on each pavement have been documented by means of graphic plans, when available, and/or by photographs.

4.2. Laboratory analyses

4.2.1. Preparation of samples

According to sampling conditions *in situ*, collected samples were made up of one or more layers of mortar. In the latter case the different layers have been separated in the laboratory by means of scalpel, chisel and rock saw when necessary. Analyses have been then performed on each mortar layer of the substrates' stratigraphy.

4.2.2. Optical microscopy

The mortars have been studied by means of reflected and transmitted polarized light optical microscopy. Observations have been carried out on cross sections using a Leica Wild M10 stereomicroscope and on thin sections using a Leitz Laborlux 12 Pol S polarizing microscope. Cross section and thin section photomicrographs have been made by means of a Nikon Coolpix 4500 digital camera coupled to the microscope through an eyepiece adapter. The mortar samples have been oriented the way that the area of the thin section to be observed was that perpendicular to the surface of the layer, so as of the pavement. The preparation of the thin sections has been committed to Mr. Saviozzi Gherardo, who realized them in his laboratory of Colignola, Pisa, Italy, according to the Italian standard NORMAL 14/83 [Nor83]. The observations in reflected light have been carried out on the mortar fragments left over from the thin sections preparation, taking advantage of their polished surfaces obtained by the cutting of the samples. The colour of the mortar samples has been classified by comparisons with the Munsell Soil Color Charts [Mun00]. The optical microscopy analyses aimed at the description of mortars porosity, mineralogy, morphology, distribution and orientation of the aggregates in the mortars. Carbonate rocks in the aggregate of the studied mortars have been classified by means of both Folk's [Fol59, Fol62] and Dunham's [Dun62] classification. For each sample, a characterization form based on the mortar description scheme proposed in the Italian standard UNI11176 [Uni06] has been filled out.

4.2.3. Mortars disaggregation

A fraction of each mortar sample, ranging in weight from less than 10 g to about 80 g, has been disaggregated following a procedure described by Pecchioni *et alii* [Pec08] for the separation of the binder from the aggregate. According to this method the sample is first ground in a porcelain mortar, paying attention in not to break the aggregates, until mortar fragments no smaller than the biggest aggregate grains are obtained. The sample is then transferred in to a glass beaker filled with distilled water and put in an ultrasonic tank, also filled by water up to the same level in the beaker, where it is disaggregated for 30 min. After the first disaggregation cycle by ultrasounds, the content of the beaker is filtered by means of a sieve with 63 μm apertures size. The passing fraction is the so called binder enriched fraction, considered to be composed mainly by the binder of the mortar. The retained fraction, constituted by the aggregate and part of the binder still adhering to the aggregate grains, has to undergo further disaggregation cycles by ultrasounds until the aggregate grains, examined under the stereomicroscope, are totally free of binder. The used beakers had 100 ml volume;

the ultrasonic bath was an Elmasonic with 0.9 l tank capacity and 35 kHz ultrasonic frequency, manufactured by Elma.

4.2.4. Mechanical sieving

Grain size distribution of the mortar layers has been determined by mechanical sieving. According to the used method the sample, about 80 g, is disaggregated according to the procedure described in the section 4.2.3 and fractionated in a column of sieves (ISO 3310 series sieves with 31.5, 16, 8, 6.3, 4, 2.5, 1, 0.5, 0.2, 0.1, 0.075, 0.063 mm openings size) stirred for 10 min by means of a Matest electronic sieve shaker. Then, the masses of the collected fractions are determined.

4.2.5. Chemical analyses

The analyses described in the following three paragraphs, namely the loss on ignition test (L.O.I.), the atomic absorption spectrometry (AAS) and the ion chromatography (IC) have been performed by the chemists of the chemical laboratory of the Civil Engineer Department of the Aristotle University of Thessaloniki. The used methodologies have been developed during years of local experimentation on building materials, adapting traditional analytical methods and referring to the existing international standards. The pyrolysis gas chromatography mass spectrometry (Py/GC/MS), described in the section 4.2.5.4, have been carried out in the Laboratory of Environmental Sciences R. Sartori of the C.I.R.S.A. University of Bologna Ravenna, Italy, by Dr. Simona Montalbani, under the supervision of Prof. Daniele Fabbri and Prof. Giuseppe Chiavari. The activity of the C.I.R.S.A. laboratory includes the characterization of the organic matter in cultural heritage materials.

4.2.5.1. Loss on Ignition

The tests have been executed on the granulometric fraction of particle size $< 75 \mu\text{m}$. According to the used method, the sample is first dried in an electric furnace at $60 \text{ }^\circ\text{C}$ until the difference between two successive weighing is less than 0,005 g. Then, 1 g of the dried sample is weighed into a porcelain crucible which has been previously ignited and tared, as described in the EN 196-2:1994 standard [EN94]. The crucible is placed in an electric furnace controlled at $975 \pm 25 \text{ }^\circ\text{C}$ and heated for 90 min. The crucible is then cooled to room temperature in a desiccator and weighed. The loss on ignition of the sample expressed in percentage is calculated from the following equation:

$$\text{L.O.I.} = \frac{(m_b - m_c)}{(m_b - m_a)} \times 100$$

where

L.O.I. is the loss on ignition of the dry mass of a solid sample, in percentages;

m_a is the mass of the empty pre-ignited crucible, in grams;

m_b is the mass of the crucible containing the sample, in grams;

m_c is the mass of the crucible containing the ignited sample, in grams.

The results of the tests are expressed to two decimal places.

4.2.5.2. Atomic Absorption Spectrometry

A wet chemical analysis of cations by means of atomic absorption spectrometry (AAS) has been carried out on the granulometric fraction of particle size $< 75 \mu\text{m}$ of the studied mortars. AAS analyses have been performed on a Perkin Elmer 3110. Two kinds of analyses by acid dissolution methods have been executed. According to the first of the two methods used, 0.25 g of the sample are weighed into a porcelain crucible and treated by wet ashing with HClO_4 and HF (37% wt.) in oven at 80°C until the sample is dried, normally after 3 – 4 hours. Then, HCl 12N is added and the sample in the crucible is kept in oven for 30 more minutes. The sample is then transferred in to a 500 ml flask filled with distilled water. At this point, three flasks for three differing sample dilutions are prepared: 10 ml of the sample are transferred from the 500 ml flask into a first 100 ml flask filled with distilled water; 10 more ml are moved into a second 100 ml flask together with 2 ml of lanthanum and distilled water until filled; 10 ml are taken from the first 100 ml flask and transferred into a third 50 ml flask together with 1 ml of lanthanum and distilled water. The sample is now ready to be analyzed by the spectrometer. The cations content is expressed in oxides (Na_2O , K_2O , CaO , MgO , Fe_2O_3 , Al_2O_3 , SiO_2). The CaO content is estimated from the loss on ignition test and the SiO_2 content is calculated by difference after all the other cations are determined. According to the second method used, 0.25 g of the sample are weighed and transferred in to a 500 ml glass beaker with 200 ml of HCl 0.1 N. After 2 hours on the magnetic stirrer the content of the beaker is filtered through a filter paper with a mean pore diameter of around $0.8 \mu\text{m}$ and the passing is transferred in a 250 ml glass flask successively filled with distilled water. Three kinds of dilution are then made: 10 ml of the sample are moved from the 250 ml flask into a first 100 ml flask filled with distilled water; 10 more ml are transferred in to a second 100 ml flask together with 2 ml of lanthanum and distilled water until filled; 10 ml are taken from the first 100 ml flask and moved in to a third 100 ml flask with 4 ml of lanthanum and distilled water until filled. At this point the sample is ready to be analyzed by the spectrometer.

4.2.5.3. Ion Chromatography

The water soluble salts content (Cl^- , NO_3^- , SO_4^{2-}) of the granulometric fraction of particle size $< 75 \mu\text{m}$ has been determined by means of ion chromatography (IC). According to the used method, 1 g of the sample is weighed and mixed with 200 ml of distilled water into a 500 ml glass beaker on the magnetic stirrer for 150 minutes. The content of the beaker is then filtered through a filter paper with a mean pore diameter of around $0.8 \mu\text{m}$ and the passing is transferred in a 250 ml glass flask successively filled with distilled water. The obtained sample is ready to be analyzed by the ion chromatograph. The analyses have been performed with an Alltech 330 column.

4.2.5.4. Pyrolysis Gas Chromatography Mass Spectrometry

The presence of organic additives in the binder fraction of some of the studied mortars has been investigated by means of pyrolysis gas chromatography mass spectrometry (Py/GC/MS). Four methods have been applied: conventional pyrolysis in combination with online GC–MS; pyrolysis/silylation with hexamethyldisilazane (HMDS) in combination with online GC–MS; pyrolysis/silylation with hexamethyldisilazane (HMDS) offline; pyrolysis/methylation with tetramethylammonium hydroxide (TMAH) in combination with online GC–MS. Hexamethyldisilazane 99% and tetramethylammonium hydroxide (25% in water) were from Aldrich. The samples consisted of 0.1 – 0.5 mg of the granulometric fraction of particle size $< 63 \mu\text{m}$, obtained by the procedure described in the paragraph 4.2.3. According to the used method the sample is inserted into a quartz capillary tube and, in case of pyrolysis/silylation and pyrolysis/methylation, 5 μl of the derivatisation agent (HMDS or TMAH, 25% aqueous) is added prior to pyrolysis. Pyrolyses are carried out at $600 \text{ }^\circ\text{C}$ for 10 s at the maximum heating rate of a CDS 1000 pyroprobe heated filament pyrolyser (Chemical Data System, Oxford, USA) directly connected to the injection port of a Varian 3400 gas chromatograph coupled to a Saturn II ion trap mass spectrometer (Varian Analytical Instruments, Walnut Creek, USA). A Supelco SPB5 capillary column (30 m, 0.32 mm i.d., 0.25 μm film thickness) has been used with a temperature programme from $50 \text{ }^\circ\text{C}$ (held for 10 min) to $300 \text{ }^\circ\text{C}$ (held for 5 min) at $5 \text{ }^\circ\text{C min}^{-1}$ with helium as carrier gas. Temperatures of split/splitless injector (split mode) and pyrolysis/GC interface were kept at $250 \text{ }^\circ\text{C}$. Mass spectra were recorded at 1 scan s^{-1} under electron impact at 70 eV, scan range from 45 to 650 m/z. Structural assignment of the products was based on match with the NIST 1992 mass spectra library.

4.2.6. Water absorption under vacuum

The open porosity of the samples has been measured according to the European Standard EN 1936:2006 [EN06]. Nevertheless the used method differs from the one described in the standard in the value of the pressure within the evacuation vessel, which has been possible to lower with the available apparatus only to 29 ± 0.7 kPa instead of 2 ± 0.7 kPa.

4.2.7. Compression test

Compression tests have been executed on some of the studied samples by means of a hydraulic universal testing machine Mohr & Federhaff AG (up to 1000 kN capacity), operated by Dr. Maria Stefanidou. The specimens have been loaded with a constant crosshead velocity. Since it has been not possible, for both technical and conservational reasons, to obtain specimens of the size and shape required by the testing standards, and since, as it is known, size and shape of a testing specimen have a significant influence on the measured strength, a correction factor has been applied to the experimental results. The correction factor used is the one developed by Drdacky *et alii* [Drd08] for lime/metakaoline mortar specimens of differing base edge length, differing height to base edge length ratio, and constant lime/aggregate ratio:

$$f_c = \frac{f_e}{\left(\frac{h}{a}\right)^{-1.6341}}$$

where

f_c is the computed compressive strength;

f_e is the experimentally attained compression strength;

h/a is the height to base edge length ratio;

Specimens in the shape of prisms with base length ranging from 2 cm to 4 cm and height ranging from 1 cm to 3 cm have been realized from some of the collected mortar samples (Figure 8). The prismatic shape has been obtained grinding each side of the sample by means of abrasive paper, paying attention in disturbing as little as possible its superficial strata [Drd08]. Depending on the characteristics of the sample, one or both the horizontal surfaces of the prism, where the compressive load is applied, have been levelled with gypsum. Every specimen has been oriented the way that the loaded surface was the one parallel to the surface of pavement.



Figure 8 Some of the specimens prepared for the execution of the compression tests.

Chapter 5

Results and Discussion

5.1. Results of the analyses

In the following paragraphs the results of the analyses performed on the studied pavements are reported. For each of the investigated case studies, the *in situ* analyses are first illustrated. Then, for each of the samples collected from the substrates, a characterization form filled out with the data obtained by the laboratory analyses is reported. In section 5.2, the results are compared by means of graphics, discussed and elaborated. Finally, in section 5.3, some practical applications of the results are suggested.

5.1.1. The ancient city of Dion

Five pavements that belonged to five different buildings within the ancient city of Dion have been studied. The location of these buildings within the city plan is showed in Figure 9. The mosaics are indicated in the text with the name of the building where they are placed.

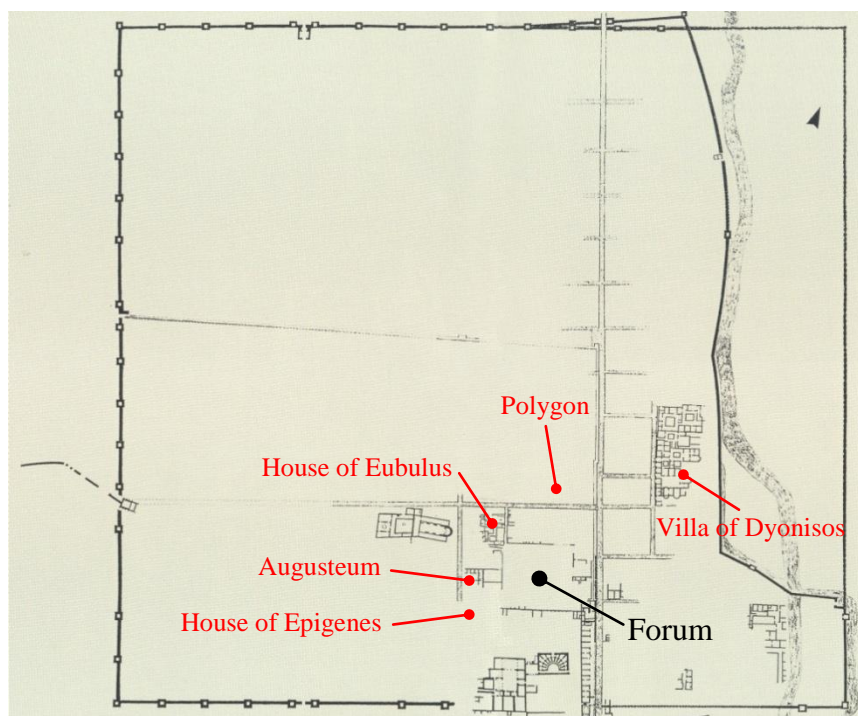


Figure 9 Plan of the city of Dion with the location of the studied mosaics. From *Pandermalis* [Pan97], modified.

– *Mosaic of the Augusteum*

The investigated floor mosaic is located in a single room building that stood in the middle of the west side of the Roman forum (Figure 9). This building, probably a temple dedicated to the cult of the Roman emperors, has a Doric front and walls painted to resemble marble cladding (Figure 10). Inside it, archaeologists found fragments of marble statues of male figures and of a semicircular platform [Geo08]. The mosaic pavement lost almost completely the *tessellatum*, which was made of stone *tesserae* with average size smaller than 1 cm, still lasting only on a narrow area next to the south wall of the room (Figure 10, Figure 11).



Figure 10 The single room of the *Augusteum* with its south and west painted walls visible under the shelter.



Figure 11 Remains of the mosaic's *tessellatum* in the area next to the south wall of the room.

Nevertheless, the mosaic's substrate is well preserved. The *in situ* analyses and the sampling have been performed in an area of the pavement where a crack is cutting the substrate through its whole thickness. The position of the sampling point, located 3.4 m from the west wall and 3 m from the south wall of the room, is showed in Figure 12.

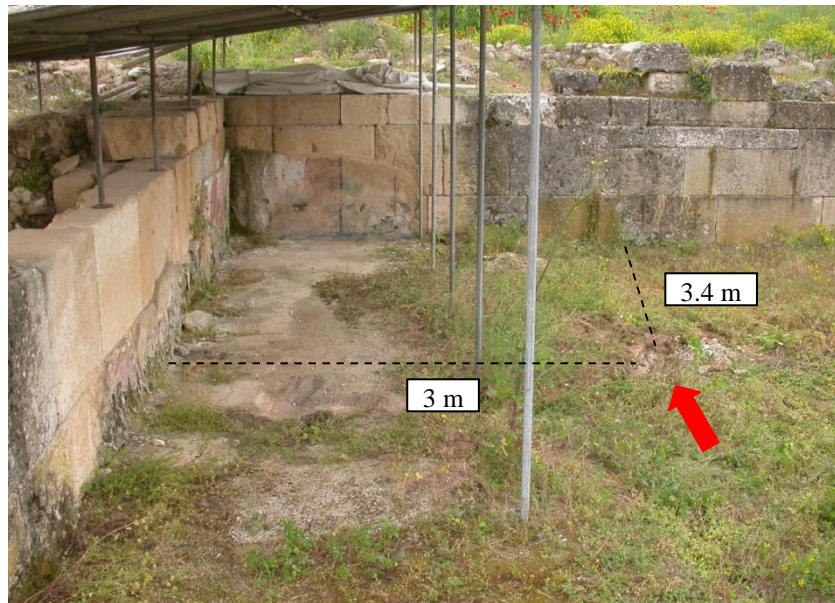


Figure 12 The point of the pavement where the substrate has been investigated.

The *in situ* investigation of the mosaic of the *Augusteum* revealed that its substrate was built on natural levelled ground and made of four preparatory mortar layers (Figure 13). The layers mutual adhesion is very good, even though layer number 3 is locally detached from the underlying one.

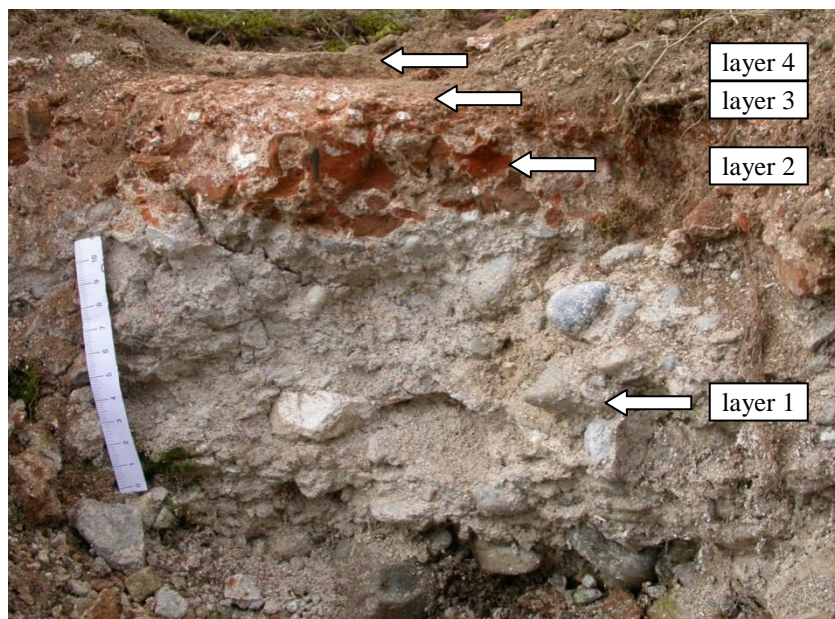


Figure 13 Cross section of the mosaic's substrate with the indication of the different mortar layers.

In Figure 14, a schematic graphic reproduction of the stratigraphy of the mosaic's substrate with the indication of the layers thickness and of the sampled layers with the correspondent sample codes is showed. A total of four mortar samples have been collected from the preparatory layers of the mosaic of the *Augusteum*.

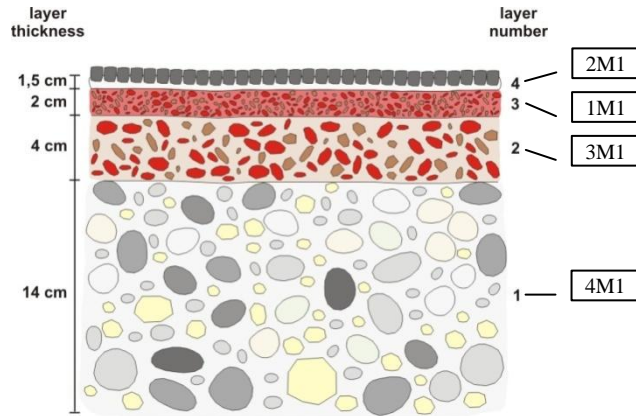


Figure 14 Schematic graphic reproduction of the stratigraphy of the mosaic of the *Augusteum* with the indication of the sampled layers and the correspondent sample codes.

In Table 1, Table 2, Table 3 and Table 4, the results of the laboratory analyses on the mortars of the 1st, 2nd, 3rd and 4th layer of the studied substrate are summarized.

Table 1 Ancient city of Dion, mosaic of the *Augusteum*: results of the laboratory analyses on the mortar layer n. 1.

Sample: 4M1		CHARACTERIZATION FORM					
OPTICAL MICROSCOPY (Figure 78, Figure 79 in Appendix)							
Stratigraphy	Layer 1	Munsell colour	White 10YR8/1				
Microscopic description of the binder on thin section							
Structure	Homogeneous	Reaction with the aggregate	None visible				
Texture	Micritic	Shape of pores	Irregular				
Microscopic description of the aggregate on thin section							
Granulometry	Maximum size: 8 mm Most abundant sizes: 8-4 mm, 4-2 mm		Roundness	From subangular to very rounded			
Sorting	Poorly sorted $\sigma = 2.00 \text{ } \emptyset$		Distribution	Homogeneous			
Shape	Natural		Orientation	None			
Sphericity	Low		Mineralogic and petrographic composition	Limestones (biomicrite, mudstone; intrasparite, grainstone), marble.			
Classification of the aggregate			Fluvial sand and gravel				
OPEN POROSITY %	13.25		COMPRESSIVE STRENGTH	ND			
GRANULOMETRIC CURVE							
CHEMICAL ANALYSES							
Total cations content % w.t.	Na ₂ O	K ₂ O	CaO	MgO	Fe ₂ O ₃	Al ₂ O ₃	SiO ₂
	0.59	0.39	42.82	5.17	0.56	1.13	19.04
Cations soluble in HCl 0.1 N % w.t.	Na ₂ O	K ₂ O	CaO	MgO	Fe ₂ O ₃	Al ₂ O ₃	SiO ₂
	0.01	0.03	41.70	4.69	0.16	0.79	1.01
Water soluble salts % w.t.	Cl ⁻	NO ₃ ⁻	SO ₄ ²⁻	Loss on Ignition %			30.30
	<0.01	<0.01	<0.01				
Py-GC-MS spectrum	ND						

Table 2 Ancient city of Dion, mosaic of the *Augusteum*: results of the laboratory analyses on the mortar layer n. 2.

Sample: 3M1		CHARACTERIZATION FORM					
OPTICAL MICROSCOPY (Figure 80, Figure 81 in Appendix)							
Stratigraphy	Layer 2	Munsell colour	Very pale brown 10YR8/2				
Microscopic description of the binder on thin section							
Structure	Homogeneous	Reaction with the aggregate	None visible				
Texture	Micritic	Shape of pores	From subcircular to irregular				
Microscopic description of the aggregate on thin section							
Granulometry	Maximum size: 11 mm Most abundant sizes: 8-4 mm, 4-2 mm		Roundness	From angular to subangular			
Sorting	Moderately sorted $\sigma = 1.00 \varnothing$		Distribution	Homogeneous			
Shape	Due to artificial crushing		Orientation	None			
Sphericity	Low	Mineralogic and petrographic composition	Ceramic fragments				
Classification of the aggregate			Artificially crushed bricks (cocciopesto)				
OPEN POROSITY %	37.31		COMPRESSIVE STRENGTH	11.80 MPa			
GRANULOMETRIC CURVE							
CHEMICAL ANALYSES							
Total cations content % w.t.	Na ₂ O	K ₂ O	CaO	MgO	Fe ₂ O ₃	Al ₂ O ₃	SiO ₂
	1.81	1.16	18.61	4.63	3.15	7.48	23.93
Cations soluble in HCl 0.1 N % w.t.	Na ₂ O	K ₂ O	CaO	MgO	Fe ₂ O ₃	Al ₂ O ₃	SiO ₂
	0.02	0.06	18.03	3.75	0.45	1.72	1.75
Water soluble salts % w.t.	Cl ⁻	NO ₃ ⁻	SO ₄ ²⁻	Loss on Ignition %			39.24
	<0.01	<0.01	<0.01				
Py-GC-MS spectrum							

Table 3 Ancient city of Dion, mosaic of the *Augusteum*: results of the laboratory analyses on the mortar layer n. 3.

Sample: 1M1		CHARACTERIZATION FORM					
OPTICAL MICROSCOPY (Figure 82, Figure 83 in Appendix)							
Stratigraphy	Layer 3	Munsell colour	Pinkish white 2.5YR8/2				
Microscopic description of the binder on thin section							
Structure	Not homogeneous	Reaction with the aggregate	Reaction rims around ceramic fragments				
Texture	Micritic	Shape of pores	Irregular				
Microscopic description of the aggregate on thin section							
Granulometry	Maximum size: 4 mm Most abundant sizes: 4-2 mm, 2-1 mm		Roundness	From angular to subrounded			
Sorting	Poorly sorted $\sigma = 2.00 \text{ } \emptyset$		Distribution	Not homogeneous			
Shape	Due to artificial crushing		Orientation	Oriented sub-parallel to the layer surface			
Sphericity	Low		Mineralogic and petrographic composition	Ceramic fragments			
Classification of the aggregate			Artificially crushed bricks (cocciopesto)				
OPEN POROSITY %	41.92		COMPRESSIVE STRENGTH	3.95 MPa			
GRANULOMETRIC CURVE							
CHEMICAL ANALYSES							
Total cations content % w.t.	Na ₂ O	K ₂ O	CaO	MgO	Fe ₂ O ₃	Al ₂ O ₃	SiO ₂
	2.24	1.28	14.83	5.04	3.89	8.84	31.25
Cations soluble in HCl 0.1 N % w.t.	Na ₂ O	K ₂ O	CaO	MgO	Fe ₂ O ₃	Al ₂ O ₃	SiO ₂
	0.02	0.07	13.57	3.83	0.90	1.93	1.98
Water soluble salts % w.t.	Cl ⁻	NO ₃ ⁻	SO ₄ ²⁻	Loss on Ignition %			32.63
	<0.01	-	-				
Py-GC-MS spectrum							

Table 4 Ancient city of Dion, mosaic of the *Augusteum*: results of laboratory analyses on mortar layer n. 4.

Sample: 2M1		CHARACTERIZATION FORM					
OPTICAL MICROSCOPY (Figure 84, Figure 85 in Appendix)							
Stratigraphy	Layer 4	Munsell colour	ND				
Microscopic description of the binder on thin section							
Structure	Homogeneous	Reaction with the aggregate	None visible				
Texture	Micritic	Shape of pores	Irregular				
Microscopic description of the aggregate on thin section							
Granulometry	Maximum size: 1 mm Most abundant sizes: 0.5-0.251 mm		Roundness	From very angular to subangular			
Sorting	Moderately sorted $\sigma = 1.00 \text{ } \emptyset$		Distribution	Homogeneous			
Shape	Due to artificial crushing		Orientation	Oriented sub-parallel to the layer surface			
Sphericity	From high to low		Mineralogic and petrographic composition	Marble fragments			
Classification of the aggregate			Artificially crushed marbles				
OPEN POROSITY %	ND		COMPRESSIVE STRENGTH	ND			
GRANULOMETRIC CURVE	ND						
CHEMICAL ANALYSES							
Total cations content % w.t.	Na ₂ O	K ₂ O	CaO	MgO	Fe ₂ O ₃	Al ₂ O ₃	SiO ₂
	0.30	0.08	33.44	1.46	0.11	0.76	22.86
Cations soluble in HCl 0.1 N % w.t.	Na ₂ O	K ₂ O	CaO	MgO	Fe ₂ O ₃	Al ₂ O ₃	SiO ₂
	0.04	0.02	32.92	1.33	0.04	0.66	0.97
Water soluble salts % w.t.	Cl ⁻	NO ₃ ⁻	SO ₄ ²⁻	Loss on Ignition %			41.00
	0.02	0.01	0.01				
Py-GC-MS spectrum	<p>The figure is a gas chromatography-mass spectrometry (GC-MS) spectrum for sample 2M1. The y-axis is labeled 'MCounts' and ranges from 0.0 to 2.5. The x-axis is labeled 'minutes' and ranges from 0 to 50. The spectrum shows several peaks, with the most prominent ones labeled with their retention times: 12:0, 14:0, 16:0, 18:0, and 18:1. There are also several smaller peaks marked with an asterisk (*).</p>						

– *Mosaic of the House of Epigenes*

The studied mosaic covers the floor of one of the two *atria* of a house that stood on the west side of the forum, south of the *Augusteum* (Figure 9). The house, which dates to the second half of the 3rd century A.D., was altered many times [Geo08]. The studied mosaic, located in the *atrium* on the west side of the house (Figure 15), shows a geometric pattern made of stone *tesserae* with average size of about 1.5 cm (Figure 16).



Figure 15 View of the House of Epigenes from its southwest corner. In the centre of the picture the two *atria* are visible.



Figure 16 The mosaic of the west *atrium* of the House of Epigenes. A wide lacuna of both the *tessellatum* and the substrate is visible.

The *in situ* analyses and the sampling have been carried out in an area of the pavement where a wide lacuna of both the *tessellatum* and the foundation layer was present (Figure 16). The position of the sampling point, located at 2.5 m from the west wall of the *atrium* and at 1 m from its north central wall, is showed in Figure 17.

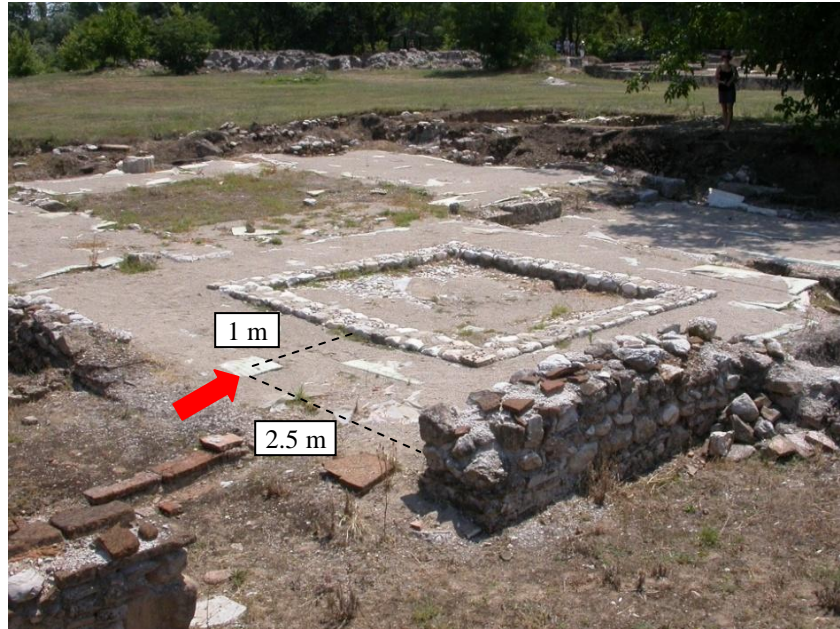


Figure 17 The west *atrium* with the position of the sampling point.

The observations carried out *in situ* showed that the studied mosaic was probably built upon artificial ground used to backfill and level an area where there were remains of older structures. In fact, dispersed in the ground below the thin mosaic's substrate, made of one mortar layer plus the *tessellatum*, there are brick fragments and lime grains which might have belonged to older structures (Figure 18).



Figure 18 Cross section of the mosaic's substrate with the indication of the different layers.

A single sample composed of the preparatory layer of mortar and of a small portion of the *tessellatum* has been collected from the mosaic of the House of *Epigenes*. In Figure 19, a schematic graphic reproduction of the mosaic's substrate with the indication of the sampled layers and the correspondent sample code is showed.

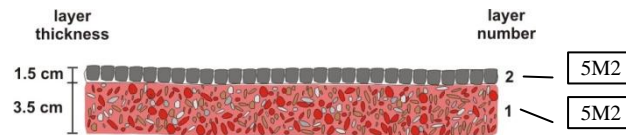


Figure 19 Ancient city of Dion, schematic graphic reproduction of the stratigraphy of the mosaic of the west *atrium* of the House of *Epigenes* with the indication of the sampled layers and the correspondent sample code.

In Table 5, the results of the laboratory analyses for the mortar of the 1st layer of the studied substrate are summarized.

Table 5 Ancient city of Dion, mosaic of the *House of Epigenes*: results of the laboratory analyses on the mortar layer n. 1.

Sample: 5M2		CHARACTERIZATION FORM																									
OPTICAL MICROSCOPY (Figure 86, Figure 87 in Appendix)																											
Stratigraphy	Layer 1	Munsell colour	Pinkish white 5YR8/2																								
Microscopic description of the binder on thin section																											
Structure	Homogeneous	Reaction with the aggregate	Reaction rims around ceramic fragments																								
Texture	Micritic	Shape of pores	Irregular																								
Microscopic description of the aggregate on thin section																											
Granulometry	Maximum size: 4 mm Most abundant sizes: 4-2, 2-1 mm		Roundness	From angular to rounded																							
Sorting	Poorly sorted $\sigma = 2.00 \text{ } \varnothing$		Distribution	Homogeneous																							
Shape	Part natural, part due to artificial crushing		Orientation	Oriented sub-parallel to layer surface																							
Sphericity	From high to low		Mineralogic and petrographic composition	Limestones (intrasparite, grainstone-packstone; intramicrite, mudstone-wackestone), ceramic fragments, marble, quartz, quartzite, k-feldspar, chert.																							
Classification of the aggregate			Fluvial sand and artificially crushed bricks (cocciopesto)																								
OPEN POROSITY %	33.80		COMPRESSIVE STRENGTH	4.50 MPa																							
GRANULOMETRIC CURVE	<table border="1"> <caption>Granulometric Curve Data (Estimated)</caption> <thead> <tr> <th>Sieves diameter (mm)</th> <th>Passing percentage (%)</th> </tr> </thead> <tbody> <tr><td>0.0</td><td>0</td></tr> <tr><td>0.2</td><td>10</td></tr> <tr><td>0.5</td><td>20</td></tr> <tr><td>1.0</td><td>35</td></tr> <tr><td>2.5</td><td>55</td></tr> <tr><td>4.0</td><td>70</td></tr> <tr><td>8.0</td><td>85</td></tr> <tr><td>16.0</td><td>95</td></tr> <tr><td>31.5</td><td>100</td></tr> </tbody> </table>							Sieves diameter (mm)	Passing percentage (%)	0.0	0	0.2	10	0.5	20	1.0	35	2.5	55	4.0	70	8.0	85	16.0	95	31.5	100
	Sieves diameter (mm)	Passing percentage (%)																									
0.0	0																										
0.2	10																										
0.5	20																										
1.0	35																										
2.5	55																										
4.0	70																										
8.0	85																										
16.0	95																										
31.5	100																										
CHEMICAL ANALYSES																											
Total cations content % w.t.	Na ₂ O	K ₂ O	CaO	MgO	Fe ₂ O ₃	Al ₂ O ₃	SiO ₂																				
	2.08	1.42	20.85	6.95	3.00	7.03	31.41																				
Cations soluble in HCl 0.1 N % w.t.	Na ₂ O	K ₂ O	CaO	MgO	Fe ₂ O ₃	Al ₂ O ₃	SiO ₂																				
	0.03	0.07	16.37	4.54	0.55	1.62	2.28																				
Water soluble salts % w.t.	Cl ⁻	NO ₃ ⁻	SO ₄ ²⁻	Loss on Ignition %			27.27																				
	<0.01	<0.01	<0.01																								
Py-GC-MS spectrum	ND																										

– *Mosaic of the House of Eubulus*

The pavement investigated is located in the *atrium* of a house that belonged to a man called *Eubulus*, as we know from the stamps on its lead water pipes [Pan97], and occupied the northwest corner of the forum (Figure 9). The *atrium* is in central position within the house, next to a large room where a fountain was placed [Pan97] (Figure 20). The actual pavement of the *atrium* misses completely the *tessellatum*, while its substrate is preserved (Figure 21).



Figure 20 View of the House of *Eubulus* from its northwest corner. It is visible the central *atrium* and, behind it, the large room that contained a fountain.



Figure 21 View of the *atrium* from its northeast corner.

The *in situ* analyses and sampling have been carried out at the edge of the northeast corner of the *atrium*, next to its entrance (Figure 22). Here, after the removal of a superficial layer of loose gravel, a fragment of the whole substrate, composed of one single mortar layer, has been collected (Figure 23). As for the mosaic of the *House of Epigenes*, described in the previous paragraph, the *in situ* investigation revealed that the mosaic of the *House of Eubulus* was probably built upon artificial backfilled ground. In fact, also in this case the ground below the mosaic's substrate contains brick fragments and lime grains referable to older structures.



Figure 22 View from east of the north corridor of the *atrium*. In the low right corner of the picture the entrance to the room is visible. The red arrow indicates the sampling point of the substrate.



Figure 23 The mortar sample collected from the substrate of the pavement of the *atrium* of the House of Eubulus. The sample consists of a fragment including the whole thickness of the substrate.

In Figure 24, a schematic graphic reproduction of the mosaic's substrate with the indication of the sampled layer and the correspondent sample code is showed.

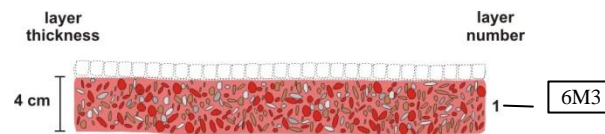


Figure 24 Ancient city of Dion, schematic graphic reproduction of the stratigraphy of the mosaic of the *atrium* of the House of Eubulus with the indication of the sampled layer and the correspondent sample code.

In Table 6, the results of the laboratory analyses on the mortar of the studied substrate are summarized.

Table 6 Ancient city of Dion, mosaic of the *House of Eubulus*: results of laboratory analyses on mortar layer n. 1.

Sample: 6M3		CHARACTERIZATION FORM					
OPTICAL MICROSCOPY (Figure 88, Figure 89 in Appendix)							
Stratigraphy	Layer 1	Munsell colour	Pinkish white 5YR8/2				
Microscopic description of the binder on thin section							
Structure	Homogeneous	Reaction with the aggregate	Reaction rims around ceramic fragments				
Texture	Micritic	Shape of pores	From sub-circular to irregular				
Microscopic description of the aggregate on thin section							
Granulometry	Maximum size: 6 mm Most abundant sizes: 4-2, 2-1 mm		Roundness	From angular to very rounded			
Sorting	Poorly sorted $\sigma = 2.00 \text{ } \emptyset$		Distribution	Homogeneous			
Shape	Part natural, part due to artificial crushing		Orientation	Oriented sub-parallel to layer surface			
Sphericity	From high to low		Mineralogic and petrographic composition	Limestones (intramicrite, mudstone-wackestone; intrasparrite, grainstone-packstone-wackestone), ceramic fragments, quartz, k-feldspar, plagioclase, marble, quartzite.			
Classification of the aggregate			Fluvial sand and artificially crushed bricks (cocciopesto)				
OPEN POROSITY %	38.26		COMPRESSIVE STRENGTH	2.96 MPa			
GRANULOMETRIC CURVE							
CHEMICAL ANALYSES							
Total cations content % w.t.	Na ₂ O	K ₂ O	CaO	MgO	Fe ₂ O ₃	Al ₂ O ₃	SiO ₂
	1.51	1.23	18.75	7.46	3.35	6.99	18.68
Cations soluble in HCl 0.1 N % w.t.	Na ₂ O	K ₂ O	CaO	MgO	Fe ₂ O ₃	Al ₂ O ₃	SiO ₂
	0.04	0.09	18.33	5.80	0.65	1.61	2.72
Water soluble salts % w.t.	Cl ⁻	NO ₃ ⁻	SO ₄ ²⁻	Loss on Ignition %			42.03
	<0.01	-	<0.01				
Py-GC-MS spectrum	ND						

– *Mosaic of the Polygon*

At the junction of the central avenue with the road that leads to the west gate (Figure 9) there stood the Polygon, a building square on the outside and organized around a twelve-sided courtyard (Figure 25). The building, which should date to the 3rd century A.D., was probably used as a market hall [Geo08]. The studied mosaic is located in a room having irregular shape, occupying the southwest corner of the building (Figure 25, Figure 26), which served as *Vespasian* (lavatories) [Geo08]. The mosaic still preserves the *tessellatum*, which is made of stone *tesserae* with average size of 2.5 cm.



Figure 25 View of the *Polygon* from its southwest corner, where the room containing the studied mosaic is located.



Figure 26 View of the room from its northwest corner, the studied mosaic is covered by a temporarily protection.

The area of the mosaic, which is located in central position within the room, is significantly smaller than that of the room floor. The *in situ* analyses and the sampling have been performed on the northwest corner of the pavement, in an area where a small lacuna uncovers the substrate. The sampling point is showed in Figure 27.

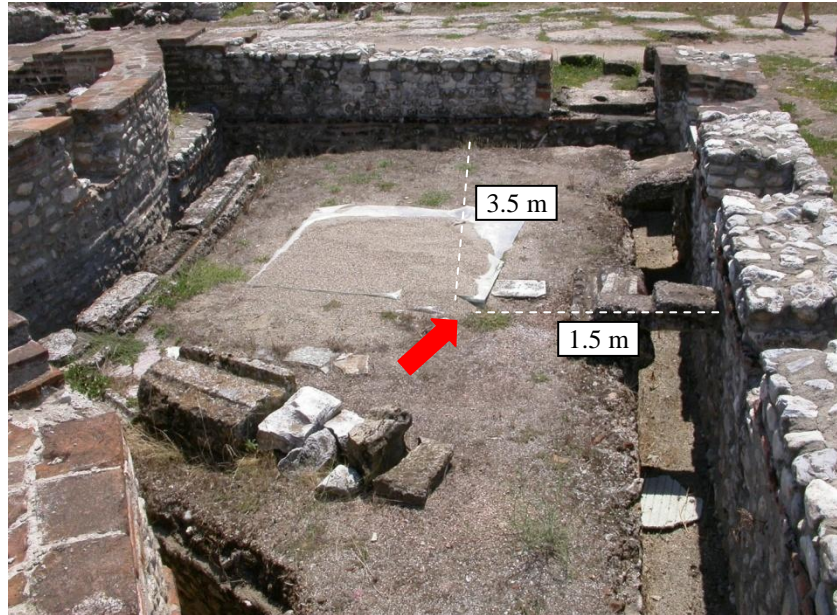


Figure 27 The position of the sampling point on the studied pavement.

As visible in Figure 26 and Figure 27 the mosaic of the *Polygon* was built upon a structure elevated above the ground, composed of an outer wall made of bricks and stones that is delimitating an internal area backfilled with artificial ground. The mosaic substrate, laid upon this structure, is composed of three preparatory layers of mortar (Figure 28).



Figure 28 Cross section of the mosaic's substrate with the indication of the different mortar layers.

The adhesion between the mortar layers is very good. In Figure 29, a schematic graphic reproduction of the mosaic's substrate with the indication of the sampled layers and the correspondent sample codes is showed.

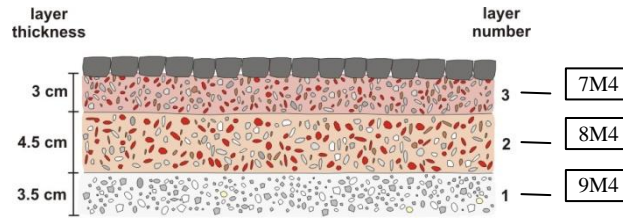


Figure 29 Ancient city of Dion, schematic graphic reproduction of the stratigraphy of the mosaic of the Polygon with the indication of the sampled layers and the correspondent sample codes.

In Table 7, Table 8, and Table 9, the results of the laboratory analyses on the mortars of the 1st, 2nd and 3rd layer of the studied substrate are summarized.

Table 7 Ancient city of Dion, mosaic of the *Polygon*: results of the laboratory analyses on the mortar layer n. 1.

Sample: 9M4		CHARACTERIZATION FORM																											
OPTICAL MICROSCOPY (Figure 90, Figure 91 in Appendix)																													
Stratigraphy	Layer 1	Munsell colour	White 2.5Y8/1																										
Microscopic description of the binder on thin section																													
Structure	Homogeneous	Reaction with the aggregate	None visible																										
Texture	Micritic	Shape of pores	From subcircular to irregular																										
Microscopic description of the aggregate on thin section																													
Granulometry	Maximum size: 6 mm Most abundant sizes: 4-2 mm, 2-1 mm		Roundness	From subangular to very rounded																									
Sorting	Poorly sorted $\sigma = 2.00 \text{ } \emptyset$		Distribution	Homogeneous																									
Shape	Natural		Orientation	None																									
Sphericity	Low		Mineralogic and petrographic composition	Limestones (intrasparite, grainstone-packstone; micrite, mudstone), marble, quartz, quartzite.																									
Classification of the aggregate			Fluvial sand and gravel																										
OPEN POROSITY %	22.45		COMPRESSIVE STRENGTH	ND																									
GRANULOMETRIC CURVE	<table border="1" style="display: none;"> <caption>Granulometric Curve Data</caption> <thead> <tr> <th>Sieves diameter (mm)</th> <th>Passing percentage (%)</th> </tr> </thead> <tbody> <tr><td>0.075</td><td>0</td></tr> <tr><td>0.15</td><td>0</td></tr> <tr><td>0.3</td><td>0</td></tr> <tr><td>0.6</td><td>5</td></tr> <tr><td>1.2</td><td>20</td></tr> <tr><td>2.5</td><td>50</td></tr> <tr><td>5</td><td>80</td></tr> <tr><td>10</td><td>95</td></tr> <tr><td>20</td><td>100</td></tr> <tr><td>40</td><td>100</td></tr> </tbody> </table>							Sieves diameter (mm)	Passing percentage (%)	0.075	0	0.15	0	0.3	0	0.6	5	1.2	20	2.5	50	5	80	10	95	20	100	40	100
	Sieves diameter (mm)	Passing percentage (%)																											
0.075	0																												
0.15	0																												
0.3	0																												
0.6	5																												
1.2	20																												
2.5	50																												
5	80																												
10	95																												
20	100																												
40	100																												
CHEMICAL ANALYSES																													
Total cations content % w.t.	Na ₂ O	K ₂ O	CaO	MgO	Fe ₂ O ₃	Al ₂ O ₃	SiO ₂																						
	2.64	0.12	39.46	6.90	0.41	1.40	14.08																						
Cations soluble in HCl 0.1 N % w.t.	Na ₂ O	K ₂ O	CaO	MgO	Fe ₂ O ₃	Al ₂ O ₃	SiO ₂																						
	0.02	0.01	38.76	6.42	0.10	0.45	0.41																						
Water soluble salts % w.t.	Cl ⁻	NO ₃ ⁻	SO ₄ ²⁻	Loss on Ignition %			35.00																						
	<0.01	<0.01	<0.01																										
Py-GC-MS spectrum	ND																												

Table 8 Ancient city of Dion, mosaic of the *Polygon*: results of the laboratory analyses on the mortar layer n. 2.

Sample: 8M4		CHARACTERIZATION FORM					
OPTICAL MICROSCOPY (Figure 92, Figure 93 in Appendix)							
Stratigraphy	Layer 2	Munsell colour	White 10YR8/1				
Microscopic description of the binder on thin section							
Structure	Homogeneous	Reaction with the aggregate	Reaction rims around ceramic fragments				
Texture	Micritic	Shape of pores	Mostly subcircular				
Microscopic description of the aggregate on thin section							
Granulometry	Maximum size: 8 mm Most abundant sizes: 4-2 mm, 2-1 mm		Roundness	From subangular to very rounded			
Sorting	Poorly sorted $\sigma = 2.00 \text{ } \emptyset$		Distribution	Homogeneous			
Shape	Part natural, part due to artificial crushing		Orientation	None			
Sphericity	Low		Mineralogic and petrographic composition	Limestones (micrite, mudstone; dismicrite, mudstone; intrasparite, grainstone-packstone), ceramic fragments, marble, quartz, k-feldspar, micaschist, quartzite.			
Classification of the aggregate			Fluvial sand and artificially crushed bricks (cocciopesto)				
OPEN POROSITY %	31.43		COMPRESSIVE STRENGTH			3.41 MPa	
GRANULOMETRIC CURVE							
CHEMICAL ANALYSES							
Total cations content % w.t.	Na ₂ O	K ₂ O	CaO	MgO	Fe ₂ O ₃	Al ₂ O ₃	SiO ₂
	1.16	0.70	29.80	6.40	1.80	3.70	32.82
Cations soluble in HCl 0.1 N % w.t.	Na ₂ O	K ₂ O	CaO	MgO	Fe ₂ O ₃	Al ₂ O ₃	SiO ₂
	0.02	0.04	28.68	5.51	0.49	1.17	1.38
Water soluble salts % w.t.	Cl ⁻	NO ₃ ⁻	SO ₄ ²⁻	Loss on Ignition %			23.61
	0.01	<0.01	0.01				
Py-GC-MS spectrum	ND						

Table 9 Ancient city of Dion, mosaic of the *Polygon*: results of the laboratory analyses on the mortar layer n. 3.

Sample: 7M4		CHARACTERIZATION FORM					
OPTICAL MICROSCOPY (Figure 94, Figure 95 in Appendix)							
Stratigraphy	Layer 3	Munsell colour	Pinkish white 7.5YR8/2				
Microscopic description of the binder on thin section							
Structure	Homogeneous	Reaction with the aggregate	Reaction rims around ceramic fragments				
Texture	Micritic	Shape of pores	From subcircular to irregular				
Microscopic description of the aggregate on thin section							
Granulometry	Maximum size: 4 mm Most abundant sizes: 2-1 mm, 1-0.5 mm		Roundness	From subangular to very rounded			
Sorting	Moderately sorted $\sigma = 1.00 \text{ } \emptyset$		Distribution	Homogeneous			
Shape	Part natural, part due to artificial crushing		Orientation	Oriented sub-parallel to layer surface			
Sphericity	From high to low		Mineralogic and petrographic composition	Ceramic fragments, limestones (micrite, mudstone; dismicrite, mudstone; intrasparite, grainstone-packstone), marbles, quartz, quartzite, vulcanite.			
Classification of the aggregate			Fluvial sand and artificially crushed bricks (cocciopesto)				
OPEN POROSITY %	50.18		COMPRESSIVE STRENGTH	3.32 MPa			
GRANULOMETRIC CURVE							
CHEMICAL ANALYSES							
Total cations content % w.t.	Na ₂ O	K ₂ O	CaO	MgO	Fe ₂ O ₃	Al ₂ O ₃	SiO ₂
	1.21	0.99	21.55	6.93	3.69	7.29	16.09
Cations soluble in HCl 0.1 N % w.t.	Na ₂ O	K ₂ O	CaO	MgO	Fe ₂ O ₃	Al ₂ O ₃	SiO ₂
	0.03	0.07	20.43	5.31	0.81	2.14	2.56
Water soluble salts % w.t.	Cl ⁻	NO ₃ ⁻	SO ₄ ²⁻	Loss on Ignition %			42.25
	<0.01	<0.01	<0.01				
Py-GC-MS spectrum	ND						

– *Mosaic of the Villa of Dyonisos*

The last studied mosaic from the ancient city of Dion is located in the Villa of Dyonisos (Figure 9). This Villa, which dates from the second half of the 2nd century A.D., consists of a complex of buildings, with a row of shops, the residence rooms, a banquet room, a cult area, the *atria*, a library and the a bathhouse [Pan97]. The mosaic investigated covered the floor of a small room in the bathhouse, at the south side of the Villa (Figure 30, Figure 31). The mosaic misses almost completely the *tessellatum* which was made of stone *tesserae* with average size of 2.5 cm.

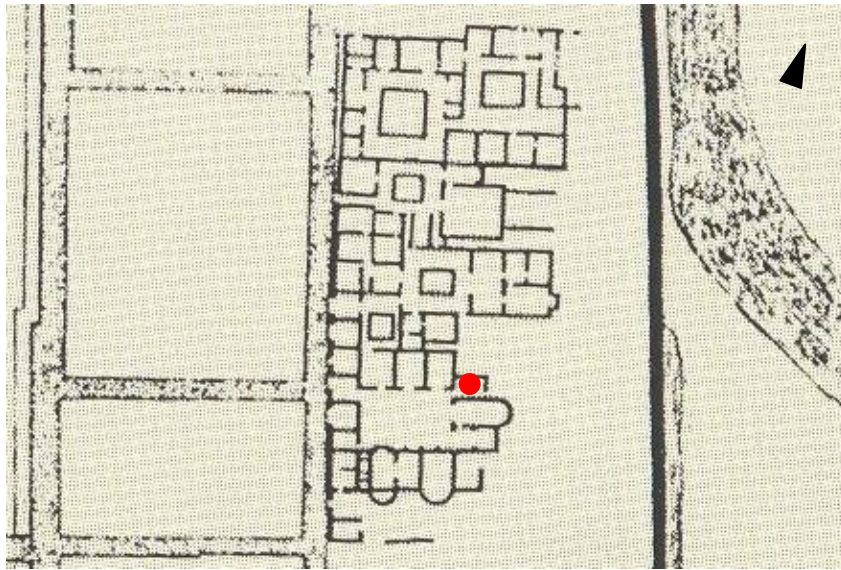


Figure 30 Plan of the Villa of Dyonisos. The red dot indicates the room in the bathhouse whose floor was covered by the studied mosaic.



Figure 31 View of part of the bathhouse from east. In the low right corner of the picture, the room with the studied pavement is visible.

The *in situ* analyses and sampling have been carried out in two areas of the pavement where cross sections of the whole substrate were visible due to the presence of deep fractures caused by a strong downward deformation of the mosaic (Figure 32). The substrate is composed of three mortar layers (Figure 33). The layers mutual adhesion is very good.

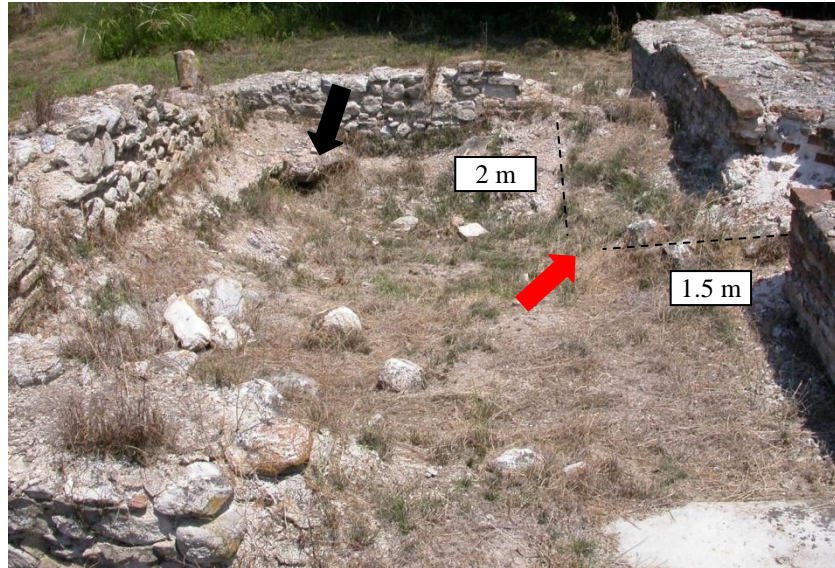


Figure 32 View of the room from west with the position of the points where the *in situ* investigations have been carried out. The sampling point is indicated by the red arrow.

The *in situ* investigation revealed that the studied mosaic was built on top of a structure made of large ceramic tiles each one about 5 cm thick (Figure 34), probably the so called *pilae* tiles that were used in Roman times as an element of the under floor heating system of baths, called the hypocaust. As it is known, this system consisted in constructing the floor at an elevated position above pillars (*pilae* stacks), in order to allow the hot air to freely circulate underneath the pavement and heat the room [Alb65] (Figure 50).

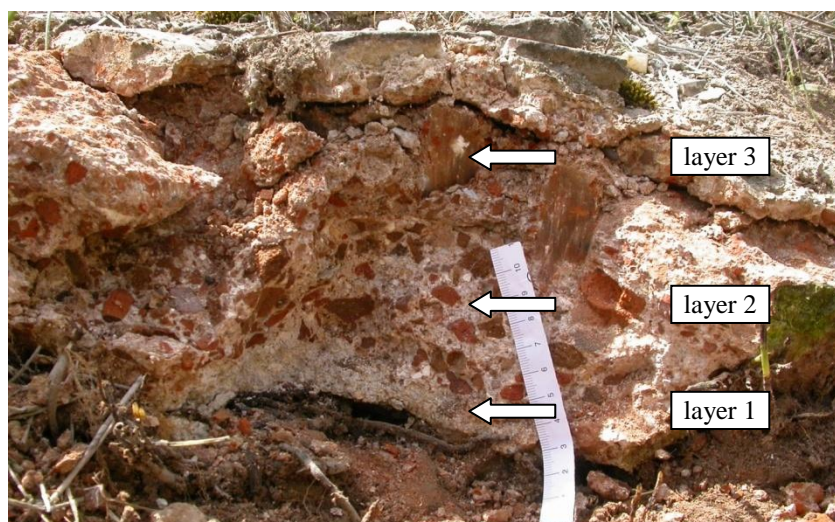


Figure 33 Cross section of the mosaic's substrate with the indication of the different mortar layers.

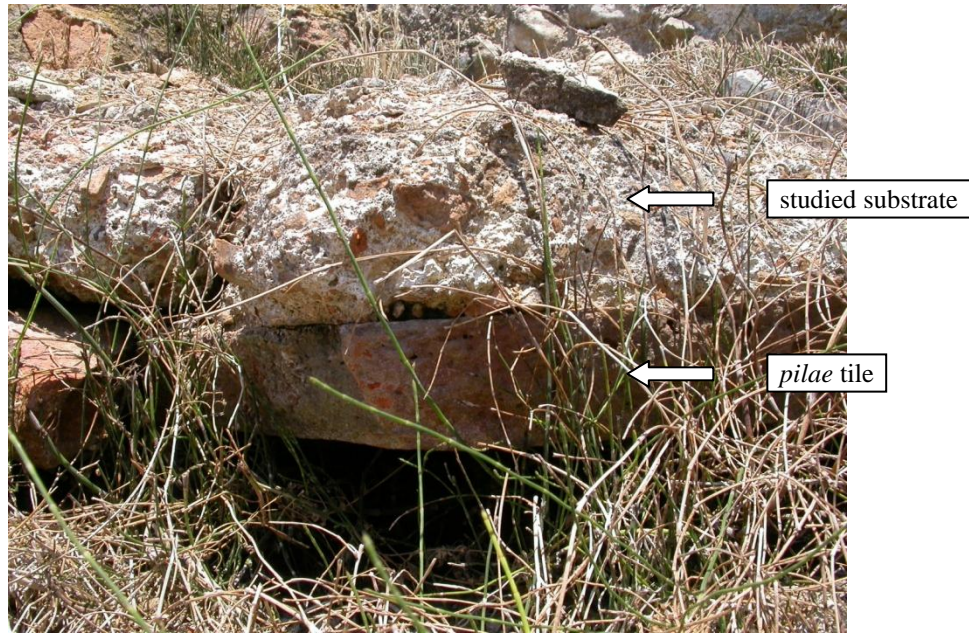


Figure 34 Southwest corner of the room (see black arrow in Figure 32): the studied pavement and the underlying raised structure made of large ceramic tiles.

In Figure 35, a schematic graphic reproduction of the studied mosaic's substrate with the indication of the sampled layers and the correspondent sample codes is showed.

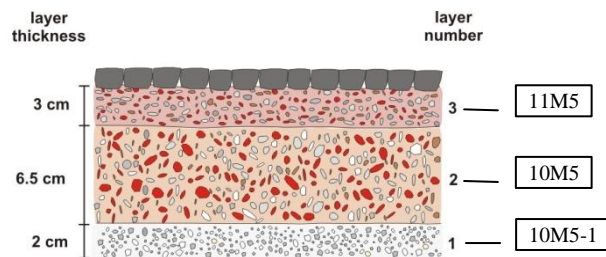


Figure 35 Ancient city of Dion, schematic graphic reproduction of the stratigraphy of the mosaic of the bathhouse of Villa Dyonisos with the indication of the sampled layers and the correspondent sample codes.

In Table 10, Table 11 and Table 12, the results of the laboratory analyses on the mortars of the 1st, 2nd and 3rd layer of the studied substrate are summarized.

Table 10 Ancient city of Dion, mosaic of the *Villa of Dyonisos*: results of the laboratory analyses on the mortar layer n. 1.

Sample: 10M5-1		CHARACTERIZATION FORM					
OPTICAL MICROSCOPY (Figure 96, Figure 97 in Appendix)							
Stratigraphy	Layer 1	Munsell colour		White 10YR8/1			
Microscopic description of the binder on thin section							
Structure	Homogeneous	Reaction with the aggregate		None visible			
Texture	Micritic	Shape of pores		From subcircular to irregular			
Microscopic description of the aggregate on thin section							
Granulometry	Maximum size: 4 mm Most abundant sizes: 4-2 mm, 2-1 mm			Roundness		From subangular to rounded	
Sorting	Poorly sorted $\sigma = 2.00 \text{ } \emptyset$			Distribution		Homogeneous	
Shape	Natural			Orientation		None	
Sphericity	From high to low			Mineralogic and petrographic composition		Limestones (micrite, mudstone; dismicrite, mudstone; intrasparite, grainstone-packstone), marble.	
Classification of the aggregate				Fluvial sand and gravel			
OPEN POROSITY %	ND			COMPRESSIVE STRENGTH		ND	
GRANULOMETRIC CURVE	ND						
CHEMICAL ANALYSES							
Total cations content % w.t.	Na ₂ O	K ₂ O	CaO	MgO	Fe ₂ O ₃	Al ₂ O ₃	SiO ₂
	0.37	0.16	46.03	4.94	0.72	1.13	9.51
Cations soluble in HCl 0.1 N % w.t.	Na ₂ O	K ₂ O	CaO	MgO	Fe ₂ O ₃	Al ₂ O ₃	SiO ₂
	0.04	0.02	41.84	4.46	0.43	0.66	1.49
Water soluble salts % w.t.	Cl ⁻	NO ₃ ⁻	SO ₄ ²⁻	Loss on Ignition %			37.14
	0.12	<0.01	0.02				
Py-GC-MS spectrum	ND						

Table 11 Ancient city of Dion, mosaic of the *Villa of Dyonisos*: results of the laboratory analyses on the mortar layer n. 2.

Sample: 10M5		CHARACTERIZATION FORM					
OPTICAL MICROSCOPY (Figure 98, Figure 99 in Appendix)							
Stratigraphy	Layer 2	Munsell colour	Very pale brown 10YR8/2				
Microscopic description of the binder on thin section							
Structure	Homogeneous	Reaction with the aggregate	Reaction rims around ceramic fragments				
Texture	Micritic	Shape of pores	Irregular				
Microscopic description of the aggregate on thin section							
Granulometry	Maximum size: 12 mm Most abundant sizes: 4-2 mm, 2-1 mm		Roundness	From subangular to rounded			
Sorting	Poorly sorted $\sigma = 2.00 \text{ } \varnothing$		Distribution	Homogeneous			
Shape	Part natural, part due to artificial crushing		Orientation	None			
Sphericity	Low		Mineralogic and petrographic composition	Limestones (micrite, mudstone; dismicrite, mudstone; intrasparite, grainstone-packstone), ceramic fragments, marble, micaschist, quartzite.			
Classification of the aggregate			Fluvial sand and artificially crushed bricks (cocciopesto)				
OPEN POROSITY %	34.02		COMPRESSIVE STRENGTH			8.00 MPa	
GRANULOMETRIC CURVE							
CHEMICAL ANALYSES							
Total cations content % w.t.	Na ₂ O	K ₂ O	CaO	MgO	Fe ₂ O ₃	Al ₂ O ₃	SiO ₂
	1.08	0.72	20.29	8.54	2.89	5.33	25.73
Cations soluble in HCl 0.1 N % w.t.	Na ₂ O	K ₂ O	CaO	MgO	Fe ₂ O ₃	Al ₂ O ₃	SiO ₂
	0.03	0.06	20.13	7.78	1.02	2.02	3.28
Water soluble salts % w.t.	Cl ⁻	NO ₃ ⁻	SO ₄ ²⁻	Loss on Ignition %			35.42
	0.04	0.01	0.03				
Py-GC-MS spectrum	ND						

Table 12 Ancient city of Dion, mosaic of the *Villa of Dyonisos*: results of the laboratory analyses on the mortar layer n. 3.

Sample: 11M5		CHARACTERIZATION FORM					
OPTICAL MICROSCOPY (Figure 100, Figure 101 in Appendix)							
Stratigraphy	Layer 3	Munsell colour	White 7.5YR8/1				
Microscopic description of the binder on thin section							
Structure	Homogeneous	Reaction with the aggregate	Reaction rims around ceramic fragments				
Texture	Micritic	Shape of pores	From sub-circular to irregular				
Microscopic description of the aggregate on thin section							
Granulometry	Maximum size: 5 mm Most abundant sizes: 4-2 mm, 2-1 mm		Roundness	From angular to rounded			
Sorting	Poorly sorted $\sigma = 2.00 \text{ } \varnothing$		Distribution	Homogeneous			
Shape	Part natural, part due to artificial crushing		Orientation	None			
Sphericity	From high to low		Mineralogic and petrographic composition	Ceramic fragments, limestones (micrite, mudstone; dismicrite, mudstone; intrasparite, grainstone-packstone), marble, quartz, k-feldspar, quartzite.			
Classification of the aggregate			Fluvial sand and artificially crushed bricks (cocciopesto)				
OPEN POROSITY %	31.89		COMPRESSIVE STRENGTH			7.72 MPa	
GRANULOMETRIC CURVE							
CHEMICAL ANALYSES							
Total cations content % w.t.	Na ₂ O	K ₂ O	CaO	MgO	Fe ₂ O ₃	Al ₂ O ₃	SiO ₂
	1.54	1.30	17.07	4.63	4.03	7.44	37.80
Cations soluble in HCl 0.1 N % w.t.	Na ₂ O	K ₂ O	CaO	MgO	Fe ₂ O ₃	Al ₂ O ₃	SiO ₂
	0.03	0.09	15.11	3.45	1.02	1.68	1.88
Water soluble salts % w.t.	Cl ⁻	NO ₃ ⁻	SO ₄ ²⁻	Loss on Ignition %			26.19
	<0.01	<0.01	0.01				
Py-GC-MS spectrum	ND						

5.1.2. The “Villa Romana delle Muracche” in Tortoreto

Two mosaics covering the floor of two adjacent rooms within the *pars urbana* (see paragraph 3.3.2) of the *Villa delle Muracche* (1st century B.C.) in Tortoreto have been investigated (Figure 36, Figure 37). In Figure 36, a plan of the Villa [Lap96] with the location of the studied mosaics is showed.

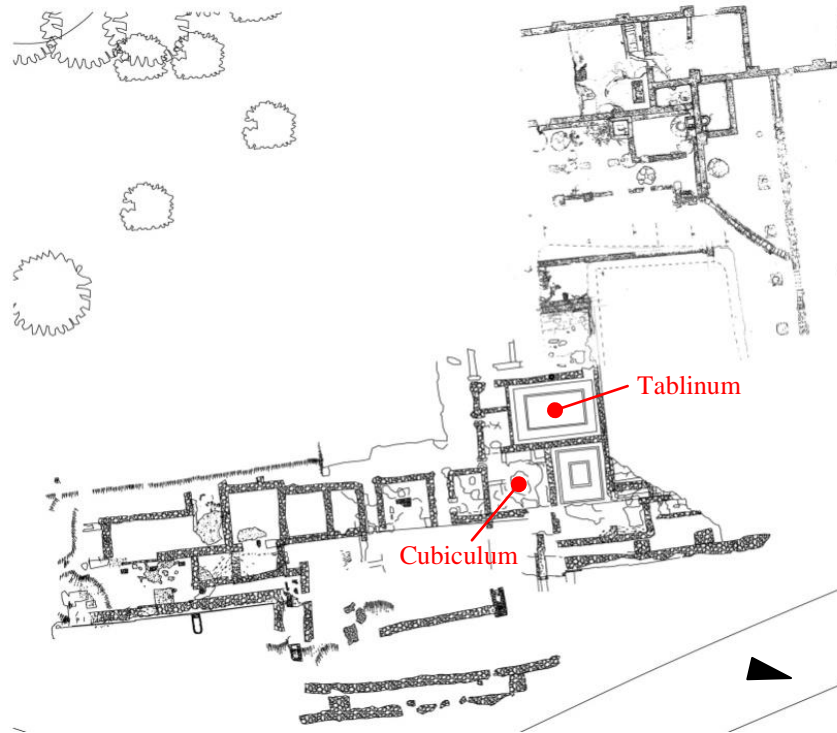


Figure 36 Plan of the Villa delle Muracche with the location of the rooms where the studied mosaics are placed. From Lapenna [Lap96], modified.

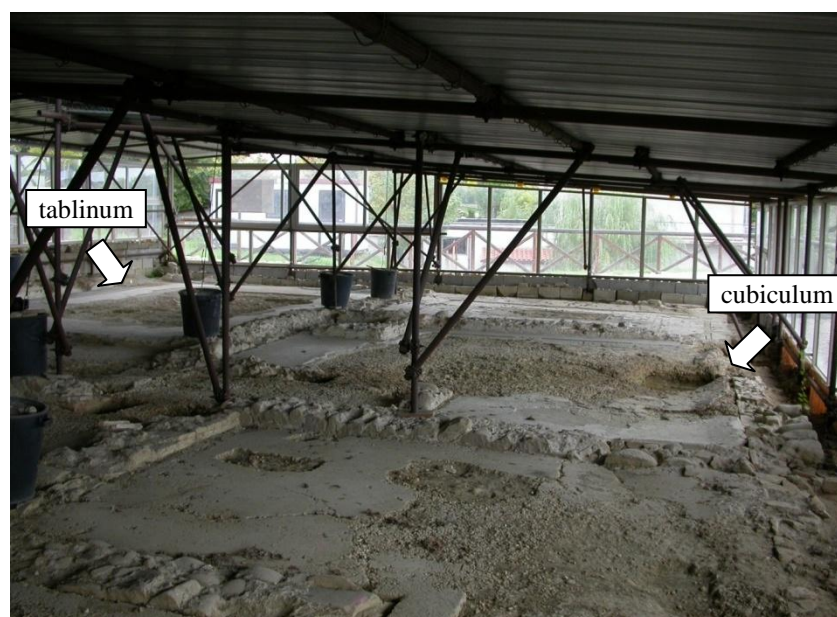


Figure 37 View from southeast of the area of the *Villa* where the studied mosaics are located.

– *Mosaic of the Cubiculum*

The studied mosaic is located in a room that served as bedroom (*cubiculum*) located on the east side of the Villa (Figure 36, Figure 37). The mosaic shows wide *lacunae* of both the *tessellatum* and the substrate. In the sampled area the *tessellatum* is made of stone *tesserae* with average size of about 1 cm. The *in situ* analyses and the sampling have been carried out on an area of the pavement where a large cavity uncovered the foundation layers (Figure 38).



Figure 38 The position of the sampling point on the pavement of the *cubiculum*.

The *in situ* investigation indicated that the mosaic of the *cubiculum* was built upon natural levelled ground. The mosaic's substrate is made of four mortar layers characterized by a good mutual adhesion (Figure 39).

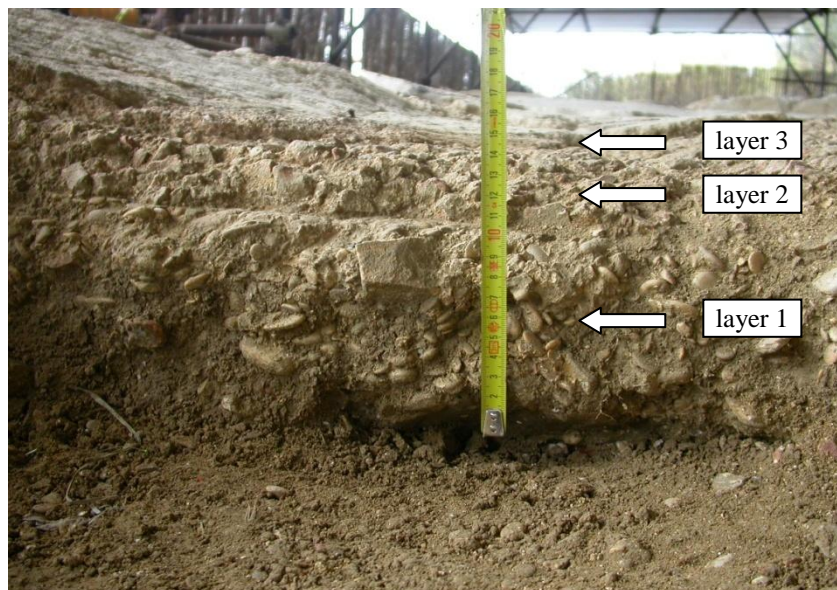


Figure 39 Cross section of the mosaic's substrate with the indication of the first three mortar layers.

In Figure 40, a schematic graphic reproduction of the stratigraphy of the mosaic's substrate with the indication of the layers thickness and of the sampled layers with the correspondent sample codes is showed.

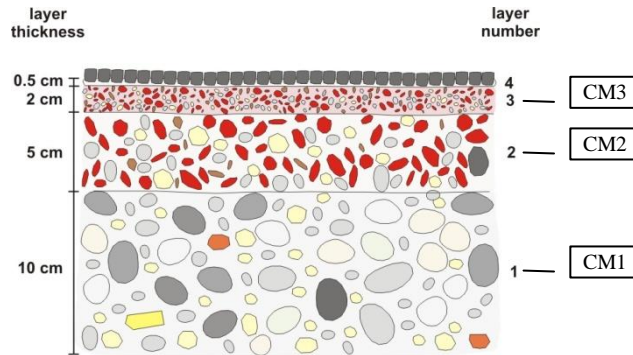


Figure 40 “Villa Romana delle Muracche”, schematic graphic reproduction of the stratigraphy of the mosaic of the *cubiculum* with the indication of the sampled mortar layers and the correspondent sample codes.

In Table 13, Table 14 and Table 15, the results of the laboratory analyses on the mortars of the 1st, 2nd and 3rd layer of the studied substrate are summarized.

Table 13 “Villa Romana delle Muracche”, mosaic of the *Cubiculum*: results of the laboratory analyses on the mortar layer n. 1.

Sample: CM1		CHARACTERIZATION FORM					
OPTICAL MICROSCOPY (Figure 102, Figure 103 in Appendix)							
Stratigraphy	Layer 1	Munsell colour		White 10YR8/1			
Microscopic description of the binder on thin section							
Structure	Homogeneous	Reaction with the aggregate		None visible			
Texture	Micritic	Shape of pores		Irregular			
Microscopic description of the aggregate on thin section							
Granulometry	Maximum size: 7 mm Most abundant sizes: 4-2 mm			Roundness	From angular to very rounded		
Sorting	Poorly sorted $\sigma = 2.00 \text{ } \emptyset$			Distribution	Homogeneous		
Shape	Part natural, part due to artificial crushing			Orientation	None		
Sphericity	Low			Mineralogic and petrographic composition	Limestones (biosparite, grainstone; biomicrite, mudstone-wackestone), ceramic fragments, quartz, k-feldspar, plagioclase, muscovite, biotite, shells.		
Classification of the aggregate				Fluvial sand and gravel and artificially crushed bricks.			
OPEN POROSITY %	31.89			COMPRESSIVE STRENGTH		ND	
GRANULOMETRIC CURVE	ND						
CHEMICAL ANALYSES							
Total cations content % w.t.	Na ₂ O	K ₂ O	CaO	MgO	Fe ₂ O ₃	Al ₂ O ₃	SiO ₂
	0.70	1.06	25.19	1.89	1.52	5.44	32.21
Cations soluble in HCl 0.1 N % w.t.	Na ₂ O	K ₂ O	CaO	MgO	Fe ₂ O ₃	Al ₂ O ₃	SiO ₂
	0.08	0.10	23.79	1.18	0.57	1.36	1.57
Water soluble salts % w.t.	Cl ⁻	NO ₃ ⁻	SO ₄ ²⁻	Loss on Ignition %			32.00
	0.03	0.02	0.03				
Py-GC-MS spectrum	ND						

Table 14 “Villa Romana delle Muracche”, mosaic of the *Cubiculum*: results of the laboratory analyses on the mortar layer n. 2.

Sample: CM2		CHARACTERIZATION FORM					
OPTICAL MICROSCOPY (Figure 104, Figure 105 in Appendix)							
Stratigraphy	Layer 2	Munsell colour		White 2.5YR8/1			
Microscopic description of the binder on thin section							
Structure	Homogeneous	Reaction with the aggregate		Reaction rims around ceramic fragments			
Texture	Micritic	Shape of pores		Irregular			
Microscopic description of the aggregate on thin section							
Granulometry	Maximum size: 9 mm Most abundant sizes: 8-4 mm, 4-2 mm		Roundness		From angular to rounded		
Sorting	Moderately sorted $\sigma = 1.00 \text{ } \emptyset$		Distribution		Homogeneous		
Shape	Part natural, part due to artificial crushing		Orientation		None		
Sphericity	Low		Mineralogic and petrographic composition		Mostly ceramic fragments, in less quantity quartz, k-feldspar, plagioclase, limestones (biomicrite, mudstone; biosparite, grainstone), chert, marble.		
Classification of the aggregate			Artificially crushed bricks (cocciopesto) and fluvial sand.				
OPEN POROSITY %	38.97		COMPRESSIVE STRENGTH		ND		
GRANULOMETRIC CURVE	ND						
CHEMICAL ANALYSES							
Total cations content % w.t.	Na ₂ O	K ₂ O	CaO	MgO	Fe ₂ O ₃	Al ₂ O ₃	SiO ₂
	0.46	0.82	26.58	1.77	0.92	4.84	29.61
Cations soluble in HCl 0.1 N % w.t.	Na ₂ O	K ₂ O	CaO	MgO	Fe ₂ O ₃	Al ₂ O ₃	SiO ₂
	0.10	0.13	25.56	1.33	0.48	1.53	2.37
Water soluble salts % w.t.	Cl ⁻	NO ₃ ⁻	SO ₄ ²⁻	Loss on Ignition %			35.00
	0.03	0.01	0.03				
Py-GC-MS spectrum	ND						

Table 15 “Villa Romana delle Muracche”, mosaic of the *Cubiculum*: results of the laboratory analyses on the mortar layer n. 3.

Sample: CM3		CHARACTERIZATION FORM					
OPTICAL MICROSCOPY (Figure 106, Figure 107 in Appendix)							
Stratigraphy	Layer 3	Munsell colour		Very pale brown 10YR8/2			
Microscopic description of the binder on thin section							
Structure	Homogeneous	Reaction with the aggregate		Reaction rims around ceramic fragments			
Texture	Micritic	Shape of pores		Irregular			
Microscopic description of the aggregate on thin section							
Granulometry	Maximum size: 2 mm Most abundant sizes: 1-0.5 mm	Roundness		From very angular to rounded			
Sorting	Moderately sorted $\sigma = 1.00 \text{ } \emptyset$	Distribution		Homogeneous			
Shape	Part natural, part due to artificial crushing	Orientation		Oriented sub-parallel to layer surface			
Sphericity	Low	Mineralogic and petrographic composition		Ceramic fragments, limestones (biomicrite, mudstone; biosparite, grainstone; intrasparite, packstone), quartz, k- feldspar, plagioclase, chert, quartzite, marble, shell fragments.			
Classification of the aggregate		Artificially crushed bricks (cocciopesto) and fluvial sand.					
OPEN POROSITY %	33.95	COMPRESSIVE STRENGTH		3.05 MPa			
GRANULOMETRIC CURVE	ND						
CHEMICAL ANALYSES							
Total cations content % w.t.	Na ₂ O	K ₂ O	CaO	MgO	Fe ₂ O ₃	Al ₂ O ₃	SiO ₂
	0.59	0.84	25.05	2.22	1.29	5.10	31.91
Cations soluble in HCl 0.1 N % w.t.	Na ₂ O	K ₂ O	CaO	MgO	Fe ₂ O ₃	Al ₂ O ₃	SiO ₂
	0.15	0.13	24.17	1.69	0.59	1.81	2.49
Water soluble salts % w.t.	Cl ⁻	NO ₃ ⁻	SO ₄ ²⁻	Loss on Ignition %			33.00
	0.09	0.06	0.05				
Py-GC-MS spectrum							

– *Mosaic of the Tablinum*

The studied mosaic is placed in a room that served as office (*tablinum*) located west of the *cubiculum* (Figure 36, Figure 37). Also in this case the mosaic shows wide *lacunae* of both the *tessellatum*, which is made of stone tesserae with average size of 1 cm, and the substrate. The *in situ* analyses and sampling have been carried out in two areas of the pavement, in the specific the inner area and the outer frame (Figure 41).

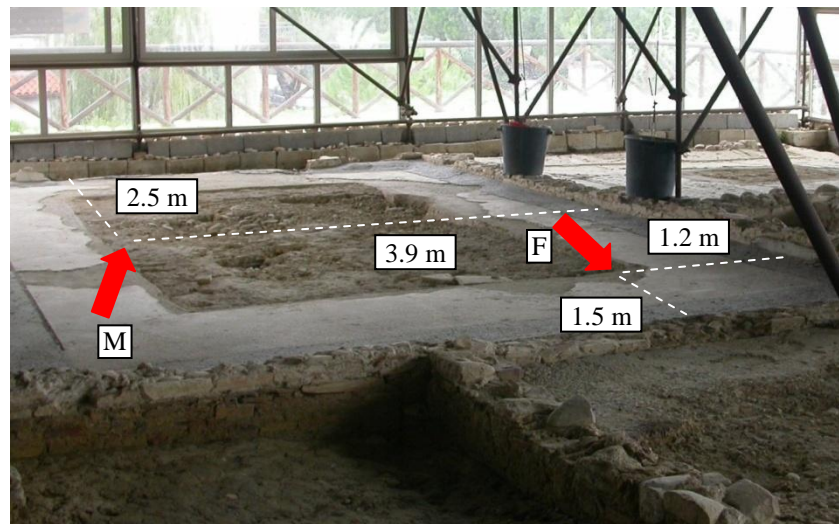


Figure 41 The position of the sampling points in the inner area (M) and in the outer frame (F).

The mosaic was built upon natural levelled ground and its substrate is composed of four preparatory layers of mortar (Figure 42) characterized by good mutual adhesion. The mosaic's substrate below the two studied areas showed some differences in the thickness of the 2nd and 3rd layer (Figure 43).

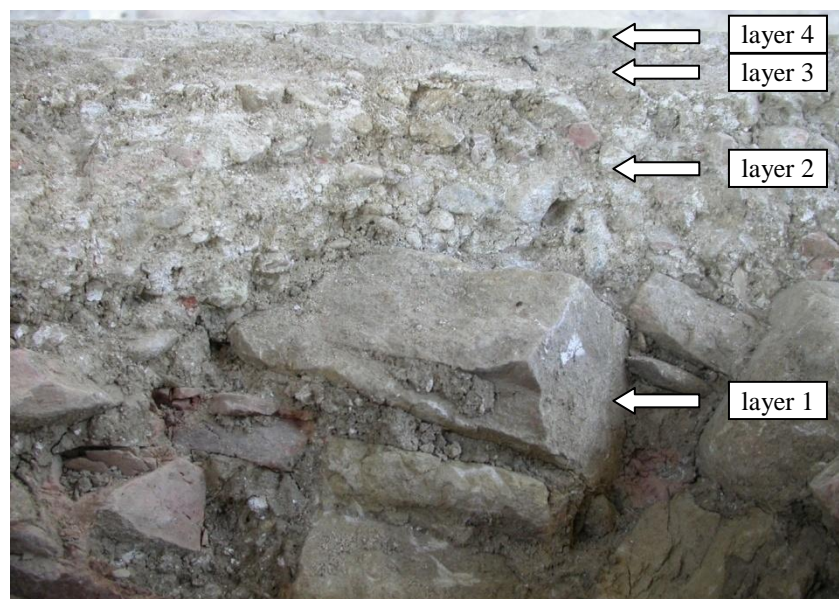


Figure 42 Cross section of the mosaic's substrate below the inner area of the pavement.

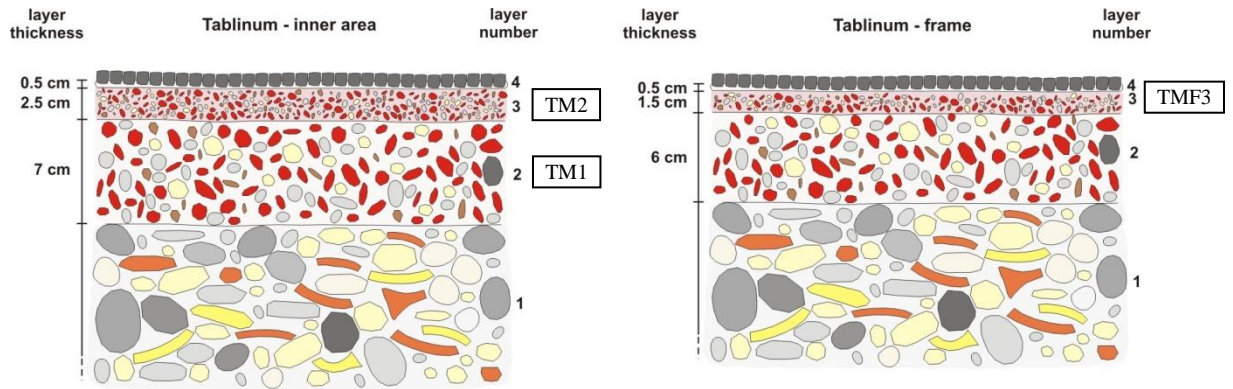


Figure 43 “Villa Romana delle Muracche”, schematic graphic reproduction of the substrate of the mosaic of the *tablinum* below the inner area (left) and the outer frame (right).

In Table 16, Table 17 and Table 18, the results of the laboratory analyses on the mortars of the 2nd and 3rd layer of the substrate in the inner area and of the 3rd layer of the substrate in the outer frame of the pavement are summarized.

Table 16 “Villa Romana delle Muracche”, mosaic of the *Tablinum*, inner area: results of the laboratory analyses on the mortar layer n. 2.

Sample: TM1		CHARACTERIZATION FORM					
OPTICAL MICROSCOPY (Figure 108, Figure 109 in Appendix)							
Stratigraphy	Layer 2	Munsell colour		Very pale brown 10YR8/2			
Microscopic description of the binder on thin section							
Structure	Homogeneous	Reaction with the aggregate		Reaction rims around ceramic fragments			
Texture	Micritic	Shape of pores		Irregular			
Microscopic description of the aggregate on thin section							
Granulometry	Maximum size: 10 mm Most abundant sizes: 8-4 mm, 4-2 mm		Roundness		From angular to rounded		
Sorting	Poorly sorted $\sigma = 2.00 \text{ } \emptyset$		Distribution		Homogeneous		
Shape	Part natural, part due to artificial crushing		Orientation		None		
Sphericity	Low	Mineralogic and petrographic composition		Ceramic fragments, limestones (biomicrite, mudstone and wackestone; intrasparite, packstone) k- feldspar, plagioclase, chert, shell fragments.			
Classification of the aggregate			Artificially crushed bricks (cocciopesto) and fluvial sand.				
OPEN POROSITY %	27.33		COMPRESSIVE STRENGTH			ND	
GRANULOMETRIC CURVE							
CHEMICAL ANALYSES							
Total cations content % w.t.	Na ₂ O	K ₂ O	CaO	MgO	Fe ₂ O ₃	Al ₂ O ₃	SiO ₂
	0.81	0.99	27.56	1.51	1.44	4.23	28.46
Cations soluble in HCl 0.1 N % w.t.	Na ₂ O	K ₂ O	CaO	MgO	Fe ₂ O ₃	Al ₂ O ₃	SiO ₂
	0.31	0.05	29.96	0.96	0.29	0.72	0.43
Water soluble salts % w.t.	Cl ⁻	NO ₃ ⁻	SO ₄ ²⁻	Loss on Ignition %			35.00
	0.22	0.05	0.12				
Py-GC-MS spectrum	ND						

Table 17 “Villa Romana delle Muracche”, mosaic of the *Tablinum*, inner area: results of the laboratory analyses on the mortar layer n. 3.

Sample: TM2		CHARACTERIZATION FORM																											
OPTICAL MICROSCOPY (Figure 110, Figure 111 in Appendix)																													
Stratigraphy	Layer 3	Munsell colour		White 2.5YR8.1																									
Microscopic description of the binder on thin section																													
Structure	Homogeneous	Reaction with the aggregate		Reaction rims around ceramic fragments and chert (rare)																									
Texture	Micritic	Shape of pores		Irregular																									
Microscopic description of the aggregate on thin section																													
Granulometry	Maximum size: 2 mm Most abundant sizes: 1-0.5 mm		Roundness		From very angular to very rounded																								
Sorting	Well sorted $\sigma = 0.50 \varnothing$		Distribution		Homogeneous																								
Shape	Part natural, part due to artificial crushing		Orientation		Oriented sub-parallel to layer surface																								
Sphericity	Low	Mineralogic and petrographic composition		Limestones (biomicrite, mudstone, wackestone and packstone; intrasparite, grainstone; biosparite, packstone), quartz, chert, k- feldspar, plagioclase, ceramic fragments, artificially crushed marbles, quartzite, muscovite, shell fragments.																									
Classification of the aggregate			Fluvial sand, artificially crushed bricks (cocciopesto) and marbles.																										
OPEN POROSITY %	29.90		COMPRESSIVE STRENGTH			0.99 MPa																							
GRANULOMETRIC CURVE		<p>The granulometric curve for Layer 3 shows the following approximate data points:</p> <table border="1"> <thead> <tr> <th>Sieves diameter (mm)</th> <th>Passing percentage (%)</th> </tr> </thead> <tbody> <tr><td>0.075</td><td>0</td></tr> <tr><td>0.15</td><td>5</td></tr> <tr><td>0.3</td><td>15</td></tr> <tr><td>0.6</td><td>35</td></tr> <tr><td>1.2</td><td>65</td></tr> <tr><td>2.5</td><td>90</td></tr> <tr><td>5.0</td><td>95</td></tr> <tr><td>10.0</td><td>98</td></tr> <tr><td>20.0</td><td>99</td></tr> <tr><td>40.0</td><td>100</td></tr> </tbody> </table>						Sieves diameter (mm)	Passing percentage (%)	0.075	0	0.15	5	0.3	15	0.6	35	1.2	65	2.5	90	5.0	95	10.0	98	20.0	99	40.0	100
Sieves diameter (mm)	Passing percentage (%)																												
0.075	0																												
0.15	5																												
0.3	15																												
0.6	35																												
1.2	65																												
2.5	90																												
5.0	95																												
10.0	98																												
20.0	99																												
40.0	100																												
CHEMICAL ANALYSES																													
Total cations content % w.t.	Na ₂ O	K ₂ O	CaO	MgO	Fe ₂ O ₃	Al ₂ O ₃	SiO ₂																						
	0.86	1.08	24.07	1.58	1.97	5.52	32.92																						
Cations soluble in HCl 0.1 N % w.t.	Na ₂ O	K ₂ O	CaO	MgO	Fe ₂ O ₃	Al ₂ O ₃	SiO ₂																						
	0.23	0.06	23.79	1.16	0.44	1.45	0.79																						
Water soluble salts % w.t.	Cl ⁻	NO ₃ ⁻	SO ₄ ²⁻	Loss on Ignition %			32.00																						
	0.07	0.03	0.03																										
Py-GC-MS spectrum	ND																												

Table 18 “Villa Romana delle Muracche”, mosaic of the *Tablinum*, outer frame: results of the laboratory analyses on the mortar layer n. 3.

Sample: TMF3		CHARACTERIZATION FORM					
OPTICAL MICROSCOPY							
Stratigraphy	Layer 3	Munsell colour			White 2.5YR8.1		
Microscopic description of the binder on thin section							
Structure	Homogeneous	Reaction with the aggregate		Reaction rims around ceramic fragments and chert (rare)			
Texture	Micritic	Shape of pores		Irregular			
Microscopic description of the aggregate on thin section							
Granulometry	Maximum size: 2 mm Most abundant sizes: 1-0.5 mm		Roundness		From very angular to very rounded		
Sorting	Well sorted $\sigma = 0.50 \text{ } \emptyset$		Distribution		Homogeneous		
Shape	Part natural, part due to artificial crushing		Orientation		Oriented sub-parallel to layer surface		
Sphericity	Low		Mineralogic and petrographic composition		Limestones (biomicrite, mudstone, wackestone and packstone; intrasparite, grainstone; biosparite, packstone), quartz, chert, k- feldspar, plagioclase, ceramic fragments, artificially crushed marbles, quartzite, muscovite, shell fragments.		
Classification of the aggregate			Fluvial sand, artificially crushed bricks (cocciopesto) and marbles.				
OPEN POROSITY %	ND			COMPRESSIVE STRENGTH		ND	
GRANULOMETRIC CURVE	ND						
CHEMICAL ANALYSES							
Total cations content % w.t.	Na ₂ O	K ₂ O	CaO	MgO	Fe ₂ O ₃	Al ₂ O ₃	SiO ₂
	0.97	1.11	24.35	1.94	1.97	6.99	31.72
Cations soluble in HCl 0.1 N % w.t.	Na ₂ O	K ₂ O	CaO	MgO	Fe ₂ O ₃	Al ₂ O ₃	SiO ₂
	0.34	0.09	22.39	1.13	0.76	2.08	1.67
Water soluble salts % w.t.	Cl ⁻	NO ₃ ⁻	SO ₄ ²⁻	Loss on Ignition %		30.95	
	0.52	0.02	0.47				
Py-GC-MS spectrum	ND						

5.1.3. The archaeological area of St. Severo, Classe

One mosaic that was brought to light during one of the most recent archaeological excavations of the area of the St. Severo's church in Classe, Ravenna, has been investigated.

– *Mosaic of the Roman Villa*

The studied mosaic belonged to a Roman *Villa* that stood in the area of the St. Severo's Basilica in the 1st century A.D. (see paragraph 3.4.2). The location of the studied pavement with respect to the structures of the St. Severo's Basilica is showed in Figure 44. In Figure 45, a view of the excavated area with the studied mosaic can be observed.

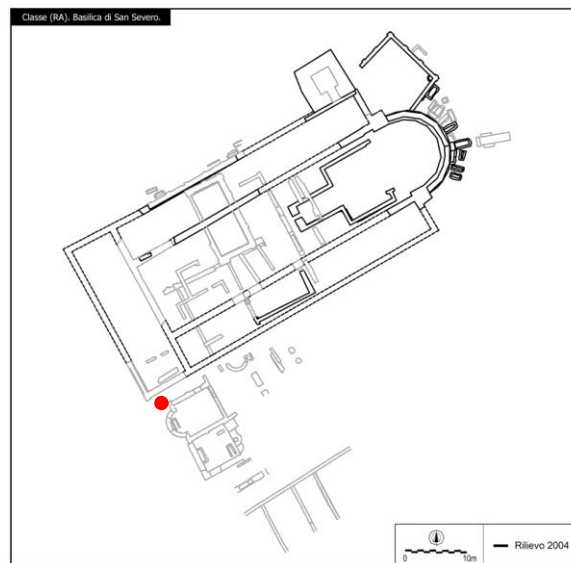


Figure 44 Plan of the St. Severo's Basilica with the excavated structures (courtesy of Prof. A. Augenti, University of Bologna, Italy). The red dot indicates the location of the studied pavement.



Figure 45 View of the area from southwest. The location of the studied mosaic is shown by the arrow.

Both the *tessellatum* and the substrate of the studied mosaic are only partially preserved. The *tessellatum* is made of stone *tesserae* with average size of 2 – 3 cm. The position of the sampling point is showed in Figure 46.



Figure 46 The position of the sampling point on the studied pavement (view from southwest).

In this case it was not possible, through the adopted methodology, to determine with sufficient certainty the type of foundation ground upon which the mosaic was built. In fact, the lower limit of the first of the three layers of the pavement was not clearly recognizable. This layer, which measures more than 15 cm in thickness on the studied cross section of the substrate, consists of a very low cohesive mortar containing mostly brick fragments with dimensions of several centimeters (Figure 47).

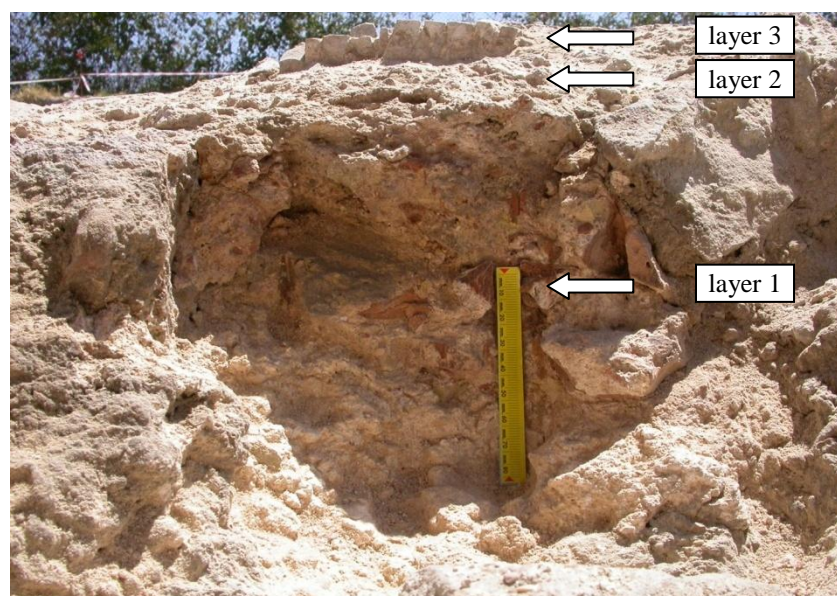


Figure 47 Cross section of the mosaic's substrate with the indication of the different mortar layers.

In Figure 48, a schematic graphic reproduction of the stratigraphy of the mosaic's substrate with the indication of the layers thickness and of the sampled layers is showed.

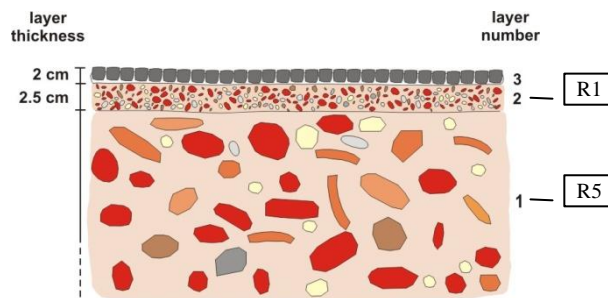


Figure 48 Schematic graphic reproduction of the stratigraphy of the studied mosaic with the indication of the sampled mortar layers and the correspondent sample codes.

In Table 19 and Table 20, the results of the laboratory analyses of the mortars of the 1st and 2nd layer of the mosaic's substrate are summarized.

Table 19 Archaeological area of St. Severo, mosaic of the Roman *Villa*: results of the laboratory analyses on the mortar layer n. 1.

Sample: R5		CHARACTERIZATION FORM																											
OPTICAL MICROSCOPY (Figure 112, Figure 113 in Appendix)																													
Stratigraphy	Layer 1	Munsell colour	Very pale brown 10YR8/2																										
Microscopic description of the binder on thin section																													
Structure	Not homogeneous	Reaction with the aggregate	Reaction rims around ceramic fragments																										
Texture	Micritic	Shape of pores	From sub-circular to irregular																										
Microscopic description of the aggregate on thin section																													
Granulometry	Maximum size: 4 mm Most abundant sizes: 4-2 mm, 2-1 mm		Roundness	From subangular to rounded																									
Sorting	Poorly sorted $\sigma = 2.00 \text{ } \emptyset$		Distribution	Homogeneous																									
Shape	Part natural, part due to artificial crushing		Orientation	None																									
Sphericity	Low		Mineralogic and petrographic composition	Ceramic fragments, quartz, k-feldspar, chert, limestones (biomicrite, mudstone, wackestone; biosparite, packstone), marbles, sandstone, mortar fragments, volcanic rocks.																									
Classification of the aggregate			Artificially crushed bricks (cocciopesto), fluvial sand and pozzolana.																										
OPEN POROSITY %	49.34		COMPRESSIVE STRENGTH	2.02 MPa																									
GRANULOMETRIC CURVE		<table border="1"> <caption>Granulometric Curve Data</caption> <thead> <tr> <th>Sieves diameter (mm)</th> <th>Passing percentage (%)</th> </tr> </thead> <tbody> <tr><td>0.075</td><td>0</td></tr> <tr><td>0.15</td><td>~5</td></tr> <tr><td>0.3</td><td>~10</td></tr> <tr><td>0.6</td><td>~15</td></tr> <tr><td>1.2</td><td>~25</td></tr> <tr><td>2.5</td><td>~45</td></tr> <tr><td>5</td><td>~75</td></tr> <tr><td>8</td><td>100</td></tr> <tr><td>16</td><td>100</td></tr> <tr><td>31.5</td><td>100</td></tr> </tbody> </table>						Sieves diameter (mm)	Passing percentage (%)	0.075	0	0.15	~5	0.3	~10	0.6	~15	1.2	~25	2.5	~45	5	~75	8	100	16	100	31.5	100
		Sieves diameter (mm)	Passing percentage (%)																										
0.075	0																												
0.15	~5																												
0.3	~10																												
0.6	~15																												
1.2	~25																												
2.5	~45																												
5	~75																												
8	100																												
16	100																												
31.5	100																												
CHEMICAL ANALYSES																													
Total cations content % w.t.	Na ₂ O	K ₂ O	CaO	MgO	Fe ₂ O ₃	Al ₂ O ₃	SiO ₂																						
	0.46	0.34	33.72	0.67	0.75	2.34	16.72																						
Cations soluble in HCl 0.1 N % w.t.	Na ₂ O	K ₂ O	CaO	MgO	Fe ₂ O ₃	Al ₂ O ₃	SiO ₂																						
	0.30	0.18	32.84	0.41	0.26	1.06	1.06																						
Water soluble salts % w.t.	Cl ⁻	NO ₃ ⁻	SO ₄ ²⁻	Loss on Ignition %			45.00																						
	0.48	0.36	0.37																										
Py-GC-MS spectrum	ND																												

Table 20 Archaeological area of St. Severo, mosaic of the Roman *Villa*: results of the laboratory analyses on the mortar layer n. 2.

Sample: R1		CHARACTERIZATION FORM					
OPTICAL MICROSCOPY (Figure 114, Figure 115 in Appendix)							
Stratigraphy	Layer 2	Munsell colour	Very pale brown 10YR8/2				
Microscopic description of the binder on thin section							
Structure	Not homogeneous	Reaction with the aggregate	Reaction rims around ceramic fragments				
Texture	Micritic	Shape of pores	From sub-circular to irregular				
Microscopic description of the aggregate on thin section							
Granulometry	Maximum size: 4 mm Most abundant sizes: 2-1 mm, 1-0.5 mm	Roundness	From subangular to subrounded				
Sorting	Poorly sorted $\sigma = 2.00 \varnothing$	Distribution	Homogeneous				
Shape	Part natural, part due to artificial crushing	Orientation	None				
Sphericity	Low	Mineralogic and petrographic composition	Ceramic fragments, quartz, k-feldspar, volcanic rocks, pyroxene, calcite, biotite, chert.				
Classification of the aggregate		Artificially crushed bricks (cocciopesto), pozzolana and fluvial sand.					
OPEN POROSITY %	41.03	COMPRESSIVE STRENGTH		ND			
GRANULOMETRIC CURVE	ND						
CHEMICAL ANALYSES							
Total cations content % w.t.	Na ₂ O	K ₂ O	CaO	MgO	Fe ₂ O ₃	Al ₂ O ₃	SiO ₂
	2.40	2.07	16.65	1.87	1.60	7.56	39.85
Cations soluble in HCl 0.1 N % w.t.	Na ₂ O	K ₂ O	CaO	MgO	Fe ₂ O ₃	Al ₂ O ₃	SiO ₂
	1.95	1.22	16.37	1.38	0.44	4.40	2.89
Water soluble salts % w.t.	Cl ⁻	NO ₃ ⁻	SO ₄ ²⁻	Loss on Ignition %			45.00
	0.26	0.09	0.09				
Py-GC-MS spectrum	<p>The figure is a gas chromatography-mass spectrometry (GC-MS) spectrum for sample R1. The x-axis represents time in minutes, ranging from 0 to 50. The y-axis represents MCounts, ranging from 0.0 to 2.0. Several peaks are labeled with their retention times: 12:0, 14:0, 16:0, 18:0, 18:1, and 18:2. There are also three small peaks marked with asterisks (*) at approximately 28, 30, and 32 minutes. The peak at 18:0 is the most prominent, reaching a maximum MCount of approximately 2.0.</p>						

5.1.4. The “Cortile Romano” in the Archaeological Museum of Florence

Four pavement fragments stored in the “Cortile Romano”, one of the internal courtyards of the Archaeological Museum of Florence, have been studied. These fragments, lifted during past excavations in different areas of the city of Florence (see paragraph 3.5.2), preserve almost entirely their original substrate. The studied floor fragments have been indicated by progressive alphabetic letters.

– *Pavement A*

The investigated floor fragment has squared shape with 50 cm edge length (Figure 49). The surface of the pavement is made of rectangular marble slabs with 40 cm and 30 cm edges, which are laid upon a substrate composed of two layers of mortar interpreted as the 1st and the 2nd layer of the pavement’s stratigraphy. The first foundation layer was probably laid on large thin ceramic tiles, of which only few remains are preserved, which could be the so called *pilae* tiles that were used in Roman times as an element of the under floor heating system of baths (Figure 50). A cross section of the studied pavement is showed in the photograph of Figure 51 and reproduced graphically in Figure 52.



Figure 49 The studied pavement fragment.



Figure 50 A reconstruction of the floor of a Roman bath. The floor was built in elevated position above pillars (*pilae* stacks), in order to allow the hot air to freely circulate underneath the pavement and heat the room (Archaeological Museum of Dion, Greece).



Figure 51 Cross section of the substrate of the pavement A with the indication of the two preparatory mortar layers.

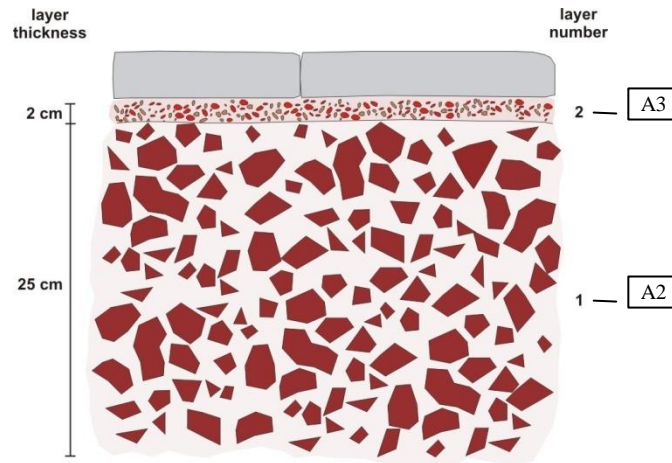


Figure 52 “Cortile Romano”, schematic graphic reproduction of the stratigraphy of the pavement A with the indication of the sampled mortar layers and the correspondent sample codes.

In Table 21 and Table 22, the results of the laboratory analyses on the mortars of the 1st and 2nd layer of the pavement’s substrate are summarized.

Table 21 “Cortile Romano”, pavement A: results of the laboratory analyses on the mortar layer n. 1.

Sample: A2		CHARACTERIZATION FORM					
OPTICAL MICROSCOPY (Figure 116, Figure 117 in Appendix)							
Stratigraphy	Layer 1	Munsell colour		Pinkish white 7.5YR8/2			
Microscopic description of the binder on thin section							
Structure	Not homogeneous	Reaction with the aggregate		Reaction rims around ceramic fragments			
Texture	Micritic	Shape of pores		From sub-circular to irregular			
Microscopic description of the aggregate on thin section							
Granulometry	Maximum size: 8 mm Most abundant sizes: 4-2 mm, 2-1 mm	Roundness		From angular to subangular			
Sorting	Moderately sorted $\sigma = 1.00 \text{ } \emptyset$	Distribution		Not homogeneous			
Shape	Due to artificial crushing	Orientation		None			
Sphericity	Low	Mineralogic and petrographic composition		Ceramic fragments, quartz, k-feldspar, plagioclase, volcanic rocks, quartzite.			
Classification of the aggregate				Artificially crushed bricks (cocciopesto)			
OPEN POROSITY %	37.38		COMPRESSIVE STRENGTH		7.21 MPa		
GRANULOMETRIC CURVE	ND						
CHEMICAL ANALYSES							
Total cations content % w.t.	Na ₂ O	K ₂ O	CaO	MgO	Fe ₂ O ₃	Al ₂ O ₃	SiO ₂
	0.38	1.29	25.89	0.88	1.65	5.46	31.71
Cations soluble in HCl 0.1 N % w.t.	Na ₂ O	K ₂ O	CaO	MgO	Fe ₂ O ₃	Al ₂ O ₃	SiO ₂
	0.15	1.05	25.37	0.30	0.79	2.58	3.21
Water soluble salts % w.t.	Cl ⁻	NO ₃ ⁻	SO ₄ ²⁻	Loss on Ignition %			32.77
	0.05	0.18	0.06				
Py-GC-MS spectrum	ND						

Table 22 “Cortile Romano”, pavement A: results of the laboratory analyses on the mortar layer n. 2.

Sample: A3		CHARACTERIZATION FORM					
OPTICAL MICROSCOPY (Figure 118, Figure 119 in Appendix)							
Stratigraphy	Layer 2	Munsell colour	Pinkish white 5YR8/2				
Microscopic description of the binder on thin section							
Structure	Not homogeneous	Reaction with the aggregate	Reaction rims around ceramic fragments and chert (rare)				
Texture	Micritic	Shape of pores	From circular to irregular				
Microscopic description of the aggregate on thin section							
Granulometry	Maximum size: 2 mm Most abundant sizes: 2-1 mm, 1-1.5 mm	Roundness	From angular to subangular				
Sorting	Moderately sorted $\sigma = 1.00 \text{ } \emptyset$	Distribution	Not homogeneous				
Shape	Due to artificial crushing	Orientation	None				
Sphericity	Low	Mineralogic and petrographic composition	Ceramic fragments, quartz, chert, micaschist.				
Classification of the aggregate		Artificially crushed bricks (cocciopesto)					
OPEN POROSITY %	52.49	COMPRESSIVE STRENGTH	4.45 MPa				
GRANULOMETRIC CURVE	ND						
CHEMICAL ANALYSES							
Total cations content % w.t.	Na ₂ O	K ₂ O	CaO	MgO	Fe ₂ O ₃	Al ₂ O ₃	SiO ₂
	0.43	2.39	16.65	1.72	3.29	7.75	43.77
Cations soluble in HCl 0.1 N % w.t.	Na ₂ O	K ₂ O	CaO	MgO	Fe ₂ O ₃	Al ₂ O ₃	SiO ₂
	0.20	1.89	16.07	0.31	0.72	3.67	1.11
Water soluble salts % w.t.	Cl ⁻	NO ₃ ⁻	SO ₄ ²⁻	Loss on Ignition %			24.00
	<0.01	0.02	0.03				
Py-GC-MS spectrum							

– *Pavement B*

The fragment, approximately of the same size of the previous one (Figure 53), is composed of marble slabs laid above two layers of mortar which were spread upon a structure made of ceramic tiles (Figure 54). Next to one of the two longer edges of the floor fragment, the remains of a vertical wall covered on one side by marble slabs, are visible. The stratigraphy of the pavement has the same characteristics as that of pavement A (Figure 55). For such a reason it can be supposed that the two fragments belonged to a same floor.



Figure 53 The studied pavement fragment.

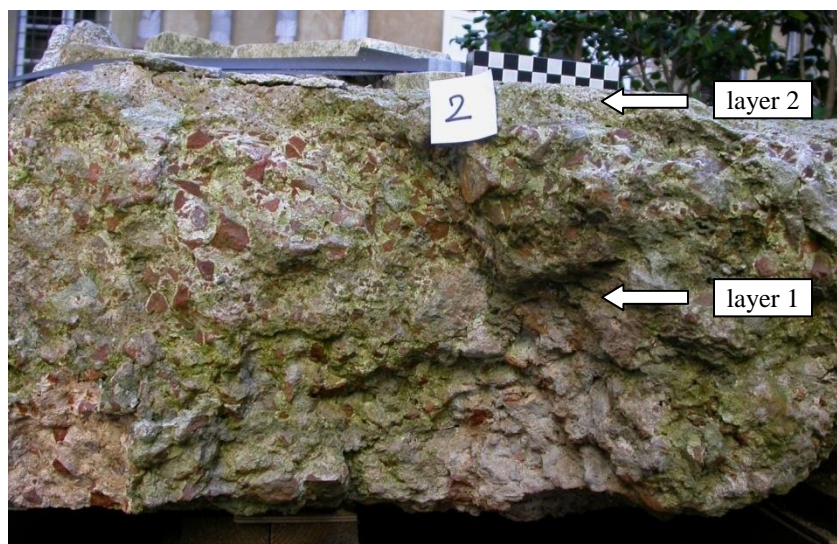


Figure 54 Cross section of the pavement's substrate with the indication of the two preparatory mortar layers.

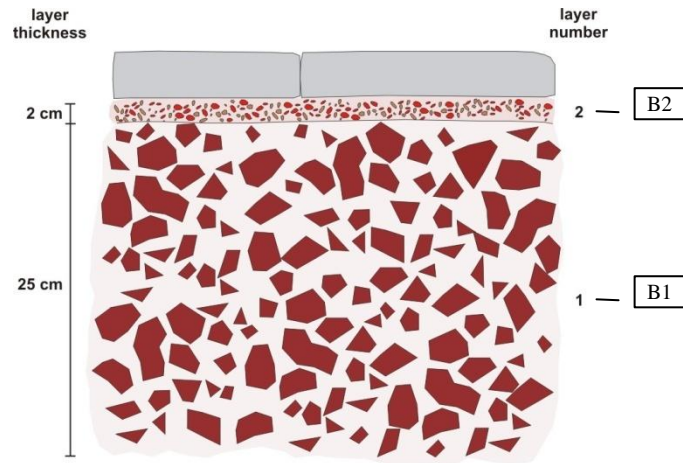


Figure 55 “Cortile Romano”, schematic graphic reproduction of the stratigraphy of the pavement B with the indication of the sampled mortar layers and the correspondent sample codes.

In Table 23 and Table 24, the results of the laboratory analyses on the mortars of the 1st and 2nd layer of the pavement’s substrate are summarized.

Table 23 “Cortile Romano”, pavement B: results of the laboratory analyses on the mortar layer n. 1.

Sample: B1		CHARACTERIZATION FORM					
OPTICAL MICROSCOPY (Figure 120, Figure 121 in Appendix)							
Stratigraphy	Layer 1	Munsell colour		Pinkish white 7.5YR8/2			
Microscopic description of the binder on thin section							
Structure	Not homogeneous	Reaction with the aggregate		Reaction rims around ceramic fragments			
Texture	Micritic	Shape of pores		Irregular			
Microscopic description of the aggregate on thin section							
Granulometry	Maximum size: 12 mm Most abundant sizes: 1-0.5 mm	Roundness		From angular to subangular			
Sorting	Well sorted $\sigma = 0.50 \text{ \AA}$	Distribution		Homogeneous			
Shape	Due to artificial crushing	Orientation		None			
Sphericity	Low	Mineralogic and petrographic composition		Ceramic fragments			
Classification of the aggregate				Artificially crushed bricks (cocciopesto)			
OPEN POROSITY %	30.99	COMPRESSIVE STRENGTH			12.86 MPa		
GRANULOMETRIC CURVE	ND						
CHEMICAL ANALYSES							
Total cations content % w.t.	Na ₂ O	K ₂ O	CaO	MgO	Fe ₂ O ₃	Al ₂ O ₃	SiO ₂
	0.46	1.11	26.58	0.85	2.03	5.25	32.72
Cations soluble in HCl 0.1 N % w.t.	Na ₂ O	K ₂ O	CaO	MgO	Fe ₂ O ₃	Al ₂ O ₃	SiO ₂
	0.22	0.82	25.33	0.17	0.69	2.31	3.89
Water soluble salts % w.t.	Cl ⁻	NO ₃ ⁻	SO ₄ ²⁻	Loss on Ignition %			31.00
	0.01	0.02	0.05				
Py-GC-MS spectrum	ND						

Table 24 “Cortile Romano”, pavement B: results of the laboratory analyses on the mortar layer n. 2.

Sample: B2		CHARACTERIZATION FORM					
OPTICAL MICROSCOPY (Figure 122, Figure 123 in Appendix)							
Stratigraphy	Layer 2	Munsell colour		Pinkish white 7.5YR8/2			
Microscopic description of the binder on thin section							
Structure	Not homogeneous	Reaction with the aggregate		Reaction rims around ceramic fragments			
Texture	Micritic	Shape of pores		From irregular to sub-circular			
Microscopic description of the aggregate on thin section							
Granulometry	Maximum size: 1 mm Most abundant sizes: 1-0.5 mm	Roundness		From angular to subrounded			
Sorting	Moderately sorted $\sigma = 1.00 \text{ } \emptyset$	Distribution		Homogeneous			
Shape	Due to artificial crushing	Orientation		None			
Sphericity	Low	Mineralogic and petrographic composition		Ceramic fragments, quartz			
Classification of the aggregate				Artificially crushed bricks (cocciopesto)			
OPEN POROSITY %	54.10	COMPRESSIVE STRENGTH			ND		
GRANULOMETRIC CURVE	ND						
CHEMICAL ANALYSES							
Total cations content % w.t.	Na ₂ O	K ₂ O	CaO	MgO	Fe ₂ O ₃	Al ₂ O ₃	SiO ₂
	0.59	1.64	21.41	1.72	0.80	5.14	37.70
Cations soluble in HCl 0.1 N % w.t.	Na ₂ O	K ₂ O	CaO	MgO	Fe ₂ O ₃	Al ₂ O ₃	SiO ₂
	0.35	1.42	19.59	0.99	0.77	3.46	2.80
Water soluble salts % w.t.	Cl ⁻	NO ₃ ⁻	SO ₄ ²⁻	Loss on Ignition %			31.00
	0.04	0.07	0.06				
Py-GC-MS spectrum	ND						

– *Pavement D*

The studied fragment consists of a small portion of pavement's substrate connected to a thick vertical wall covered on one side by a large marble slab (Figure 56). The stratigraphy of the substrate is similar to that of pavements A and B, composed of two mortar layers laid upon large ceramic tiles (Figure 57, Figure 58). It can be supposed that this structure constituted one of the walls delimitating the room to which the studied pavement fragments belonged.



Figure 56 The studied fragment of substrate connected to the remains of a vertical wall.

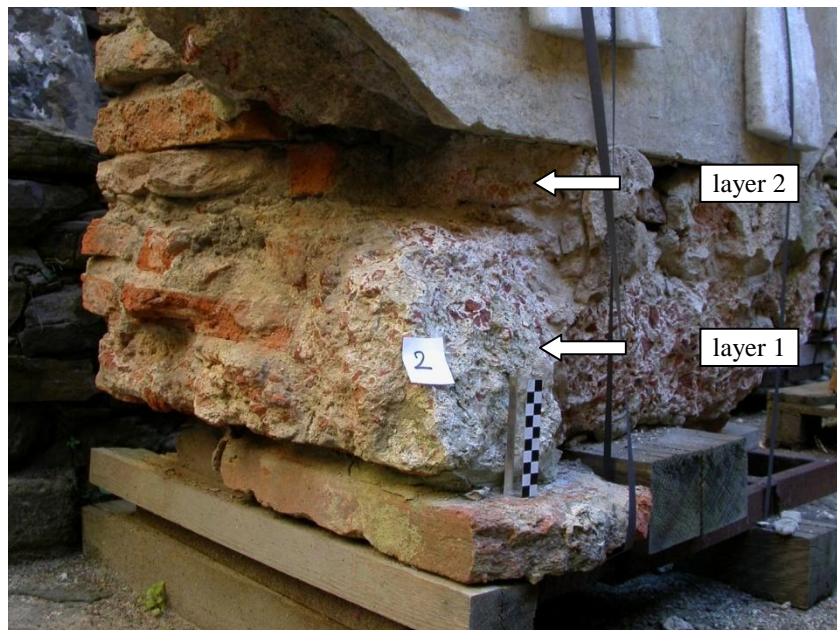


Figure 57 The studied portion of substrate with the indication of the sampled mortar layers.

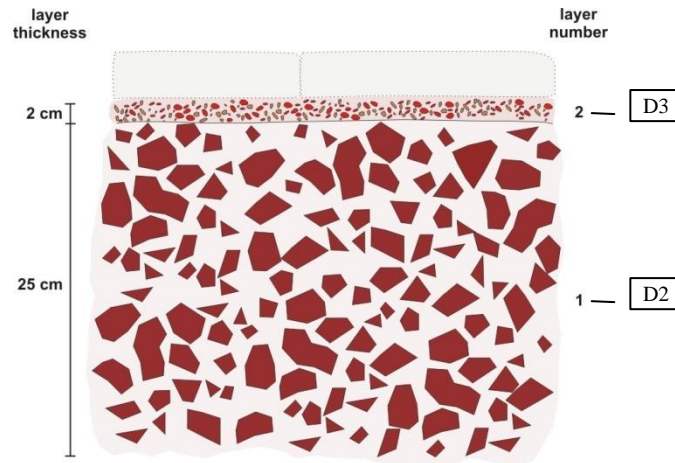


Figure 58 “Cortile Romano”, schematic graphic reproduction of the stratigraphy of the pavement D with the indication of the sampled mortar layers and the correspondent sample codes.

In Table 25 and Table 26, the results of the laboratory analyses on the mortars of the 1st and 2nd layer of the pavement’s substrate are summarized.

Table 25 “Cortile Romano”, pavement D: results of the laboratory analyses on the mortar layer n. 1.

Sample: D2		CHARACTERIZATION FORM					
OPTICAL MICROSCOPY (Figure 124, Figure 125 in Appendix)							
Stratigraphy	Layer 1	Munsell colour		Very pale brown 10YR8/2			
Microscopic description of the binder on thin section							
Structure	Not homogeneous	Reaction with the aggregate		Reaction rims around ceramic fragments			
Texture	Micritic	Shape of pores		Irregular			
Microscopic description of the aggregate on thin section							
Granulometry	Maximum size: 4 mm Most abundant sizes: 4-2 mm, 2-1 mm	Roundness		From subangular to subrounded			
Sorting	Poorly sorted $\sigma = 2.00 \text{ } \emptyset$	Distribution		Not homogeneous			
Shape	Part natural, part due to artificial crushing	Orientation		None			
Sphericity	Low	Mineralogic and petrographic composition		Ceramic fragments, quartz, K-feldspar, calcite, biotite, micaschist, limestones (biomicrite, mudstone), marble.			
Classification of the aggregate		Artificially crushed bricks (cocciopesto) and fluvial sand.					
OPEN POROSITY %	28.03	COMPRESSIVE STRENGTH			ND		
GRANULOMETRIC CURVE		ND					
CHEMICAL ANALYSES							
Total cations content % w.t.	Na ₂ O	K ₂ O	CaO	MgO	Fe ₂ O ₃	Al ₂ O ₃	SiO ₂
	0.20	0.77	28.54	0.83	1.11	3.21	31.33
Cations soluble in HCl 0.1 N % w.t.	Na ₂ O	K ₂ O	CaO	MgO	Fe ₂ O ₃	Al ₂ O ₃	SiO ₂
	0.06	0.57	28.26	0.32	0.58	1.78	1.78
Water soluble salts % w.t.	Cl ⁻	NO ₃ ⁻	SO ₄ ²⁻	Loss on Ignition %			34.00
	0.02	0.02	0.10				
Py-GC-MS spectrum	ND						

Table 26 “Cortile Romano”, pavement D: results of the laboratory analyses on the mortar layer n. 2.

Sample: D3		CHARACTERIZATION FORM					
OPTICAL MICROSCOPY (Figure 126, Figure 127 in Appendix)							
Stratigraphy	Layer 2	Munsell colour		Pinkish white 7.5R8.2			
Microscopic description of the binder on thin section							
Structure	Not homogeneous	Reaction with the aggregate		Reaction rims around ceramic fragments			
Texture	Micritic	Shape of pores		Mostly sub-circular			
Microscopic description of the aggregate on thin section							
Granulometry	Maximum size: 2 mm Most abundant sizes: 1-0.5 mm	Roundness		From angular to subrounded			
Sorting	Poorly sorted $\sigma = 1.00 \text{ } \emptyset$	Distribution		Not homogeneous			
Shape	Part natural, part due to artificial crushing	Orientation		Oriented sub-parallel to layer surface			
Sphericity	Low	Mineralogic and petrographic composition		Ceramic fragments, quartz, K-feldspar, plagioclase, quartzite, marble, micaschist, limestones (biomicrite, mudstone), sandstone, shell fragments.			
Classification of the aggregate		Artificially crushed bricks (cocciopesto) and fluvial sand.					
OPEN POROSITY %	38.31	COMPRESSIVE STRENGTH			ND		
GRANULOMETRIC CURVE	ND						
CHEMICAL ANALYSES							
Total cations content % w.t.	Na ₂ O	K ₂ O	CaO	MgO	Fe ₂ O ₃	Al ₂ O ₃	SiO ₂
	0.67	2.14	22.25	0.77	1.41	5.97	38.78
Cations soluble in HCl 0.1 N % w.t.	Na ₂ O	K ₂ O	CaO	MgO	Fe ₂ O ₃	Al ₂ O ₃	SiO ₂
	0.32	1.76	21.41	0.28	0.52	2.44	2.08
Water soluble salts % w.t.	Cl ⁻	NO ₃ ⁻	SO ₄ ²⁻	Loss on Ignition %			28.00
	0.02	0.01	1.04				
Py-GC-MS spectrum	ND						

– *Pavement E*

The studied pavement fragment, which is leaning against a wall on the opposite side of the courtyard with respect to the above described fragments, has almost squared shape with edge length of about 50 cm. The pavement is composed of two mortar layers, the second of which is polished on the surface (Figure 59). The limit between the two mortar layers is not visible, but they can be distinguished according to the size of the aggregate in the mortars, (Figure 60, Figure 61).



Figure 59 The polished surface of the pavement fragment E.



Figure 60 The back side of the pavement fragment E with the first layer made of large pebbles.



Figure 61 Cross section of the pavement with the indication of the two mortar layers.

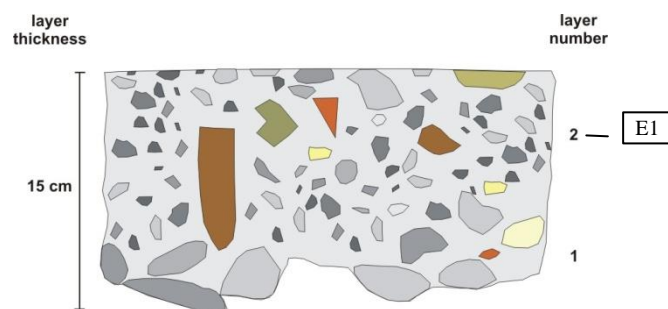


Figure 62 Schematic graphic reproduction of the stratigraphy of the studied pavement with the indication of the sampled mortar layer and the correspondent sample code.

In Table 27, the results of the laboratory analyses on the mortar of the 2nd layer of the pavement are summarized.

Table 27 “Cortile Romano”, pavement E: results of the laboratory analyses on the mortar layer n. 2.

Sample: E1		CHARACTERIZATION FORM					
OPTICAL MICROSCOPY (Figure 128, Figure 129 in Appendix)							
Stratigraphy	Layer 2	Munsell colour		White 10YR8/4			
Microscopic description of the binder on thin section							
Structure	Homogeneous	Reaction with the aggregate		None visible			
Texture	Micritic	Shape of pores		From sub-circular to irregular			
Microscopic description of the aggregate on thin section							
Granulometry	Maximum size: 4 mm Most abundant sizes: 2-1 mm, 1-0.5 mm		Roundness		From very angular to very rounded		
Sorting	Poorly sorted $\sigma = 2.00 \text{ } \emptyset$		Distribution		Homogeneous		
Shape	Part natural, part due to artificial crushing		Orientation		None		
Sphericity	Low		Mineralogic and petrographic composition		Limestones (intramicrite, mudstone), marble, quartzite, sandstone, quartz, k-feldspar, biotite, volcanic rocks.		
Classification of the aggregate			Fluvial sand and artificially crushed marbles				
OPEN POROSITY %	20.52		COMPRESSIVE STRENGTH			ND	
GRANULOMETRIC CURVE	ND						
CHEMICAL ANALYSES							
Total cations content % w.t.	Na ₂ O	K ₂ O	CaO	MgO	Fe ₂ O ₃	Al ₂ O ₃	SiO ₂
	0.38	0.87	23.37	0.64	1.32	2.31	37.12
Cations soluble in HCl 0.1 N % w.t.	Na ₂ O	K ₂ O	CaO	MgO	Fe ₂ O ₃	Al ₂ O ₃	SiO ₂
	0.08	0.55	22.28	0.39	0.70	1.62	1.11
Water soluble salts % w.t.	Cl ⁻	NO ₃ ⁻	SO ₄ ²⁻	Loss on Ignition %			34.00
	0.02	<0.01	0.03				
Py-GC-MS spectrum	ND						

5.1.5. The Palace of Aegae in Vergina

The pavements of two adjacent rooms that served as banquet halls [Dro00], located at the west side of the Palace of Aegae, have been investigated. In Figure 63, a plan of the Palace with the location of the studied mosaics and the position of the sampling points within the area of the pavements is showed.

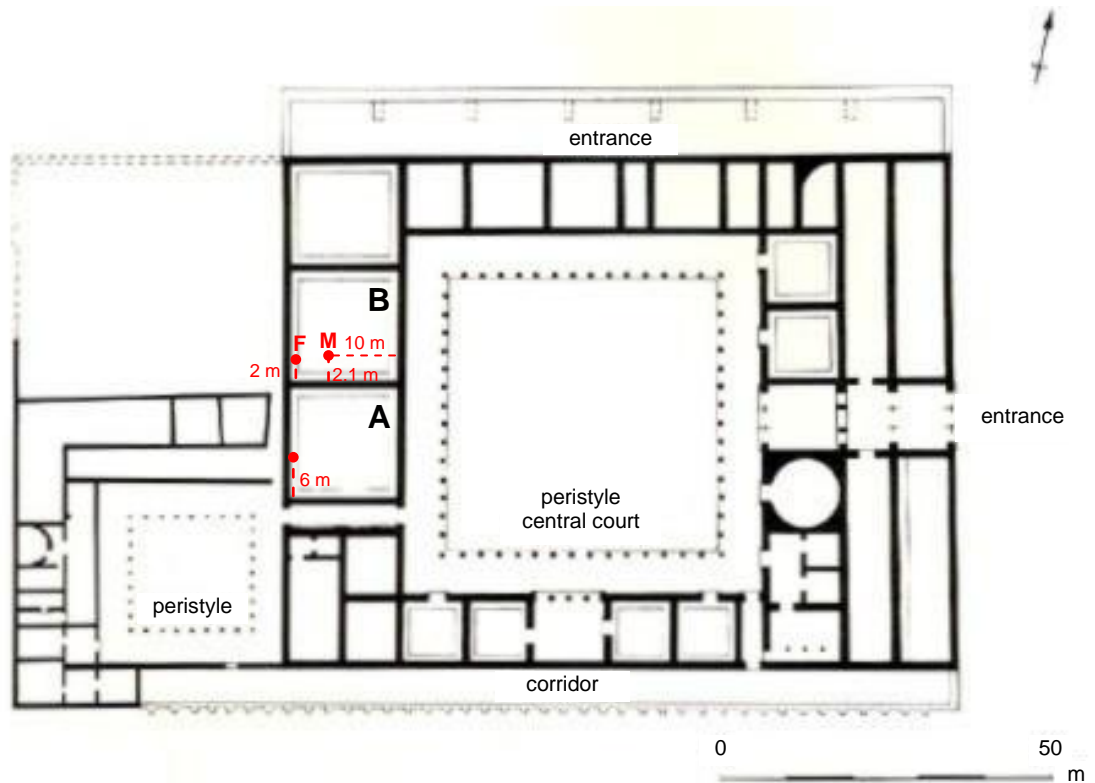


Figure 63 Plan of the Palace of Aegae with the location of the studied pavements and the indication of the sampling points. Plan by I. Travlos and D. Pandermalis [Dro00], modified.

– Mosaic A

The studied mosaic is located in the room indicated with the letter A in Figure 63. The *in situ* analyses and the sampling have been carried out at the west edge of the room, on the outer frame of the pavement. The mosaic's substrate, built on natural levelled ground, in this point is composed of three preparatory layers, the first of which consists of large stones, up to 10 cm in diameter, laid on the ground, without any mortar. The surface of the mosaic is made of black pebbles with average size of 1 – 2 cm (Figure 64, Figure 65). The mortar cohesion and the layers mutual adhesion is very good, even though fractures sub-parallel to the surface of the pavement are present, especially in the upper part of the substrate (Figure 64).

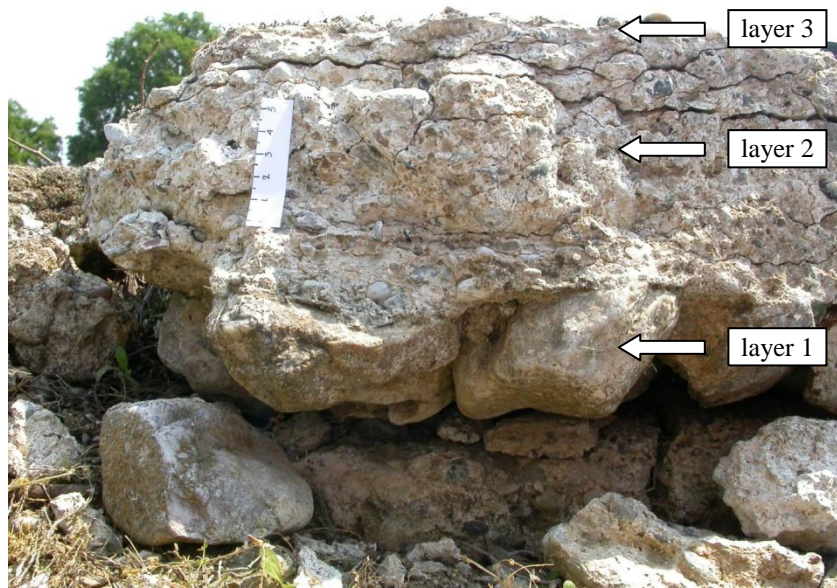


Figure 64 Cross section of the pavement's substrate with the indication of the preparatory mortar layers.

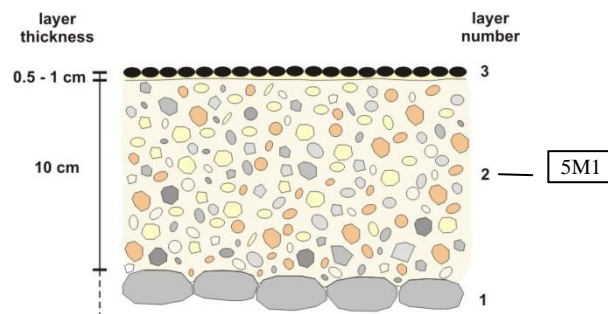


Figure 65 Palace of Aegae, schematic graphic reproduction of the stratigraphy of the mosaic A with the indication of the sampled mortar layer and the correspondent sample code.

In Table 28, the results of the laboratory analyses on the mortar of the 2nd layer of the mosaic's substrate are summarized.

Table 28 Palace of Aegae, mosaic A: results of the laboratory analyses on the mortar layer n. 2.

Sample: 5M1		CHARACTERIZATION FORM					
OPTICAL MICROSCOPY (Figure 130, Figure 131 in Appendix)							
Stratigraphy	Layer 2	Munsell colour	White 10YR8/1				
Microscopic description of the binder on thin section							
Structure	Not homogeneous	Reaction with the aggregate	None visible				
Texture	Micritic	Shape of pores	Irregular				
Microscopic description of the aggregate on thin section							
Granulometry	Maximum size: 5 mm Most abundant sizes: 8-4 mm, 4-2 mm	Roundness	From angular to rounded				
Sorting	Poorly sorted $\sigma = 2.00 \text{ } \emptyset$	Distribution	Not homogeneous				
Shape	Natural	Orientation	None				
Sphericity	From high to low	Mineralogic and petrographic composition	Schist, gneiss, chert, volcanic rocks, limestones (oosparite, grainstone), marble, quartz, k-feldspar, plagioclase, serpentinite.				
Classification of the aggregate				Fluvial sand and gravel and pozzolana			
OPEN POROSITY %	32.15		COMPRESSIVE STRENGTH			3.96 MPa	
GRANULOMETRIC CURVE							
CHEMICAL ANALYSES							
Total cations content % w.t.	Na ₂ O	K ₂ O	CaO	MgO	Fe ₂ O ₃	Al ₂ O ₃	SiO ₂
	0.41	0.14	37.99	1.76	1.52	2.29	24.03
Cations soluble in HCl 0.1 N % w.t.	Na ₂ O	K ₂ O	CaO	MgO	Fe ₂ O ₃	Al ₂ O ₃	SiO ₂
	0.02	0.05	36.17	1.01	0.98	1.97	2.40
Water soluble salts % w.t.	Cl ⁻	NO ₃ ⁻	SO ₄ ²⁻	Loss on Ignition %			31.88
	0.03	0.02	0.01				
Py-GC-MS spectrum	ND						

– *Mosaic B*

The studied mosaic is located in the room indicated with the letter B in Figure 63. The *in situ* analyses and the sampling have been carried out in two different points of the pavement, namely the inner area (point M) and the outer frame (point F) (Figure 63, Figure 66). The mosaic was built on natural leveled ground. The pavement in the inner area is composed of four layers (Figure 67, Figure 68) characterized by good mutual adhesion. The fourth layer constitutes the surface of the floor, which is made of a mortar with fine aggregates bedding stone slabs having irregular shape with up to 10 cm long edges.



Figure 66 The southwest corner of mosaic B with the indication of the sampling points on the outer frame (F) and the inner area (M) of the pavement. Photo by M. Stefanidou.

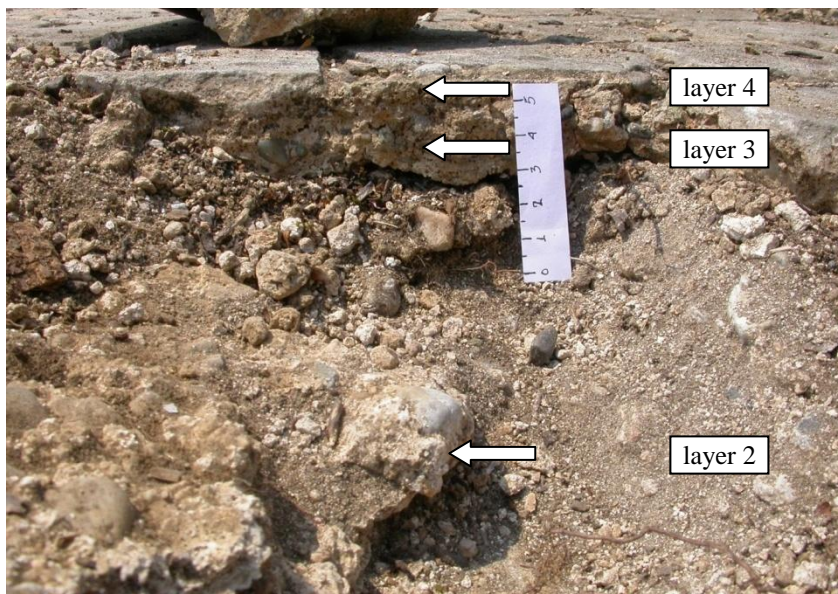


Figure 67 Stratigraphy of the substrate in the inner area (sampling point M) of the mosaic.

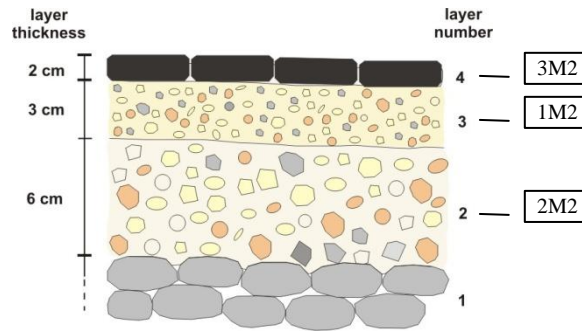


Figure 68 Palace of Aegae, schematic graphic reproduction of the stratigraphy of the mosaic in the inner area (point M) with the indication of the sampled mortar layers and the correspondent sample codes.

The substrate of the outer frame of the mosaic is composed of three preparatory layers (Figure 69, Figure 70). As for the mosaic A, the first layer is made of large stones, up to 10 cm in diameter, laid on the ground, without any mortar, while the surface of the mosaic consists of black pebbles with average size of 2 – 3 cm (Figure 69).



Figure 69 A sample of the mosaic of the outer frame (sampling point F). The layer number 2 and the layer number 3 with black pebbles inserted in it are visible.

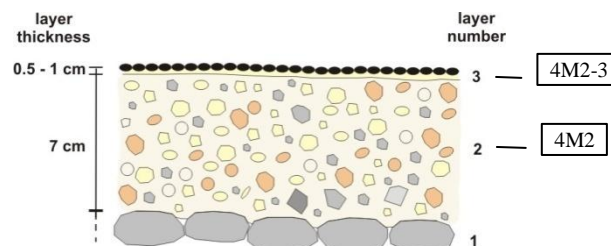


Figure 70 Schematic graphic reproduction of the stratigraphy of the mosaic in the outer frame with the indication of the sampled mortar layers and the correspondent sample codes.

In Table 29, Table 30, Table 31, Table 32 and Table 33 the results of the laboratory analyses on the mortars of the 2nd, 3rd and 4th layer of the mosaic's substrate in the inner area and on the mortar of 2nd and 3rd layer of the mosaic's substrate in the outer frame are summarized.

Table 29 Palace of Aegae, mosaic B, inner area: results of the laboratory analyses on the mortar layer n. 2.

Sample: 2M2		CHARACTERIZATION FORM																										
OPTICAL MICROSCOPY (Figure 132, Figure 133 in Appendix)																												
Stratigraphy	Layer 2	Munsell colour		Very pale brown 10YR8/2																								
Microscopic description of the binder on thin section																												
Structure	Not homogeneous	Reaction with the aggregate		None visible																								
Texture	Micritic	Shape of pores		Irregular																								
Microscopic description of the aggregate on thin section																												
Granulometry	Maximum size: 10 mm Most abundant sizes: 8-4 mm, 4-2 mm	Roundness		From subangular to rounded																								
Sorting	Poorly sorted $\sigma = 2.00 \text{ } \emptyset$	Distribution		Not homogeneous																								
Shape	Natural	Orientation		None																								
Sphericity	From high to low	Mineralogic and petrographic composition		Limestones (dismicrite, mudstone; micrite, mudstone), schist, marble, quartz, k-feldspar, plagioclase, quartzite.																								
Classification of the aggregate				Fluvial sand and gravel																								
OPEN POROSITY %	29.57		COMPRESSIVE STRENGTH			ND																						
GRANULOMETRIC CURVE																												
	<table border="1"> <caption>Approximate data points from the granulometric curve for layer 2</caption> <thead> <tr> <th>Sieves diameter (mm)</th> <th>Passing percentage (%)</th> </tr> </thead> <tbody> <tr><td>0.075</td><td>0</td></tr> <tr><td>0.15</td><td>10</td></tr> <tr><td>0.3</td><td>20</td></tr> <tr><td>0.6</td><td>25</td></tr> <tr><td>1.2</td><td>30</td></tr> <tr><td>2.5</td><td>35</td></tr> <tr><td>5</td><td>40</td></tr> <tr><td>8</td><td>45</td></tr> <tr><td>16</td><td>95</td></tr> <tr><td>31.5</td><td>100</td></tr> </tbody> </table>							Sieves diameter (mm)	Passing percentage (%)	0.075	0	0.15	10	0.3	20	0.6	25	1.2	30	2.5	35	5	40	8	45	16	95	31.5
Sieves diameter (mm)	Passing percentage (%)																											
0.075	0																											
0.15	10																											
0.3	20																											
0.6	25																											
1.2	30																											
2.5	35																											
5	40																											
8	45																											
16	95																											
31.5	100																											
CHEMICAL ANALYSES																												
Total cations content % w.t.	Na ₂ O	K ₂ O	CaO	MgO	Fe ₂ O ₃	Al ₂ O ₃	SiO ₂																					
	0.30	0.26	38.90	1.77	1.77	1.40	28.52																					
Cations soluble in HCl 0.1 N % w.t.	Na ₂ O	K ₂ O	CaO	MgO	Fe ₂ O ₃	Al ₂ O ₃	SiO ₂																					
	0.03	0.11	38.20	0.66	0.56	1.47	0.94																					
Water soluble salts % w.t.	Cl ⁻	NO ₃ ⁻	SO ₄ ²⁻	Loss on Ignition %			27.78																					
	0.01	0.01	0.01																									
Py-GC-MS spectrum	ND																											

Table 30 Palace of Aegae, mosaic B, inner area: results of the laboratory analyses on the mortar layer n. 3.

Sample: 1M2		CHARACTERIZATION FORM																												
OPTICAL MICROSCOPY (Figure 134, Figure 135 in Appendix)																														
Stratigraphy	Layer 3	Munsell colour	Very pale brown 10YR7/3																											
Microscopic description of the binder on thin section																														
Structure	Homogeneous	Reaction with the aggregate	None visible																											
Texture	Micritic	Shape of pores	Sub-circular																											
Microscopic description of the aggregate on thin section																														
Granulometry	Maximum size: 7 mm Most abundant sizes: 8-4 mm, 4-2 mm	Roundness	From subangular to very rounded																											
Sorting	Poorly sorted $\sigma = 2.00 \varnothing$	Distribution	Homogeneous																											
Shape	Natural	Orientation	None																											
Sphericity	From high to low	Mineralogic and petrographic composition	Schist, quartzite, gneiss, serpentinite, volcanic rocks, marble, chert, limestones (intramicrite, wackestone), quartz, k-feldspar, micas.																											
Classification of the aggregate		Fluvial sand and gravel and pozzolana																												
OPEN POROSITY %	21.31	COMPRESSIVE STRENGTH				11.42 MPa																								
GRANULOMETRIC CURVE																														
	<table border="1"> <caption>Granulometric Curve Data (Estimated)</caption> <thead> <tr> <th>Sieves diameter (mm)</th> <th>Passing percentage (%)</th> </tr> </thead> <tbody> <tr><td>0.075</td><td>0</td></tr> <tr><td>0.15</td><td>5</td></tr> <tr><td>0.3</td><td>10</td></tr> <tr><td>0.6</td><td>15</td></tr> <tr><td>1.2</td><td>20</td></tr> <tr><td>2.5</td><td>25</td></tr> <tr><td>5</td><td>35</td></tr> <tr><td>10</td><td>50</td></tr> <tr><td>20</td><td>75</td></tr> <tr><td>40</td><td>95</td></tr> <tr><td>80</td><td>100</td></tr> </tbody> </table>							Sieves diameter (mm)	Passing percentage (%)	0.075	0	0.15	5	0.3	10	0.6	15	1.2	20	2.5	25	5	35	10	50	20	75	40	95	80
Sieves diameter (mm)	Passing percentage (%)																													
0.075	0																													
0.15	5																													
0.3	10																													
0.6	15																													
1.2	20																													
2.5	25																													
5	35																													
10	50																													
20	75																													
40	95																													
80	100																													
CHEMICAL ANALYSES																														
Total cations content % w.t.	Na ₂ O	K ₂ O	CaO	MgO	Fe ₂ O ₃	Al ₂ O ₃	SiO ₂																							
	0.43	0.39	34.84	2.31	1.37	1.97	24.20																							
Cations soluble in HCl 0.1 N % w.t.	Na ₂ O	K ₂ O	CaO	MgO	Fe ₂ O ₃	Al ₂ O ₃	SiO ₂																							
	0.04	0.16	33.44	0.85	0.52	1.02	1.30																							
Water soluble salts % w.t.	Cl ⁻	NO ₃ ⁻	SO ₄ ²⁻	Loss on Ignition %			35.90																							
	0.01	0.01	0.02																											
Py-GC-MS spectrum																														
	<table border="1"> <caption>Py-GC-MS Spectrum Data (Estimated)</caption> <thead> <tr> <th>Retention Time (minutes)</th> <th>Approximate MCounts</th> </tr> </thead> <tbody> <tr><td>12:0</td><td>1.0</td></tr> <tr><td>14:0</td><td>0.5</td></tr> <tr><td>16:0</td><td>1.2</td></tr> <tr><td>18:0</td><td>1.2</td></tr> <tr><td>18:1</td><td>0.7</td></tr> <tr><td>18:2</td><td>0.5</td></tr> </tbody> </table>							Retention Time (minutes)	Approximate MCounts	12:0	1.0	14:0	0.5	16:0	1.2	18:0	1.2	18:1	0.7	18:2	0.5									
Retention Time (minutes)	Approximate MCounts																													
12:0	1.0																													
14:0	0.5																													
16:0	1.2																													
18:0	1.2																													
18:1	0.7																													
18:2	0.5																													

Table 31 Palace of Aegae, mosaic B, inner area: results of the laboratory analyses on the mortar layer n. 4.

Sample: 3M2		CHARACTERIZATION FORM					
OPTICAL MICROSCOPY (Figure 136, Figure 137 in Appendix)							
Stratigraphy	Layer 4	Munsell colour		Very pale brown 10YR7/3 Light red 2.5YR7/3 (upper surface)			
Microscopic description of the binder on thin section							
Structure	Homogeneous	Reaction with the aggregate		None visible			
Texture	Micritic	Shape of pores		Sub-circular			
Microscopic description of the aggregate on thin section							
Granulometry	Maximum size: 0.7 mm Most abundant sizes: 0.5-0.25 mm, 0.25-0.125 mm		Roundness		From angular to subrounded		
Sorting	Poorly sorted $\sigma = 2.00 \text{ } \emptyset$		Distribution		Homogeneous		
Shape	Natural		Orientation		None		
Sphericity	From high to low		Mineralogic and petrographic composition		Schist, quartzite, serpentinite, volcanic rocks, marble, chert, limestones (intrasparite, grainstone).		
Classification of the aggregate				Fluvial sand and pozzolana			
OPEN POROSITY %	21.82		COMPRESSIVE STRENGTH			ND	
GRANULOMETRIC CURVE	ND						
CHEMICAL ANALYSES							
Total cations content % w.t.	Na ₂ O	K ₂ O	CaO	MgO	Fe ₂ O ₃	Al ₂ O ₃	SiO ₂
	0.46	0.70	33.02	2.27	2.52	3.44	25.45
Cations soluble in HCl 0.1 N % w.t.	Na ₂ O	K ₂ O	CaO	MgO	Fe ₂ O ₃	Al ₂ O ₃	SiO ₂
	0.09	0.34	31.62	0.95	0.61	1.89	1.48
Water soluble salts % w.t.	Cl ⁻	NO ₃ ⁻	SO ₄ ²⁻	Loss on Ignition %			32.14
	0.01	<0.01	0.01				
Py-GC-MS spectrum	ND						

Table 32 Palace of Aegae, mosaic B, outer frame: results of the laboratory analyses on the mortar layer n. 2.

Sample: 4M2		CHARACTERIZATION FORM					
OPTICAL MICROSCOPY (Figure 138, Figure 139 in Appendix)							
Stratigraphy	Layer 2	Munsell colour	Very pale brown 10YR8/2				
Microscopic description of the binder on thin section							
Structure	Homogeneous	Reaction with the aggregate	None visible				
Texture	Micritic	Shape of pores	From sub-circular to irregular				
Microscopic description of the aggregate on thin section							
Granulometry	Maximum size: 6 mm Most abundant sizes: 8-4 mm, 4-2 mm	Roundness	From very angular to rounded				
Sorting	Poorly sorted $\sigma = 2.00 \text{ } \emptyset$	Distribution	Not homogeneous				
Shape	Natural	Orientation	None				
Sphericity	From high to low	Mineralogic and petrographic composition	Limestones (dismicrite, mudstone), schist, gneiss, quartzite, volcanic rocks, serpentinite, quartz, k-feldspar, micas.				
Classification of the aggregate				Fluvial sand and gravel and pozzolana			
OPEN POROSITY %	18.11		COMPRESSIVE STRENGTH			ND	
GRANULOMETRIC CURVE							
CHEMICAL ANALYSES							
Total cations content % w.t.	Na ₂ O	K ₂ O	CaO	MgO	Fe ₂ O ₃	Al ₂ O ₃	SiO ₂
	0.49	0.55	33.16	3.42	2.23	2.80	24.03
Cations soluble in HCl 0.1 N % w.t.	Na ₂ O	K ₂ O	CaO	MgO	Fe ₂ O ₃	Al ₂ O ₃	SiO ₂
	0.04	0.23	30.78	1.08	0.58	1.15	0.59
Water soluble salts % w.t.	Cl ⁻	NO ₃ ⁻	SO ₄ ²⁻	Loss on Ignition %			33.33
	0.02	0.01	<0.01				
Py-GC-MS spectrum	ND						

Table 33 Palace of Aegae, mosaic B, outer frame: results of the laboratory analyses on the mortar layer n. 3.

Sample: 4M2-3		CHARACTERIZATION FORM	
OPTICAL MICROSCOPY (Figure 140, Figure 141 in Appendix)			
Stratigraphy	Layer 3	Munsell colour	Very pale brown 10YR8/3
Microscopic description of the binder on thin section			
Structure	Not homogeneous	Reaction with the aggregate	None visible
Texture	Micritic	Shape of pores	From sub-circular to irregular
Microscopic description of the aggregate on thin section			
Granulometry	Maximum size: 0.7 mm Most abundant sizes: 0.5-0.25 mm, 0.25-0.125 mm	Roundness	From subangular to rounded
Sorting	Moderately sorted $\sigma = 1.00 \text{ } \emptyset$	Distribution	Not homogeneous
Shape	Natural	Orientation	None
Sphericity	From high to low	Mineralogic and petrographic composition	Quartz, k-feldspar, serpentinite, marble, quartzite, schist, limestones (dismicrite, mudstone; oosparite, grainstone).
Classification of the aggregate		Fluvial sand	
OPEN POROSITY %	ND	COMPRESSIVE STRENGTH	ND
GRANULOMETRIC CURVE	ND		
CHEMICAL ANALYSES			
Total cations content % w.t.	ND		
Cations soluble in HCl 0.1 N % w.t.	ND		
Water soluble salts % w.t.	ND	Loss on Ignition %	ND
Py-GC-MS spectrum	ND		

5.2. Discussion

The results of the *in situ* and laboratory analyses indicated that the characteristics of the studied substrates vary with respect to the type of surface upon which they were built and to the ancient use of the room where the pavements are placed.

The foundation surface and the stratigraphy of the substrate

In the case of pavements built upon natural levelled ground, like the mosaics of the two banquet halls of the Palace of Aegae in Vergina (Figure 68), the mosaic of the *Augusteum* in the ancient city of Dion (Figure 14), and the mosaics of the *cubiculum* and the *tablinum* of the “Villa delle Muracche” in Tortoreto (Figure 40, Figure 43), the substrate is composed of four preparatory layers.

In the case of pavements built on structures elevated above the ground, two different substrate stratigraphies have been observed: the pavement fragments A, B and D stored in the “Cortile Romano” in Florence (Figure 52, Figure 55, Figure 58), have substrates constituted by two layers; the mosaics of the lavatory in the Polygon and of the bathhouse of Villa Dyonisos (Figure 29, Figure 35), both in Dion, have substrates similar to those of the pavements A, B and D of the “Cortile Romano” but for the presence of one more thin layer at the bottom of the substrate.

Pavements built on artificial backfilled ground, like the mosaics of the *atria* of the House of Epigenes and of the House of Eubulus, both in Dion, showed to have a thin (about 4 cm) substrate composed of a single mortar layer, beside the *tessellatum* (Figure 19, Figure 24).

In the case of the mosaic of the Roman Villa in Classe, Ravenna, as already mentioned in the section 5.1.3, it has not been possible to determine with sufficient certainty the type of foundation ground upon which the mosaic was built. In fact, the lower limit of the first of the three layers of the pavement was not clearly recognizable. This layer could maybe be interpreted as artificial infill material, used to cover previous structures, upon which a thin substrate represented by the 2nd and the 3rd recognized layers, was built (Figure 47, Figure 48). The type of foundation ground stayed unclassified also in the case of the pavement E stored in the “Cortile Romano” in Florence, where the 1st layer is made of well rounded stones up to 10 cm in diameter, upon which a superficial, beaten and polished mortar layer is laid (Figure 60, Figure 61, Figure 62).

Characteristics and function of the first preparatory layer of substrates built on ground

As already stated by L.B. Alberti in his “Ten Books on Architecture” [Alb65], the function of the first foundation layer of a pavement is to protect the upper layers from uprising humidity. The description of the 1st preparatory layer given by Alberti (see section 2.1) matches with that of the 1st layer of the Hellenistic pavements of the Palace of Aegae, made of stones laid on natural levelled ground, without any mortar (Figure 64). Nevertheless, the same protective function can be attributed also to the first layer in contact with the natural ground of the Roman pavements, which is instead made of a mortar composed of calcitic lime mixed with fluvial sand and gravel (Figure 13) and, in the case of the “Villa delle Muracche”, also with brick fragments with dimensions of several centimetres (Figure 39, Figure 42). In fact, the results of the laboratory analyses indicated that this mortar has a low open porosity due to the use of a poorly sorted aggregate composed of low porous rock types [Pec08, Ste05] (Figure 78, Figure 79 in appendix). The Roman pavements built upon natural ground (*Augusteum, cubiculum, tablinum*) showed to have a 1st foundation layer characterized by both high thickness and low open porosity. This datum is probably to be connected with the fact that since laid on natural ground, the pavement is at higher risk of uprising humidity penetration, so it needs a first foundation layer that assures proper protection against it, which is to be reached through both a high layer thickness and low mortar porosity.

Pavements built upon artificial backfilled ground (House of Epigenes, House of Eubulus) showed to have instead a substrate made of a single mortar layer composed of calcitic lime mixed with fluvial sand and artificially crushed bricks (Figure 18, Figure 23). It is not clear whether this peculiarity is to be connected with the use of the room where these pavements are placed, or with the kind of foundation ground, or just with the money invested by the owner in the construction of the house. The fact that these pavements are both located in *atria* of Roman houses seems to support the first hypothesis. On the other hand, the reduced thickness of their substrate is maybe to be connected with the fact that the artificial ground upon which the mosaic’s substrate is founded could have been used to fill and level a structure including a previous pavement, whose presence would have made not necessary the construction of a “complete” new pavement’s substrate above it. Examples of pavements characterized by such a thin substrate can be found in two works by Wooton [Woo08] and Macchiarola *et alii* [Mac08], the latter referring to mosaics covering the floor of corridors in a Roman bathhouse dated to the 3rd century A.D. in the archaeological site of Torretta Vecchia, Livorno, Italy.

Characteristics and function of substrates built on elevated structures

In the case of pavements built on structures elevated above the ground, the characteristics of the substrate are mostly related to the function of the pavement in the room where it is placed, in the specific Roman baths and lavatories.

– *Roman Baths*

The fragments A, B and D stored in the “Cortile Romano” probably belonged to a pavement that was built upon *pilae* stacks, which are pillars that served to allow the hot air to freely circulate underneath the pavement and heat the room [Alb65] (Figure 50). Above *pilae* stacks it was also built the mosaic of the bathhouse of Villa Dyonisos (Figure 34). However, the substrates of the two pavements show some differences. In the case of the “Cortile Romano”, the substrate is composed of two mortar layers the first of which, about 25 cm thick, is made of a mortar composed of calcitic lime mixed with artificially crushed bricks, the so called *cocciopesto* (Figure 51, Figure 54, Figure 57), laid directly upon the *pilae* tiles. Above this layer a thin (about 2 cm) mortar layer was applied to bed the large marble slabs constituting the surface of the floor (Figure 52, Figure 55, Figure 58). In the case of Villa Dyonisos, an additional thin (2 – 3.5 cm) layer made of a mortar composed of calcitic lime mixed with fluvial sand and gravel (Figure 28, Figure 33) constitute the 1st layer of the substrate. The 2nd layer of this substrate can be considered the equivalent of the 1st layer of the pavement in the “Cortile Romano”, though is much thinner than it (Figure 35). This lower thickness is probably to be connected with the fact that in the case of Villa Dyonisos the surface of the pavement is made of *tesserae* with average size no bigger than 3 cm, which being lighter than the marble slabs of the pavement stored in the “Cortile Romano” did not need a same thick substrate. Further reasons could be related with the dimensions of the rooms, maybe smaller in the case of the pavement in Dion.

– *Roman lavatories*

The mosaic of the Vespasian (lavatories) of the *Polygon*, in the ancient city of Dion, was built upon a structure elevated above the ground, composed of an outer wall made of bricks and stones that is delimitating an internal area backfilled with artificial ground. The mosaic’s substrate, laid upon this structure, is composed of three preparatory layers of mortar whose characteristics are similar to those of the mortar layers of the substrate of the mosaic of Villa Dyonisos, described in the previous paragraph.

Characteristics and function of the fourth mortar layer

The mortar of the 4th layer of the mosaic of the *Augusteum* is composed by calcitic lime mixed with aggregates (artificially crushed marble dusts) selected to make the mortar fulfil aesthetic harmonization with the colour of the *tesserae* (Figure 84, Figure 85 in appendix). The same scope was maybe reached, in the mortar of the 4th layer of the mosaic B of the Palace of Aegae (Figure 136, Figure 137 in appendix), by painting its surface.

Open porosity of the different mortar layers

The results of the open porosity test indicated that for each of the studied substrates but for that of the mosaic of the Roman Villa in Ravenna, the mortar of the 1st layer has lower open porosity than that of the upper layers (Figure 71). This datum can be again connected with the granulometric distribution and the nature of the aggregates in the mortars. The aggregate of the mortars of the 2nd and 3rd layer can be defined granulometrically well sorted, which means that it misses smaller grains that can fit into the spaces left by the bigger ones, resulting in higher shrinking phenomena of the binder and, consequently, in an increased porosity [Pec08]. On the other hand, the aggregate of these mortars contains a high percentage of brick fragments (Figure 80, Figure 82 in appendix), which with their own porosity further contribute to increase the porosity of the mortar [Pec08, Ste05].

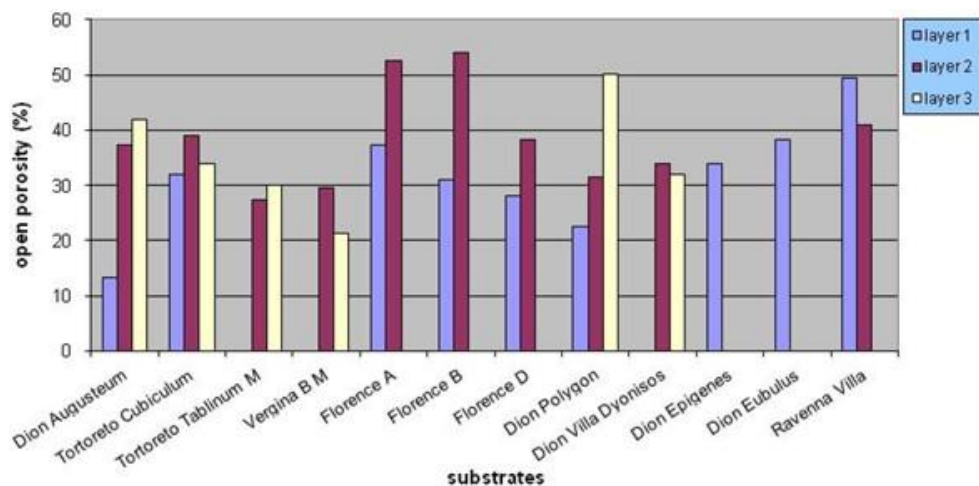


Figure 71 Open porosity of the preparatory mortar layers of the studied pavements.

Always looking at the graph of Figure 71, it can be seen that in most of the cases the mortar layer occupying the highest position in the substrate has higher open porosity than that of the lower layers. This is especially true in the cases where this layer is also the bedding layer of the elements (large *tesserae* or marble slabs) constituting the surface of the pavement (Florence A, B, D, Polygon). The higher porosity of this mortar could be related with the fact

that probably these layers needed to have high workability, because they had to be levelled to give to the pavement the right inclination, or were used to bed the elements constituting its surface (*tesserae* or marble slabs), which were inserted into the mortar before it set. The desired workability was probably reached using more water in the mortar mix, which resulted in a higher porosity of the final product [Pap06, Pec08]. As a confirmation that these mortar layers were spread with special procedures, their aggregate grains are mostly oriented with their longer edge sub-parallel to the surface of the layer (Figure 94, Figure 106 in appendix), so as of the pavement, which indicates that a pressure was applied by the craftsmen while spreading the mortar [Pec08].

Compressive strength of the different mortar layers

In Figure 72, the results of the compression tests, which because of the exiguity of some of the samples have been executed only on a reduced number of the studied mortar layers, are showed. In the graph, it can be observed that in the Roman pavements the 2nd layer of substrates built on natural ground seems to be the one characterized by the highest strength (*Augusteum*, *cubiculum*). The same it can be said, in the pavements built upon elevated structures, for the 1st layer of the pavements A and B stored in the “Cortile Romano” and for the 2nd layer of the mosaics of the Polygon and of Villa Dyonisos in Dion, which can all be considered to have the same function within the substrate. On the whole, it can be said that these layers represent the main structural elements of the pavement, the ones that make it resistant to loads.

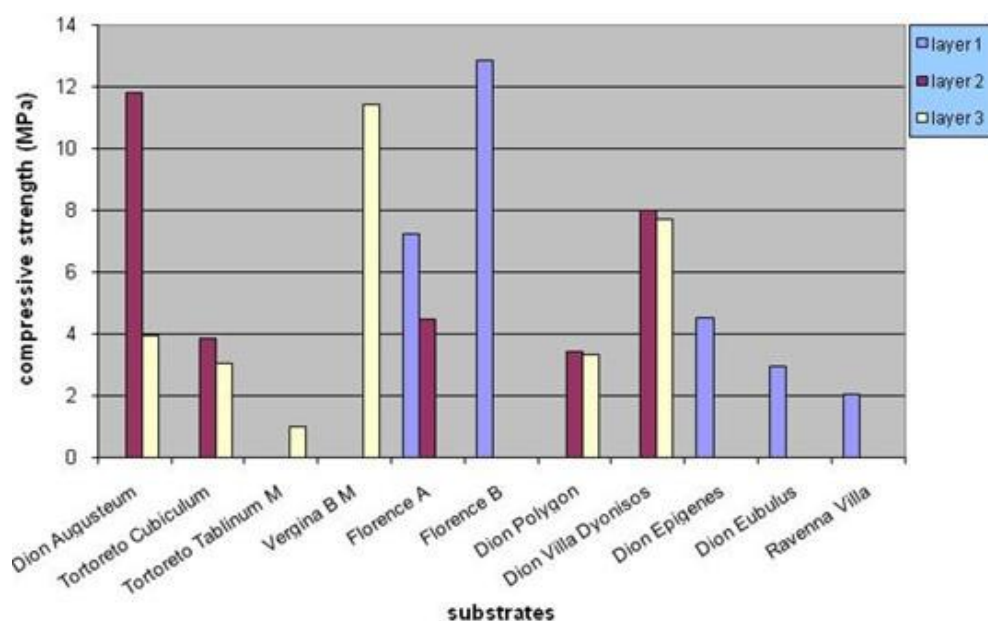


Figure 72 Compressive strength of the preparatory mortar layers of some of the studied pavements.

Hydraulic properties of the different mortar layers

The combined results of the optical microscopy observations and of the chemical analysis of the acid soluble binder enriched fraction (granulometric fraction of particle size smaller than 75 μm), indicated that most of the studied mortar layers have hydraulic properties due to the addition of pozzolanic materials to an air lime binder (see section 2.6.3). In Figure 73, the results of the chemical analysis of the HCl 0.1 N soluble granulometric fraction < 75 μm of the studied mortar layers are showed. In the graph, the $\text{SiO}_2 + \text{Al}_2\text{O}_3 + \text{Fe}_2\text{O}_3$ content is plotted versus the $\text{CaO} + \text{MgO}$ content. The quantity of silica and alumina detected by this kind of analysis is supposed to be indicative of the content of calcium silicates and aluminates hydrates [Pue94a, Mid04], which are hydraulic compounds that formed in the reaction of the pozzolanic materials with lime and water in the mortar mixture (see section 2.5.1.3). The position of the samples in the area of the graph in Figure 73 is then representative of the hydraulicity of the mortars.

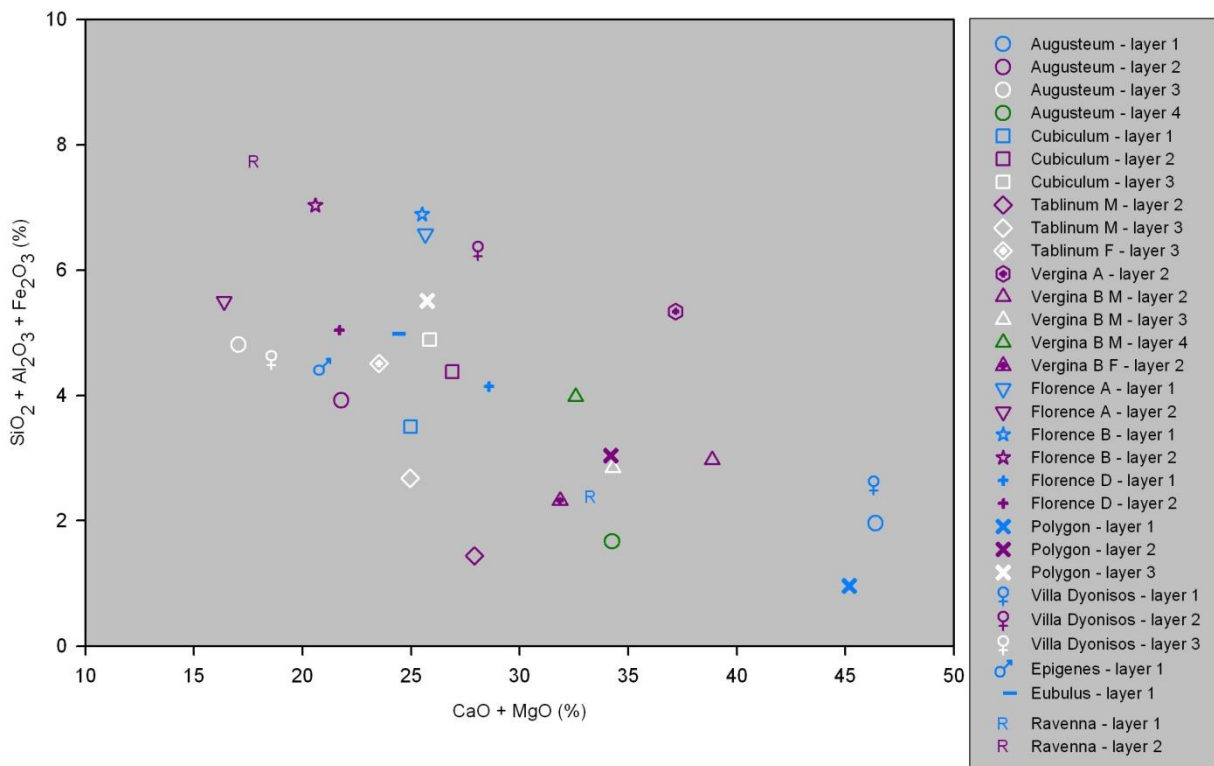


Figure 73 $\text{SiO}_2 + \text{Al}_2\text{O}_3 + \text{Fe}_2\text{O}_3$ content versus $\text{CaO} + \text{MgO}$ content of the HCl 0.1 N soluble fraction of particle size < 75 μm of the studied mortar layers. The mortar layers of a same pavement are indicated by a same symbol. 1st layers are indicated in blue colour, 2nd layers in purple, 3rd layers in white, 4th layers in green.

It can be seen that in the case of the mosaics of the *Augusteum*, of the Polygon and of Villa Dyonisos, all in Dion, while the mortars of the 1st layer of the substrate can be defined as air mortars, those of the 2nd and 3rd layer have a certain grade of hydraulicity. Furthermore, in the

case of the mosaics of the *Augusteum* and of the Polygon, the hydraulicity of the mortar of the 3rd layer seems to be higher than that of the 2nd layer. The same trend could be maybe recognized also in the case of the pavement fragments B and D stored in the “Cortile Romano” in Florence, where the mortar of the 2nd layer showed a slightly higher grade of hydraulicity than that of the 1st layer. The higher hydraulicity of the mortars of these layers is probably due to the fact that they contain brick fragments of finer granulometric size than those contained in the underlying mortar layer. In fact, as it is known, to a finer granulometric size of the pozzolanic material corresponds a higher pozzolanic reactivity [Bar97, All03]. To the same reason is probably due the higher hydraulicity of the mortar of the 2nd layer with respect to that of the 1st layer of the mosaic of the Roman Villa in Ravenna where, as indicated by the optical microscopy observations, in addition to brick fragments, volcanic sand (pozzolana) was used as pozzolanic material (Figure 112, Figure 113, Figure 114, Figure 115 in appendix).

Always looking at the graph, it can be observed that the single (beside the *tessellatum*) mortar layer of the thin substrates of the mosaics of the *atria* of the House of Epigenes and of the House of Eubulus, in Dion, have a grade of hydraulicity that is similar to that of the 3rd layer of the mosaics of the *Augusteum*, of the Polygon and of Villa Dyonisos, as well as to that of the 2nd layer of the pavement D in Florence. Considering the other similarities existing among these layers in terms of open porosity, compressive strength and granulometry, it can be said that the single mortar layer of the mosaics of the two *atria*, built on artificial backfilled ground, plays within the pavement the same role as the 3rd layer of the other above mentioned pavements. For such a reason, it can be said that in the construction of a pavement upon artificial backfilled ground it was maybe made the assumption, as already mentioned before, that the artificial ground and the previous structures covered by it, played in the new pavement the role of the lower part of the substrate.

In the case of the mosaics of the *cubiculum* and the *tablinum* of the “Villa Romana delle Muracche” in Tortoreto, all the mortar layers of the substrates showed to have a similar grade of hydraulicity, included the mortar of the first layer of the mosaic of the *cubiculum*, where the brick fragments, having big dimensions and being present in low quantities could hardly be responsible of the detected grade of hydraulicity. For such a reason, it can be hypothesized that a limestone containing a certain percentage of clay was used for the calcination process, which determined the production of a slightly hydraulic lime that was used to prepare the mortars of all the layers. The plausibility of this hypothesis is strengthened by the results of a

series of analyses I performed on the stone *tesserae* of the mosaics of the Villa before the beginning of the present research. The analyses, which aimed at the characterization of the materials of the mosaics in view of a restoration intervention, revealed that the mosaics' *tesserae* were made using an argillaceous limestone of local provenance that was likely the same used for the lime production process.

In the graph of Figure 73, it can be seen also that the mortar layers of the mosaics of the Palace of Aegae in Vergina have homogeneous characteristics when hydraulicity is concerned. Considering also the results of the optical microscopy observations, it can be said that the hydraulicity of these mortars is due to the addition of natural pozzolanic material, namely volcanic sand (*pozzolana*), to an air lime binder, in a constant proportion and granulometric size in the mortars of all the layers (Figure 130, Figure 131, Figure 138, Figure 139).

Organic additives content of the mortar layers

The results of the investigation of the presence of organic additives in the binder enriched fraction (granulometric fraction of particle size $< 63 \mu\text{m}$) of seven of the studied mortar layers are showed in Table 2, Table 3, Table 4, Table 15, Table 20, Table 22 and Table 30. Of the four analytical methods applied (see section 4.2.5.4), the only pyrolysis/methylation with tetramethylammonium hydroxide (TMAH) in combination with online GC-MS detected a series of fatty acids methyl esters in the analysed mortars. The series includes both saturated (lauric C12, myristic C14, palmitic C16, stearic C18), and unsaturated (oleic C18:1) fatty acids. The methyl esters of stearic, palmitic, oleic and miristic acid are common in the composition of siccative oils [Chi01, Chi04, Fab05] but the marker for the presence of siccative oils, the azelaic acid, which is produced with the aging of the oil [Chi01, Chi04] it has not been detected. On the other hand, the presence of the lauric acid methyl ester could suggest the use of additives of animal origin [Fab09] containing this fatty acid, like cow's and goat's milk, both used as additives in mortars in the past [Dav65, Sic81, Arc01]. Nevertheless, it must be pointed out that since the distribution of the peaks is very similar in all the obtained spectra, there is the possibility of the presence of a contamination of all the samples, of which one should be aware in the interpretation of the results. In conclusion, it can be said that it was not possible with the employed techniques to determine with a sufficient grade of certainty the origin of the organic content of the studied mortars.

Soluble salts content of the mortar layers

The analysis of the water soluble salts content by means of ion chromatography registered no relevant concentrations of Cl^- , NO_3^- , SO_4^{2-} in the mortar layers of all the substrates under study but in that of the mosaic of the Roman Villa in Classe, Ravenna. In this case chloride salts have been found, with higher concentrations in the lower part of the substrate's stratigraphy. Presence of chlorides in buried structures is probably related, in the area of Ravenna, to underground sea water upraise phenomena [Gia07].

5.3. Practical application of the results

5.3.1. Suggestions for the design of repair mortars for pavements

Basing on the results obtained by the work of the RILEM TC167-COM on the requirements for mortars meant to repair or replace historic mortars, Papayianni [Pap08] specified which are the functional and technical requirements needed in the case of flooring repair mortars. On the base of the results of the present research, it has been considered relevant to underline, referring to the investigated case studies, some of the aspects to be taken into consideration when designing repair mortars for pavements, most of them already mentioned in the work by Papayianni. The results of the investigated case studies indicated that the characteristics of the mortars constituting the foundation layers of a pavement are related with the function of each layer within the pavement's structure and with the function of the pavement itself in the room where it is placed. In the specific, the number and thickness of the mortar layers, the granulometric distribution of the aggregate, the open porosity, the compressive strength and the hydraulicity grade of the mortars, vary according to the kind of surface on which the pavement is built (natural levelled ground, artificial backfilled ground, elevated structures), to the use of the room where the pavement is placed (baths and lavatories on one side, rooms without special facilities on the other) and to the type surface of the pavement (marble slabs, large or small *tesserae*). For such a reason, the whole stratigraphy of the pavement's substrate should be investigated, paying attention that the type of surface upon which the preparatory layers are founded is correctly classified, and that the size of the elements (*tesserae* or marble slabs) constituting the surface of the pavement is taken into consideration. Once the structure of the pavement and its context are determined, the mortar of each single layer has to be characterized from the mineralogical, petrographical, granulometric, physical, mechanical and chemical point of view [Van04, Pap08]. Mortars design should be then based on the understanding of the relationship between the characteristics and the function of the mortar layer within the pavement. The data obtained by the characterization of the mortars, if

interpreted in conjunction with those coming from the analysis of the pavement context (type of foundation surface, use of the room, type of pavement's surface) will be useful to understand the role played by each layer within the considered pavement's substrate. With this kind of information at disposal, it will be possible to design a new mortar that would keep unaltered the functional role of the layer that it is replacing or repairing within the considered pavement.

5.3.2. A model for the documentation of ancient pavements in the conservation practice

Considering the large amount of information that, as it has been proved, can be obtained investigating a pavement following a methodology like the one illustrated in this thesis, it has been considered relevant to propose a model for a detailed documentation of ancient floors. This model could be based on the kind of information obtained through the methodology adopted for each of the investigated case studies, and therefore include the following description fields:

- stratigraphy of the pavement's substrate;
- type of surface upon which the pavement is built;
- ancient use of the room where the pavement is placed;
- type of pavement's surface;
- mineralogical, petrographical, chemical, physical, mechanical characteristics of the mortars of each of the preparatory layers.

5.3.3. Suggestions for the presentation of ancient pavements *in situ* and in museums

The data obtained from the study of ancient pavements conducted according to a methodology like the one adopted in the present research could be elaborated to be presented to public together with the pavement, either it is conserved *in situ* or in a museum. One kind of information suitable for presentation to public could be the influence on the technology of the pavements of factors such as the kind of foundation surface and the ancient use of the room containing the pavement. For instance, considering the results of the investigated case studies, it would be important to present to an hypothetical visitor of the archaeological site of Dion how the characteristics of the mosaics' substrate vary from the four preparatory layers laid on natural levelled ground of the mosaic of the Augusteum, to the single foundation layer spread on artificial backfilled ground of the mosaics of the *atria* of the Roman houses of Epigenes and Eubulus, to the three preparatory layers of the small mosaic of the lavatories in the Polygon, built on a trapezoidal platform made of stones and brick elevated above the ground,

to the three mortar layers laid on *pilae* stacks of the bathhouse of Villa Dyonisos. The best way to present these data in case of mosaics conserved *in situ* is probably illustrating them by means of both text and figures on presentation boards, to be mounted next to the entrance of the building or the room containing the mosaic. In Figure 74, an example of this kind of presentation board, exposed at the entrance of the “Villa Romana delle Muracche” in Tortoreto, is showed.



Figure 74 Presentation board illustrating the stratigraphy of the substrate of one of the mosaic of the Villa and the description of the mortar layers. The drawing of the substrate is by Claudio Giampaolo (courtesy of Soprintendenza Archeologica per l’Abruzzo).

In the case of presentation in museums, the additional task of resembling to the public the original context of the pavement has to be faced. In this case, the presentation boards should contain also pictures of the pavement *in situ* and graphic reproductions of the architectural complex to which it belonged. Further solutions aimed at recovering the functional value of the pavement could be also taken into consideration in this case. One of them could be the presentation to public of three-dimensional models reproducing the pavement in reduced or real scale, with a cross section of its substrate visible. An example of the application of this kind of solution can be found in the Archaeological Museum of Dion (Figure 50, Figure 75, Figure 76, Figure 77).

In the specific case of the “Cortile Romano” of the Archaeological Museum of Florence, the pavement fragments A, B and D could be restored, reassembled and re-laid upon *pilae* stacks perhaps reconstructed with the original *pilae* tiles also stored in the same courtyard. This way the considered artefact would recover much of its original significance and, if presented to public accompanied with a description board, it would acquire a considerable didactic potential.



Figure 75 Archaeological Museum of Dion, Greece: real scale reconstruction of the structure of a pavement built on natural levelled ground.



Figure 76 Archaeological Museum of Dion, Greece: real scale reconstruction of the structure of the pavement of a Roman bath built on *pilae* stacks.



Figure 77 Archaeological Museum of Dion, Greece: real scale reconstruction of the structure of the pavement of a Roman bath built on *pilae* stacks.

Chapter 6

Conclusions

6.1. Results of the research

This thesis has focused on the study of the materials, the function and the technology of ancient pavements' substrate. The theoretical section included a review of the literature on ancient pavements' study, which evidenced that only in a reduced number of works the investigation takes account of the whole structure of the pavement, and that only an even smaller number of studies contain hypotheses on the function of the different preparatory layers of the pavement. The theoretical section included also an overview of the modern practice in mosaic conservation, which underlined the constant need of enhancements in the fields of maintenance, documentation and presentation to public of ancient pavements.

Five case studies represented by archaeological sites containing floor mosaics and other kind of pavements, dated to the Hellenistic and the Roman period, have been investigated by means of *in situ* and laboratory analyses. The characteristics of the studied pavements, namely the number and the thickness of the preparatory layers, and the properties of the mortars constituting them, vary according to the ancient use of the room where the pavements are placed and to the type of surface upon which they were built. In the specific, rooms in bathhouses (Villa Dyonisos, pavements A, B and D in the "Cortile Romano") and lavatories (Polygon) had pavements built on structures elevated above the ground which were created to serve the particular function of the room. These pavements have substrates with common characteristics made of two or three mortar layers, the thickness of which varies depending on the size of the elements (either large *tesserae* or marble slabs) constituting the surface of the pavement and maybe also according to the dimensions of the room. On the other hand, rooms which did not contain special facilities or equipments, such are the temple (*Augusteum*), the hall (*atria* of the Houses of Epigenes and Eubulus), the bedroom (*cubiculum*), the office (*tablinum*), the banquet hall (mosaic A and B in the Palace of Aegae), had pavements built either on natural levelled ground or on artificial backfilled ground. These pavements have "complete" substrates composed of four layers when built on natural ground (*Augusteum*,

cubiculum, *tablinum*, mosaic A and B in the Palace of Aegae), and thin substrates composed by a single layer when built on artificial backfilled ground (*atria*). The first layer has, in pavements built on natural ground, the function to protect the upper layers of the substrate from uprising humidity. Instead, in pavements built on artificial backfilled ground, it was maybe made the assumption that this function was fulfilled by the artificial ground itself together with the previous structure that was covered by it. In all the substrates there are two layers which were made with a mortar having hydraulic properties due to the addition of pozzolanic materials (brick fragments and/or volcanic sand) to an air lime binder. The thicker of these two layers, placed below the other in the substrate, is, thanks to its mechanical strength, the main structural element of the pavement, the one that makes it resistant to loads. The upper layer is made of a mortar that needed to have high workability since it was levelled to give to the pavement the right inclination and, in some cases, the elements constituting the surface of the pavement (either *tesserae* or marble slabs) were inserted directly into it before the setting. The mortar of the 4th layer had also aesthetic functions, which were fulfilled either by using selected aggregates (artificially crushed marble dusts in the case of the mosaic of the *Augusteum*) or by painting its surface (mosaic B of the Palace of Aegae).

The results of the analyses contributed to the understanding of the function and the technology of the pavements' substrate and to the characterization of its constituent materials. Furthermore, the research underlined the importance of the study of the whole structure of the pavement, included the foundation surface, in the interpretation of the archaeological context where it is located.

A series of practical applications of the results of the research have been suggested:

- The design of repair mortars for pavements should be based on the understanding of the relationship between mortar's characteristics and function within the pavement, so as the new mortar would keep unaltered the functional role of the layer that it is replacing or repairing within the considered pavement;
- A model for a detailed documentation of ancient floors could be based on the kind of information obtained through the analytical methodology adopted for each of the investigated case studies;
- The data obtained from the study of ancient pavements conducted according to a methodology like the one adopted in the present research could be elaborated to be presented to public together with the pavement, either it is conserved *in situ* or in a museum.

6.2. Suggestions for further work

On the base of the results obtained in this work, some suggestions for further studies can be given:

- The Hellenistic and Roman pavements showed differences in the nature of the 1st layer of substrates built on natural ground and in the composition of the mortar of the upper layers, in the specific with regard to the kind of pozzolanic materials that were used. Nevertheless, since only two pavements dated to the Hellenistic period have been investigated, it has been not possible to make a comparison with the Roman pavements that would allow the formulation of hypotheses about eventual differences or similarities in the function of the different mortar layers of the substrate of pavements dating to the two periods. The investigation of further Hellenistic pavements and the integration with the data obtained so far would maybe make this possible.
- The mortar of the 4th layer, used to bed *tesserae* of average size up to 1 cm in the Roman pavements, although composed just by air lime mixed with artificially crushed marble dusts, showed to be extremely well manufactured and very well preserved. Its function consisted in both bedding the *tesserae* and fulfilling aesthetic harmonization with their colour. Also in the Hellenistic pavements the manufacturing of this mortar was taken under special care, it contained pozzolanic material (pozzolana), and its surface was painted. Further laboratory analyses to be performed on a broader number of samples collected from different mosaics could be aimed at detecting the presence of eventual additives in the mortar of this layer, at determining the nature of the used pigments and the exact purpose of their use.
- The data obtained by investigating each pavement through the proposed methodology could be used to create a database of the ancient pavements. This database could be used by experts of various disciplines (archaeologists, art historians, conservation scientists, restorers etc.) to compare pavements from different sites and gain information useful for their work.

References

- [Alb65] Alberti, L.B., 'Of Pavements according to the Opinion of Pliny and Vitruvius, and the Works of the Ancients', in *Ten Books on Architecture, translated by J. Leoni*, London (1965) 61-63.
- [All03] Allen, G.; Allen, J.; Elton, N.; Farey, M.; Holmes, S.; Livesey, P.; Radonjic, M., *Hydraulic Lime Mortar for Stone, Brick, and Block Masonry*, Donhead Publishing Ltd, Shaftesbury (2003).
- [Arc01] Arcolao, C.; Dal Bò, A., 'L'influenza delle sostanze proteiche naturali su alcune proprietà degli stucchi', in *Lo stucco: Cultura, Tecnologia, Conoscenza. Atti del Convegno di Studi Scienza e Beni Culturali, Bressanone, Libreria Progetto Padova* (2001) 527-538.
- [Aug03] Augenti, A.; Cirelli, E.; Mancassola, N.; Manzelli, V., 'Archeologia medievale a Ravenna: un progetto per la città ed il territorio', in *Atti del III Congresso Nazionale di Archeologia Medievale, Salerno, Ottobre 2003*, P. Peduto, Firenze (2003) 271-278.
- [Ban08] Bankart, G.P., *The art of the plaster*, B.T. Batsford, London (1908).
- [Bar97] Baronio, G.; Binda, L.; Lombardini, N., 'The role of brick pebbles and dust in conglomerates based on hydrated lime and crushed bricks', *Construction and Building Materials* **11** (1) (1997) 33-40.
- [Bea00] Beall, C., *Masonry and Concrete*, 1st edn, McGraw-Hill Professional, New York (2000).
- [Ber83] Bermond Montanari, G., *Ravenna e il porto di Classe. Vent'anni di ricerche archeologiche tra Ravenna e Classe*, Ravenna (1983).
- [Ber98] Beruto, D.; Botter, R.; Casarino, A.; Fieni, L.; Giordani, M.; La Rosa, C.; Mannoni, T.; Vecchiattini, R., 'New laboratory researches to produce lime putty with controlled microstructure', *Compatible Materials for Protection of European Cultural Heritage* **56** (2) (1998) 131-140.

- [Cag00] Cagnana, A., 'I Leganti, gli intonaci, gli stucchi', in *Archeologia dei materiali da costruzione. Manuali per l'Archeologia*, ed. G.P. Crogiolo and G. Olcese, S.A.P. s.r.l. (2000) 123-154.
- [Chi04] Chiavari, G.; Fabbri, D.; Prati, S., 'Effect of pigments on the analysis of fatty acids in siccative oils by pyrolysis methylation and silylation', *Journal of Analytical and applied Pyrolysis* **74** (2005) 39–44.
- [Chi01] Chiavari, G.; Fabbri, D.; Prati, S., 'In-situ Pyrolysis and Silylation for Analysis of Lipid Materials Used in Paint Layers', *Chromatographia* **53** (2001) 311-314.
- [Chl08] Chlouveraki, S.N.; Lugli, S.; Giannakaki, M.Y.; Politis, K.D., 'Observations on the technology of the Early Christian mosaics at the basilica of Saint Lot, Jordan', in *The 10th Conference of the International Committee for the Conservation of Mosaics, Conservation An Act of Discovery, Palermo, 20-26 October 2008* (unpublished).
- [Chl03] Chlouveraki, S.N.; Politis, K.D., 'The documentation and conservation of the nave mosaic in the basilica of Agios Lot at Deir 'Ain 'Abata, Jordan', in *Mosaics make a site: the conservation in situ of mosaics on archaeological sites. Proceedings of the VIth conference of the International Committee for the Conservation of Mosaics, Nicosia, Cyprus, 1996*, D. Michaelides (2003) 149-156.
- [Cor03] Corfield, M., 'A framework for the documentation of *in situ* mosaic conservation projects', in *Mosaics make a site: the conservation in situ of mosaics on archaeological sites. Proceedings of the VIth conference of the International Committee for the Conservation of Mosaics, Nicosia, Cyprus, 1996*, D. Michaelides (2003) 123-148.
- [Dav65] Davey, N., *A history of building materials*, Phoenix House, London (1965).
- [deG06] de Guichen, G.; Nardi, R., 'Mosaic conservation: fifty years of modern practice', *Conservation: the Getty Conservation Institute newsletter* **21** (1) (2006) 4-8.
- [Drd08] Drdácký, M.; Mašín, D.; Mekonone, M.D.; Slížková, Z., 'Compression tests on non-standard historic mortars specimens', in *HMC08 1st Historical Mortars Conference, Lisbon, 24-26 September 2008*.
- [Dro00] Drogou, S.; Saatsoglou Paliadeli, C., *Vergina: Wandering through the Archaeological Site*, Athens (2000).

- [Dun62] Dunham, R.J., ‘Classification of carbonate rocks according to depositional texture’, in *Classification of carbonate rocks: American Association of Petroleum Geologists Memoir*, ed. Ham, W. E. (1962) 108-121.
- [EN06] EN 1936:2006, *Natural stone test methods – Determination of real density and apparent density, and of total and open porosity*, European Committee for Standardization (2006).
- [EN94] EN 196-2:1994, *Methods of testing cement - Part 2: Chemical analysis of cement*, European Committee for Standardization (1994).
- [Fab09] Fabbri, D., personal communication.
- [Fab05] Fabbri, D.; Baravelli, V.; Chiavari, G.; Prati, S., ‘Profiling fatty acids in vegetable oils by reactive pyrolysis–gas chromatography with dimethyl carbonate and titanium silicate’, *Journal of Chromatography A*, **1100** (2005) 218–222.
- [Fio83] Fiore, F.P., ‘Capitolati e contratti nell’architettura borrominiana: un capitolo della letteratura artistica e della precettistica materiale in età barocca’, in *Ricerche di Storia dell’Arte* 11, Carrocci, Roma (1980) 17-34.
- [Fio02] Fiori, C.; Vandini, M., *Teoria e tecniche per la conservazione del mosaico. Collana i Talenti. Metodologie, tecniche e formazione nel mondo del restauro* 11, P. Cremonesi, Il Prato, Padova (2002).
- [Fio87] Fiori, C.; Donati, F.; Mambelli, R.; Racagni, P., ‘Studio della struttura e dei materiali presenti nei vari strati di due pavimenti musivi della zona archeologica di Ravenna’, in *Mosaico e restauro musivo Quaderni Irtec* 1, C. Fiori, R. Mambelli, Longo, Faenza (1988) 66-79.
- [Fol62] Folk, R.L., ‘Spectral subdivision of limestone types’, in *Classification of Carbonate Rocks - A Symposium: American Association of Petroleum Geologists Memoir* 1, ed. Ham, W.E. (1962) 62-84.
- [Fol59] Folk, R.L., 1959, ‘Practical petrographic classification of limestones’, *American Association of Petroleum Geologists Bulletin* **43** (1959) 1-38.
- [Geo08] Archaeological walk: City. *Dion Archaeological Park On-line Tour*. [Online] Geo Analysis, 2008. [Cited: 3 August 2009.] www.ancientdion.org.

- [Ghi08] Ghilardi, M.; Fouache, E.; Queyrel, F.; Syrides, G.; Vouvalidis, K.; Kunesch, S.; Styllas, M.; Stiros, S., 'Human occupation and geomorphological evolution of the Thessaloniki Plain (Greece) since mid Holocene', *Journal of Archaeological Science* **35** (2008) 111-125.
- [Gia07] Giambastiani, B.M.S.; Antonellini, M.; Oude Essink, G.H.O.; Stuurman, R.J., 'Saltwater intrusion in the unconfined coastal aquifer of Ravenna (Italy): A numerical model', *Journal of Hydrology* **340** (2007) 91– 104.
- [Got78] Gottardi, V., *I Leganti*, Pàtron, Bologna (1978).
- [Gro04] Groot, C., 'Glossary', in *Characterisation of Old Mortars with Respect to their Repair – Final Report of RILEM TC 167-COM*, ed. C. Groot, G. Ashall and J. Hughes, RILEM Publications SARL, (2004) 163-178.
- [Igm85] Institute of Geology and Mineral Exploration, *Geological Map of Greece 1:50000 Kontariotissa – Litochoro Sheet*, IGME (1985).
- [Igm82] Institute of Geology and Mineral Exploration, *Geological Map of Greece 1:50000 Veroia Sheet*, IGME (1982).
- [Idi82] Idil, Ali Cetin., 'Conservation and restoration of mosaics at Aphrodisias, Turkey', *International Committee for Mosaics Conservation, Newsletter/Chronique. Comite International pour la Conservation des Mosaiques* **5** (1982) 14-18.
- [Lap96] Lapenna, S., 'Villa Romana. Tortoreto, località Muracche', in *Documenti dell'Abruzzo Teramano IV, 1, Le Valli della Val Vibrata e del Salinello*, Fondazione Cassa di Risparmio della Provincia di Teramo Tercas spa, CARSA Edizioni (1996) 386-396.
- [Lav88] Lavagne, H., *Il mosaico attraverso i secoli*, Longo, Ravenna (1988).
- [Lop03] Lopreato, P.; Fiori, C.; Perpignani, P., 'Basilica di Santa Eufemia a Grado: storia, restauro e indagine scientifica', in *Les mosaïques: conserver pour présenter? VIIème conférence du Comité international pour la conservation des mosaïques, 22-28 novembre 1999, Arles, France: actes*, P. Blanc, V. Blanc-Bijon (2003) 177-190.
- [Mac08] Macchiarola, M.; Moh'd Saoud Abu Aysheh; Fiorella, G.; Fontanelli, R., 'Conservazione musiva e conoscenza: un binomio imprescindibile. Esempi di interventi in situ e in laboratorio', in *The 10th Conference of the International Committee for the*

Conservation of Mosaics, Conservation An Act of Discovery, Palermo, 20-26 October 2008 (unpublished).

[Mai91] Maioli, M.G., 'La topografia della zona di Classe', in *Storia di Ravenna, I, L'evo antico*, G. Susini, Venezia (1991) 375-414.

[Mar76] Mariani, E., *I leganti aerei e idraulici*, Ambrosiana, Milano (1976).

[Men92] Menicali, U., *I Materiali dell'edilizia storica. Tecnologia e impiego dei materiali tradizionali*, La Nuova Italia Scientifica, Roma (1992).

[Mid04] Middendorf, B.; Hughes, J.J.; Callebaut, K.; Baronio, G.; Papayianni, I., 'Investigative methods for the characterisation of historic mortars – Part 2: Chemical characterisation', in *Report rep028: Characterisation of Old Mortars with Respect to their Repair - Final Report of RILEM TC 167-COM*, ed. C. Groot, G. Ashall and J. Hughes (2004).

[Mon98] Montanaro, M.; Barboni, R.; Macchiarola, M., 'Trasporto e restauro del mosaico con tigre marina proveniente dall'area archeologica dell'antica Histonium (Vasto, Chieti)', in *Atti del V colloquio dell'Associazione italiana per lo studio e la conservazione del mosaico, Roma, 3-6 novembre 1997*, F. Guidobaldi, A. Paribeni, Edizioni del Girasole, Ravenna (1998) 385-398.

[Mos03] The Getty Conservation Institute and the Israel Antiquities Authorities, *Mosaics In Situ Project – Illustrated Glossary*, The Getty Conservation Institute (2003) 17 pp.

[Mun00] Munsell Soil Color Charts, Munsell Color Company (2000).

[Nar03] Nardi, R., 'The treatment of mosaics in situ', in *Mosaics make a site: the conservation in situ of mosaics on archaeological sites. Proceedings of the VIth conference of the International Committee for the Conservation of Mosaics, Nicosia, Cyprus, 1996*, D. Michaelides (2003) 187-202.

[Nor83] Commissione NORMAL, *Documento NORMAL 14/83 Sezioni sottili e lucide di materiali lapidei: tecnica di allestimento*, C.N.R. – I.C.R. (1983).

[Nor80] Commissione NORMAL, *Documento NORMAL 3/80 Materiali lapidei: Campionamento*, C.N.R. - I.C.R. (1980).

[Pan97] Pandermalis, D., *Dion*, Adam Editions, Athens (1997).

- [Pap08] Papayianni, I., ‘Requirements for flooring lime-based mortars’, in *HMC08 1st Historical Mortars Conference, Lisbon, 24-26 September 2008*.
- [Pap06] Papayianni, I.; Stefanidou, M., ‘Strength–porosity relationships in lime–pozzolan mortars’, *Construction and Building Materials* **20** (2006) 700–705.
- [Pap03] Papayianni, I.; Pacht, V., ‘Technology of mortars Used for the Substratum of Mosaics’, in *Proceedings of the 4th Symposium of the Hellenic Society for Archaeometry, Athens, 28-31 May 2003*, Y. Facorellis, N. Zacharias, K. Polikreti (2003).
- [Pec08] Pecchioni, E.; Fratini, F.; Cantisani, E., *Le malte antiche e moderne tra tradizione e innovazione*, Pàtron, Bologna (2008).
- [Peg62] Pegna, M.L., *Firenze dalle origini al medioevo*, Del Re Editore, Firenze (1962).
- [Pli71] Pliny, *Natural History*, W. Heinemann LTD, London (1971) Book XXXVI.
- [Pue94a] Puertas, F.; Blanco-Varela, M.T.; Palomo, A.; Ariño, X.; Ortega-Calvo, J.J.; Saiz-Jimenez, C., ‘Decay of Roman and repair mortars in mosaics from Italica, Spain’, *The Science of the Total Environment* **153** (1994) 123-131.
- [Pue94b] Puertas, F.; Blanco-Varela, M.T.; Palomo, A.; Ariño, X.; Ortega-Calvo, J.J.; Saiz-Jimenez, C., ‘Characterization of mortars from the mosaics of Italica: causes of deterioration’, in *III International Symposium on the Conservation of Monuments in the Mediterranean Basin, Venice, 22-25 June 1994*, V. Fassina, H. Ott and F. Zezza, Venice (1994) 577-583.
- [Ren03] Sivan, R., ‘Presenting mosaics to the public: an Israeli experience’, in *Mosaics make a site: the conservation in situ of mosaics on archaeological sites. Proceedings of the VIth conference of the International Committee for the Conservation of Mosaics, Nicosia, Cyprus, 1996*, D. Michaelides (2003) 313-319,
- [Rob95] Roby, T.C., ‘Site conservation during excavation: treatment of masonry, wall plaster and floor mosaic remains of a Byzantine church in Petra, Jordan’, *Conservation and management of archaeological sites* **1** (1995) 43-57.
- [Sat00] Soprintendenza Archeologica della Toscana, *Firenze Romana. La colonia Romana di Florentia: un itinerario didattico*, Sezione Didattica della Soprintendenza Archeologica della Toscana, Firenze (2000).

- [Sca83] Scavizzi, C.P., *Edilizia nei secoli XVII e XVIII a Roma. Ricerca per una storia delle tecniche. Quaderni del Ministero dei Beni Culturali e Ambientali, Ufficio Studi, n.6*, Roma (1983).
- [Sic81] Sickels, L.B., *Organic additives in mortars. Edinburgh Architecture Research Vol. 8*, University of Edinburgh, Dept. of Architecture, Edinburgh (1981) 7-20.
- [Ser69] Servizio Geologico d'Italia, *Carta Geologica d'Italia 1:100000 Foglio 133-134 Ascoli Piceno – Giulianova*, Reparto Riproduzione e Stampa E.I.R.A., Firenze (1969).
- [Ser67] Merla, G.; Bortolotti, V.; Passerini, P., *Note Illustrative della Carta Geologica d'Italia alla scala 1:100000 Foglio 106 Firenze*, Servizio Geologico d'Italia, Nuova Tecnica Grafica, Roma (1967).
- [Ser65] Servizio Geologico d'Italia, *Carta Geologica d'Italia 1:100000 Foglio 106 Firenze*, Istituto Italiano d'Arti Grafiche, Bergamo (1965).
- [Ser56] Servizio Geologico d'Italia, *Carta Geologica d'Italia 1:100000 Foglio 89 Ravenna*, Istituto Italiano d'Arti Grafiche, Bergamo (1956).
- [Ste05] Stefanidou, M.; Papayianni, I., 'The role of aggregates on the structure and properties of lime mortars', *Cement & Concrete Composites* **27** (2005) 914–919.
- [Ste06] Steward, J.D.; Neguer, J.; Demas, M., 'Assesing the protective function of shelters over mosaics', *Conservation: the Getty Conservation Institute newsletter* **21** (1) (2006) 16-19.
- [Tod75] Todua, T.I., 'Removal and restoration of the Bichvinta mosaic', in *Icom committee for conservation. 4th triennial meeting, Venice, 13-18 October. Preprints*, Icom, Paris (1975) 75113-1 -7.
- [UNI06] Norma UNI 11176, 2006, *Cultural heritage - Petrographic description of a mortar*, UNI Ente Nazionale Italiano Unificazione, Milan (2006).
- [UNI01] Norma UNI 10924, 2001, *Cultural heritage - Mortars for building and decorative elements - Classification and terminology*, UNI Ente Nazionale Italiano Unificazione, Milan (2001).
- [Van04] Van Balen, K.; Papayianni, I.; Van Hees, R.; Binda, L.; Waldum, A., 'Introduction to requirements for and functions and properties of repair mortars', in *Report rep028:*

Characterisation of Old Mortars with Respect to their Repair - Final Report of RILEM TC 167-COM, ed. C. Groot, G. Ashall and J. Hughes (2004).

[Vit62] Vitruvius, *On Architecture*, W. Heinemann LTD, London (1962) Book VII.

[Woo08] Wootton, W., 'Ancient mosaic technology and modern conservation: an archaeologist's perspective', in *The 10th Conference of the International Committee for the Conservation of Mosaics, Conservation An Act of Discovery, Palermo, 20-26 October 2008* (unpublished).

Appendix

Photomicrographs



Figure 78 Ancient city of Dion, mosaic of the *Augusteum*, cross section photomicrograph of mortar layer n. 1.

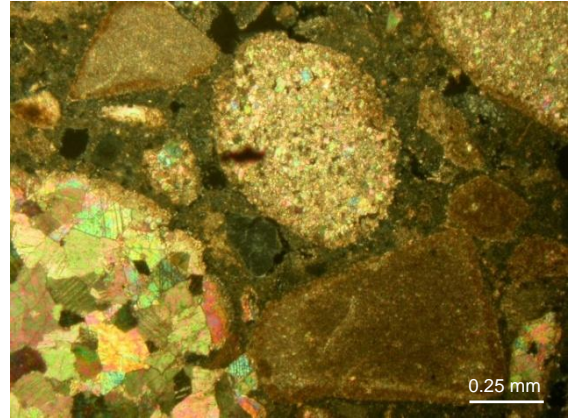


Figure 79 Ancient city of Dion, mosaic of the *Augusteum*, thin section photomicrograph of mortar layer n. 1 (crossed nicols).



Figure 80 Ancient city of Dion, mosaic of the *Augusteum*, cross section photomicrograph of mortar layer n. 2.

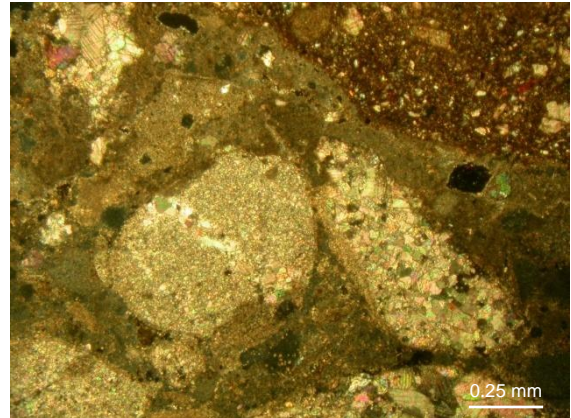


Figure 81 Ancient city of Dion, mosaic of the *Augusteum*, thin section photomicrograph of mortar layer n. 2 (crossed nicols).



Figure 82 Ancient city of Dion, mosaic of the *Augusteum*, cross section photomicrograph of mortar layer n. 3 and n.4.

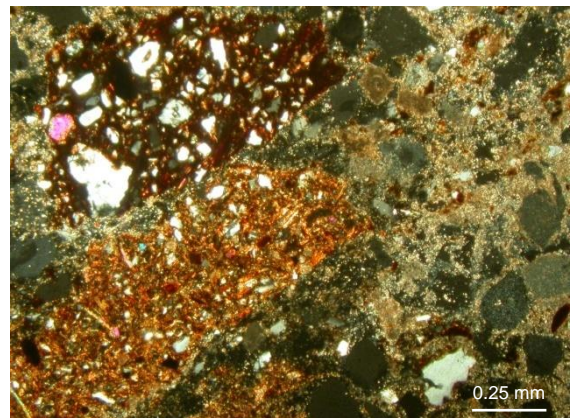


Figure 83 Ancient city of Dion, mosaic of the *Augusteum*, thin section photomicrograph of mortar layer n. 3 (crossed nicols).



Figure 84 Ancient city of Dion, mosaic of the Augusteum, cross section photomicrograph of mortar layer n. 3 and n.4.

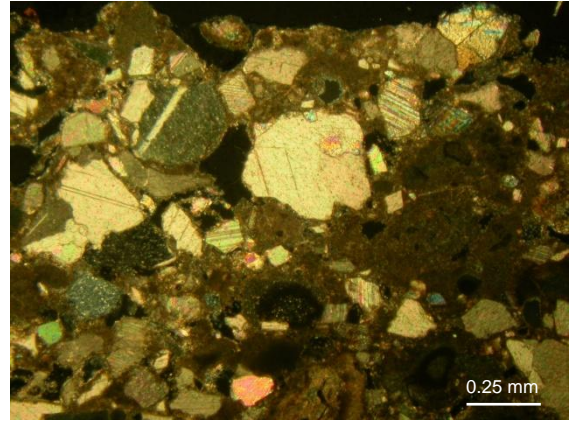


Figure 85 Ancient city of Dion, mosaic of the Augusteum, thin section photomicrograph of mortar layer n. 4 (crossed nicols).



Figure 86 Ancient city of Dion, mosaic of the House of Epigenes, cross section photomicrograph of mortar layer n. 1.

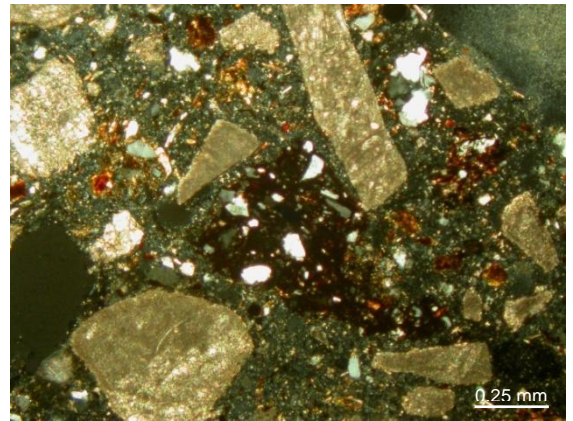


Figure 87 Ancient city of Dion, mosaic of the House of Epigenes, thin section photomicrograph of mortar layer n. 1 (crossed nicols).



Figure 88 Ancient city of Dion, mosaic of the House of Eubulus, cross section photomicrograph of mortar layer n. 1.

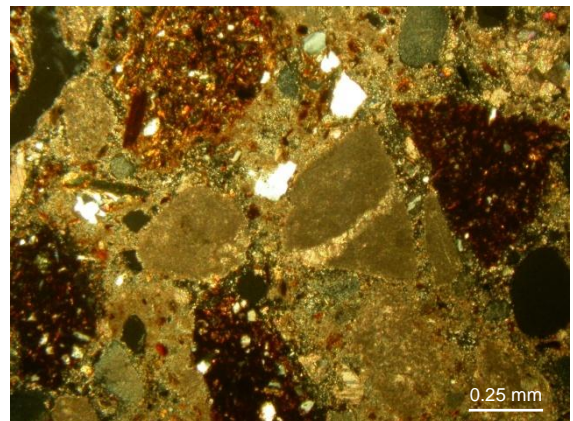


Figure 89 Ancient city of Dion, mosaic of the House of Eubulus, thin section photomicrograph of mortar layer n. 1 (crossed nicols).

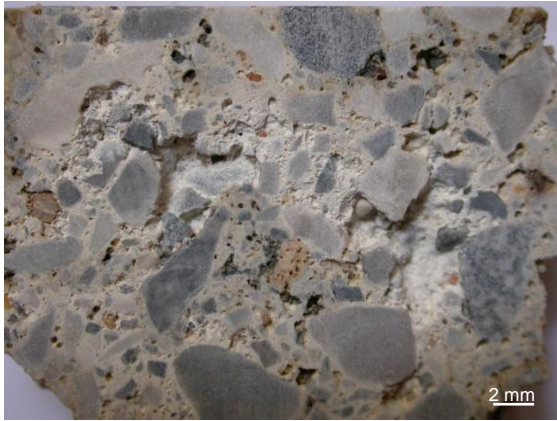


Figure 90 Ancient city of Dion, mosaic of the Polygon, cross section photomicrograph of mortar layer n. 1.

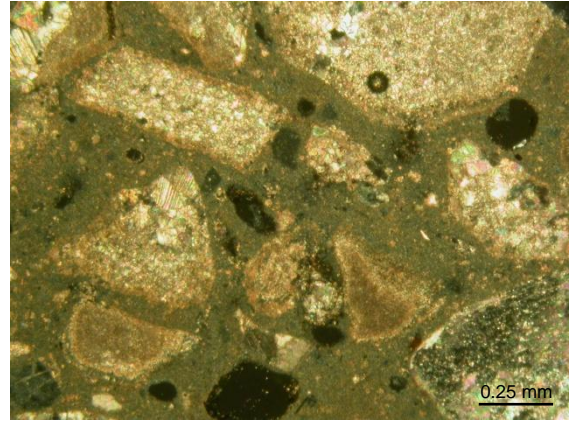


Figure 91 Ancient city of Dion, mosaic of the Polygon, thin section photomicrograph of mortar layer n. 1 (crossed nicols).



Figure 92 Ancient city of Dion, mosaic of the Polygon, cross section photomicrograph of mortar layer n. 2.



Figure 93 Ancient city of Dion, mosaic of the Polygon, thin section photomicrograph of mortar layer n. 2 (crossed nicols).



Figure 94 Ancient city of Dion, mosaic of the Polygon, cross section photomicrograph of mortar layer n. 3.

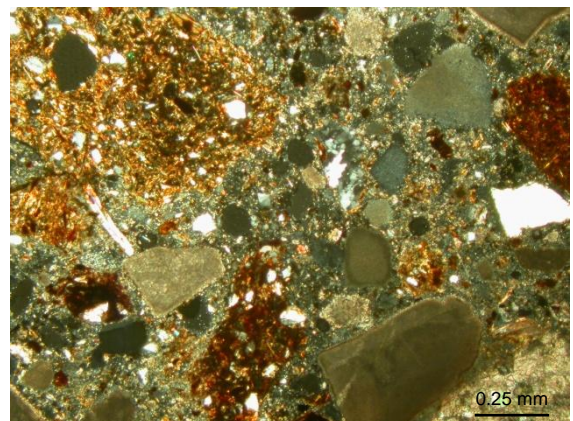


Figure 95 Ancient city of Dion, mosaic of the Polygon, thin section photomicrograph of mortar layer n. 3 (crossed nicols).

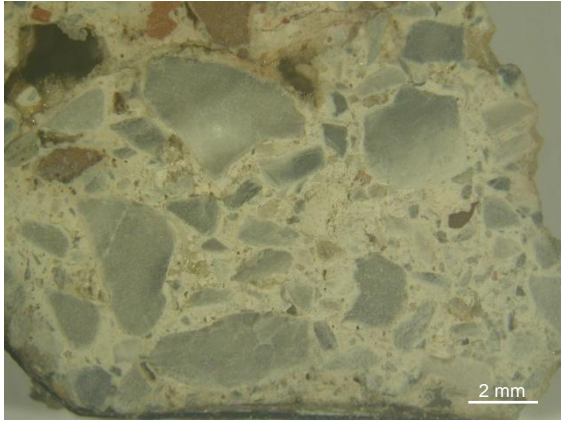


Figure 96 Ancient city of Dion, mosaic of Villa Dyonisos, cross section photomicrograph of mortar layer n. 1.

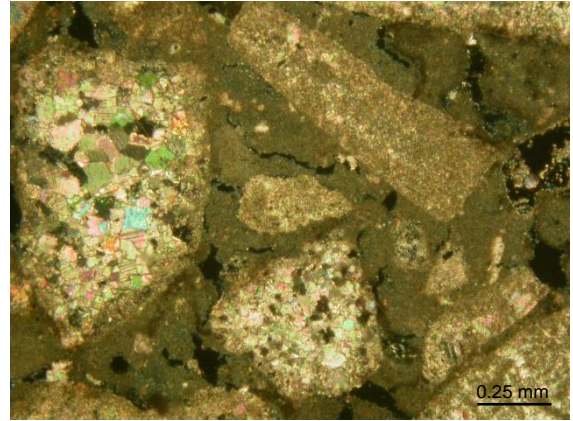


Figure 97 Ancient city of Dion, mosaic of Villa Dyonisos, thin section photomicrograph of mortar layer n. 1 (crossed nicols).

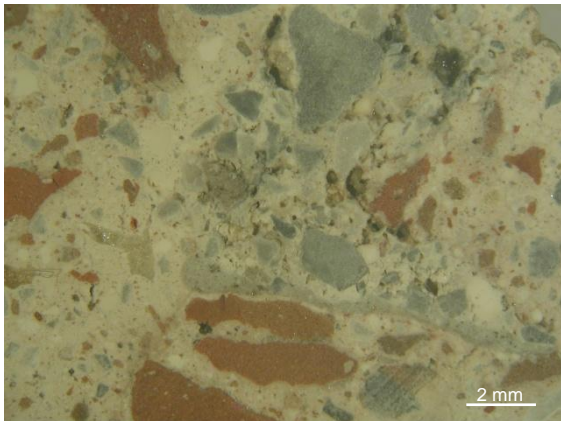


Figure 98 Ancient city of Dion, mosaic of Villa Dyonisos, cross section photomicrograph of mortar layer n. 2.

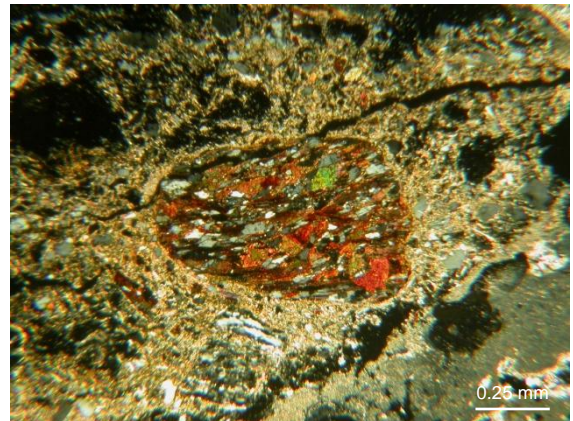


Figure 99 Ancient city of Dion, mosaic of Villa Dyonisos, thin section photomicrograph of mortar layer n. 2 (crossed nicols).

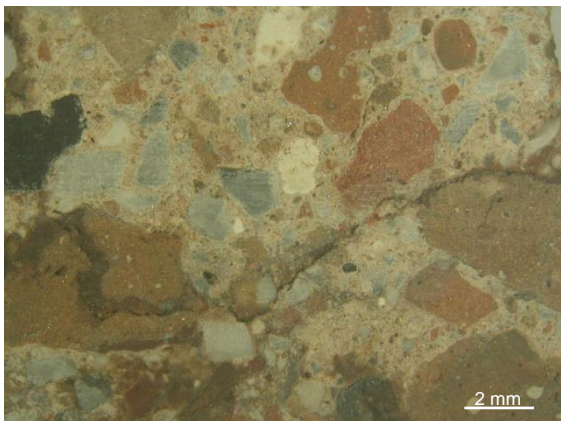


Figure 100 Ancient city of Dion, mosaic of Villa Dyonisos, cross section photomicrograph of mortar layer n. 3.

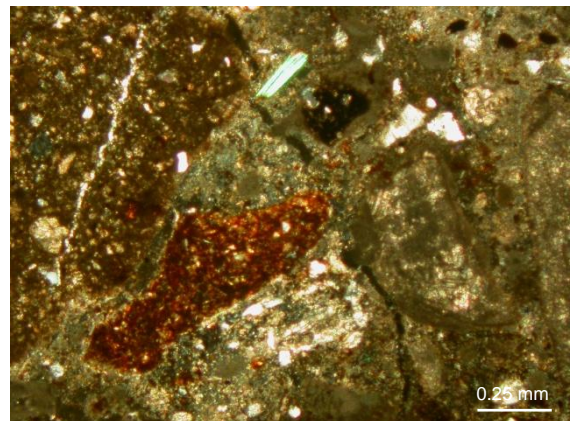


Figure 101 Ancient city of Dion, mosaic of Villa Dyonisos, thin section photomicrograph of mortar layer n. 3 (crossed nicols).



Figure 102 “Villa Romana delle Muracche”, mosaic of the *cubiculum*, cross section photomicrograph of mortar layer n. 1.

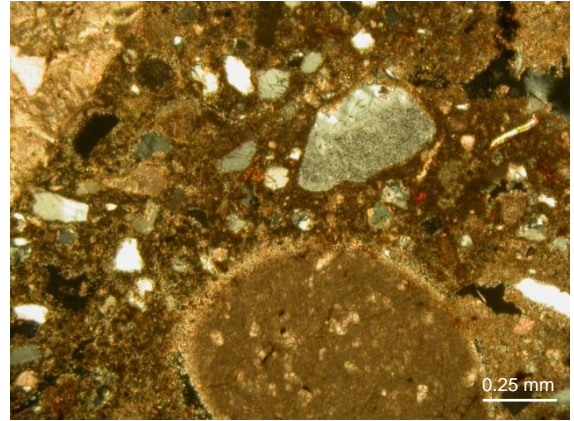


Figure 103 “Villa Romana delle Muracche”, mosaic of the *cubiculum*, thin section photomicrograph of mortar layer n. 1 (crossed nicols).



Figure 104 “Villa Romana delle Muracche”, mosaic of the *cubiculum*, cross section photomicrograph of mortar layer n. 2.

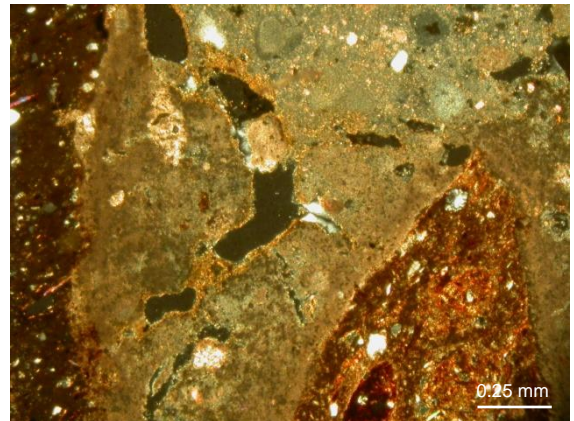


Figure 105 “Villa Romana delle Muracche”, mosaic of the *cubiculum*, thin section photomicrograph of mortar layer n. 2 (crossed nicols).



Figure 106 “Villa Romana delle Muracche”, mosaic of the *cubiculum*, cross section photomicrograph of mortar layer n. 3.

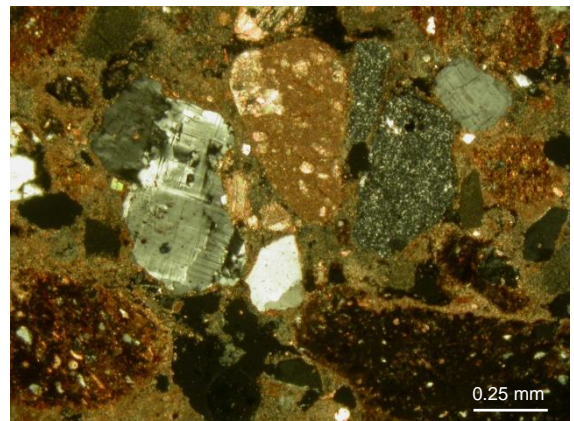


Figure 107 “Villa Romana delle Muracche”, mosaic of the *cubiculum*, thin section photomicrograph of mortar layer n. 3 (crossed nicols).



Figure 108 “Villa Romana delle Muracche”, mosaic of the *tablinum*, cross section photomicrograph of mortar layer n. 2.



Figure 109 “Villa Romana delle Muracche”, mosaic of the *tablinum*, thin section photomicrograph of mortar layer n. 2 (crossed nicols).



Figure 110 “Villa Romana delle Muracche”, mosaic of the *tablinum*, cross section photomicrograph of mortar layer n. 3.

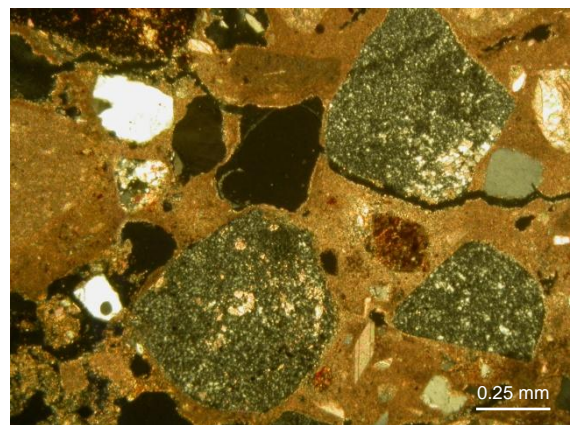


Figure 111 “Villa Romana delle Muracche”, mosaic of the *tablinum*, thin section photomicrograph of mortar layer n. 3 (crossed nicols).



Figure 112 Roman Villa of Classe, Ravenna, cross section photomicrograph of mortar layer n. 1.

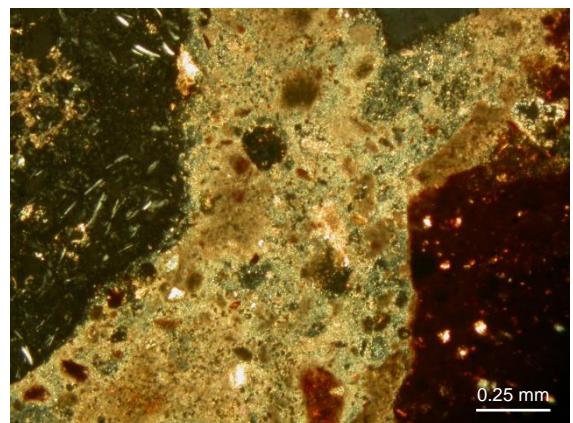


Figure 113 Roman Villa of Classe, Ravenna, thin section photomicrograph of mortar layer n. 1 (crossed nicols).



Figure 114 Roman Villa of Classe, Ravenna, cross section photomicrograph of mortar layer n. 2.

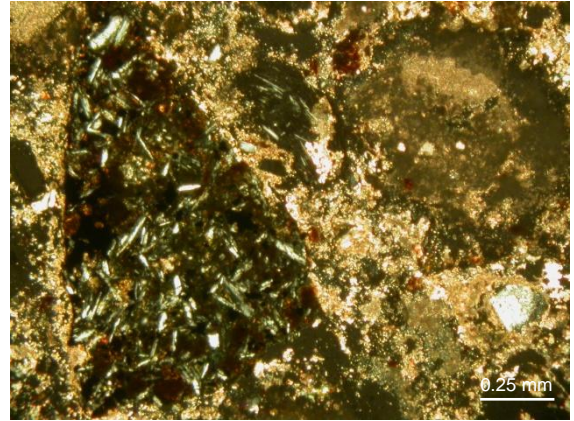


Figure 115 Roman Villa of Classe, Ravenna, thin section photomicrograph of mortar layer n. 2 (crossed nicols).



Figure 116 "Cortile Romano", Florence, pavement A, cross section photomicrograph of mortar layer n. 1.

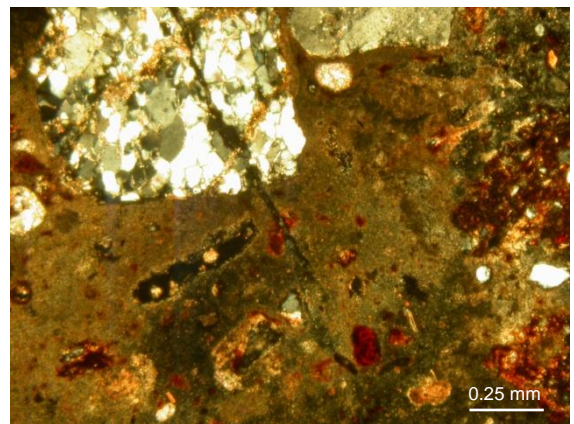


Figure 117 "Cortile Romano", Florence, pavement A, thin section photomicrograph of mortar layer n. 1 (crossed nicols).



Figure 118 "Cortile Romano", Florence, pavement A, cross section photomicrograph of mortar layer n. 2.

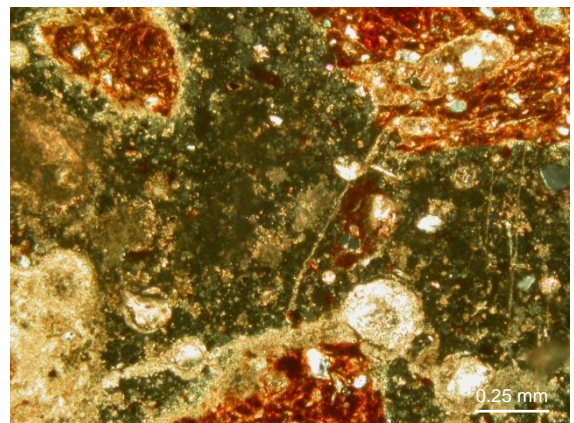


Figure 119 "Cortile Romano", Florence, pavement A, thin section photomicrograph of mortar layer n. 2 (crossed nicols).



Figure 120 “Cortile Romano”, Florence, pavement B, cross section photomicrograph of mortar layer n. 1.

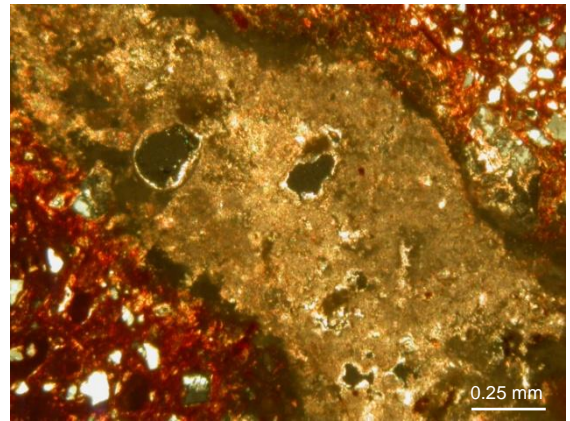


Figure 121 “Cortile Romano”, Florence, pavement B, thin section photomicrograph of mortar layer n. 1 (crossed nicols).



Figure 122 “Cortile Romano”, Florence, pavement B, cross section photomicrograph of mortar layer n. 2.

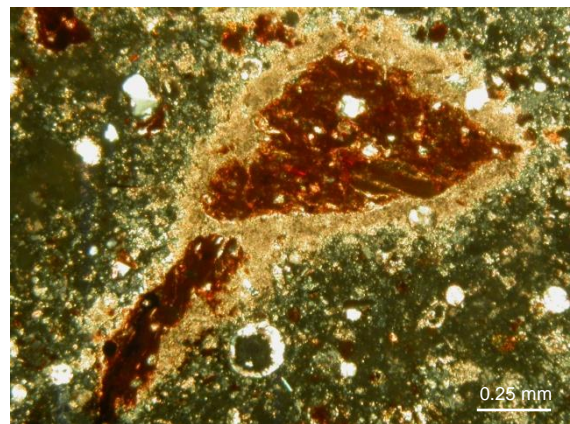


Figure 123 “Cortile Romano”, Florence, pavement B, thin section photomicrograph of mortar layer n. 2 (crossed nicols).



Figure 124 “Cortile Romano”, Florence, pavement D, cross section photomicrograph of mortar layer n. 1.

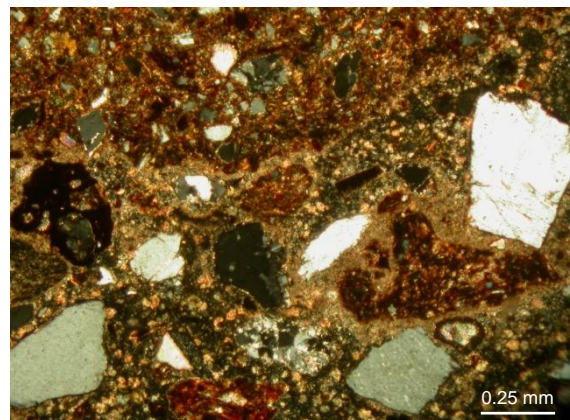


Figure 125 “Cortile Romano”, Florence, pavement D, thin section photomicrograph of mortar layer n. 1 (crossed nicols).



Figure 126 “Cortile Romano”, Florence, pavement D, cross section photomicrograph of mortar layer n. 2.

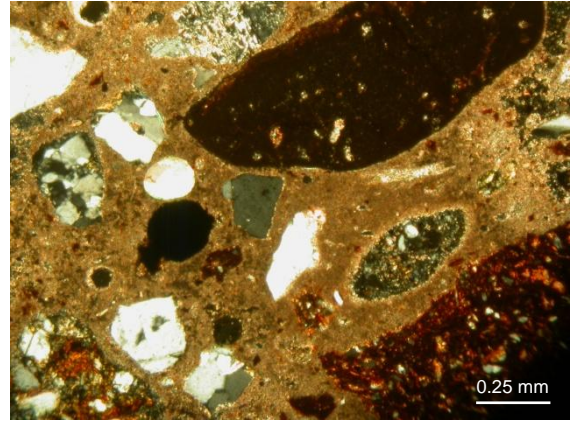


Figure 127 “Cortile Romano”, Florence, pavement D, thin section photomicrograph of mortar layer n. 2 (crossed nicols).



Figure 128 “Cortile Romano”, Florence, pavement E, cross section photomicrograph of mortar layer n. 2.

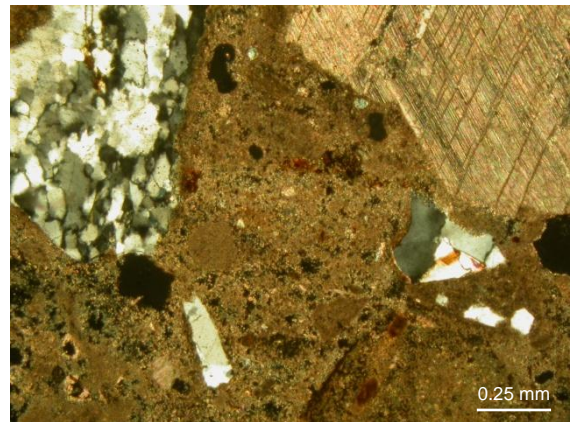


Figure 129 “Cortile Romano”, Florence, pavement E, thin section photomicrograph of mortar layer n. 2 (crossed nicols).



Figure 130 Palace of Aegae, Vergina, mosaic A, cross section photomicrograph of mortar layer n. 2.

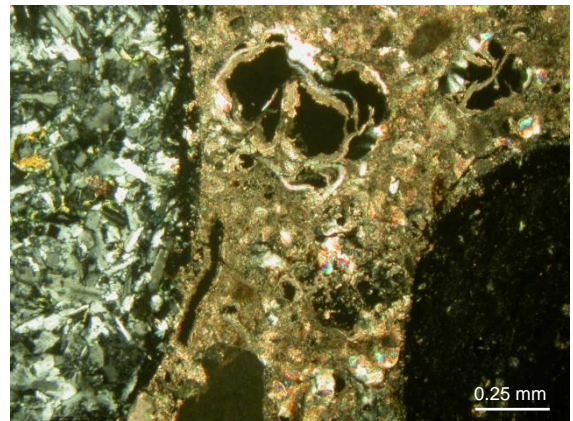


Figure 131 Palace of Aegae, Vergina, mosaic A, thin section photomicrograph of mortar layer n. 2 (crossed nicols).



Figure 132 Palace of Aegae, Vergina, mosaic Bm, cross section photomicrograph of mortar layer n. 2.

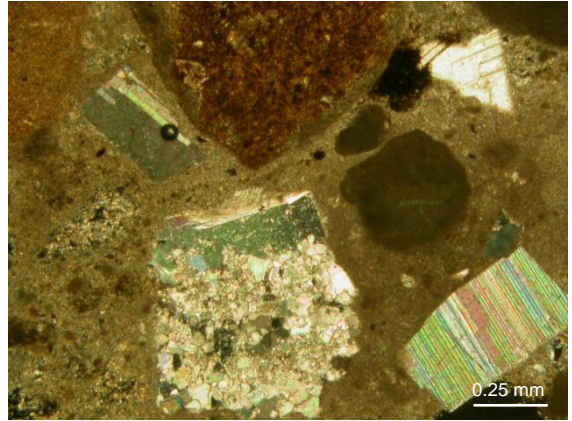


Figure 133 Palace of Aegae, Vergina, mosaic Bm, thin section photomicrograph of mortar layer n. 2 (crossed nicols).



Figure 134 Palace of Aegae, Vergina, mosaic Bm, cross section photomicrograph of mortar layer n. 3 and 4.

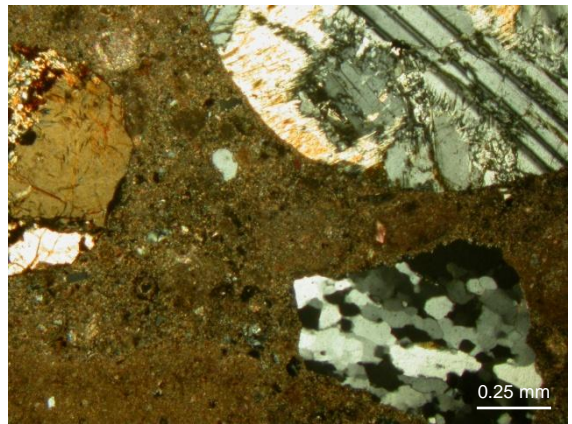


Figure 135 Palace of Aegae, Vergina, mosaic Bm, thin section photomicrograph of mortar layer n. 3 (crossed nicols).

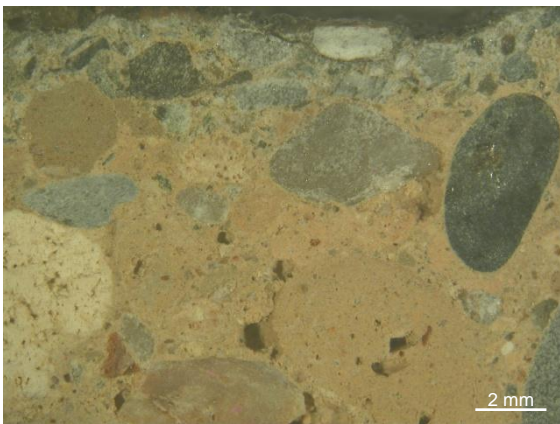


Figure 136 Palace of Aegae, Vergina, mosaic Bm, cross section photomicrograph of mortar layer n. 3 and 4.

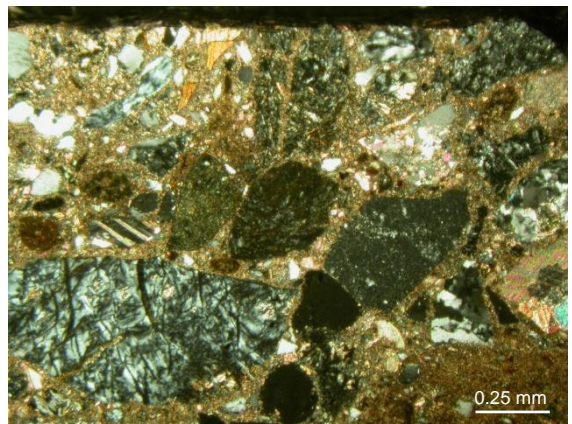


Figure 137 Palace of Aegae, Vergina, mosaic Bm, thin section photomicrograph of mortar layer n. 4 (crossed nicols).



Figure 138 Palace of Aegae, Vergina, mosaic Bf, cross section photomicrograph of mortar layer n. 2 and n. 3.



Figure 139 Palace of Aegae, Vergina, mosaic Bf, thin section photomicrograph of mortar layer n. 2 (crossed nicols).



Figure 140 Palace of Aegae, Vergina, mosaic Bf, cross section photomicrograph of mortar layer n. 2 and n. 3.

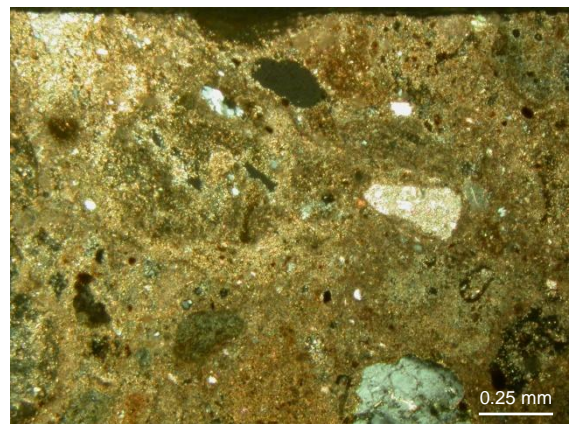


Figure 141 Palace of Aegae, Vergina, mosaic Bf, thin section photomicrograph of mortar layer n. 3 (crossed nicols).

Abstract

Study of materials and technology of ancient floor mosaics' substrate

Ancient pavements are composed of a variety of preparatory or foundation layers constituting the substrate, and of a layer of *tesserae* or marble slabs forming the surface of the floor. In other cases, the surface consists of a mortar layer beaten and polished. The term mosaic is associated with the presence of *tesserae* or pebbles, while the more general term pavement is used in all the cases. As past and modern excavations of ancient pavements demonstrated, all pavements do not necessarily display the stratigraphy of the substrate described in the ancient literary sources. In fact, the number and thickness of the preparatory layers, as well as the nature and the properties of their constituent materials, are often varying in pavements which are placed either in different sites or in different buildings within a same site or even in a same building. For such a reason, an investigation that takes account of the whole structure of the pavement is important when studying the archaeological context of the site where it is placed, when designing materials to be used for its maintenance and restoration, when documenting it and when presenting it to public. Five case studies represented by archaeological sites containing floor mosaics and other kind of pavements, dated to the Hellenistic and the Roman period, have been investigated by means of *in situ* and laboratory analyses. The results indicated that the characteristics of the studied pavements, namely the number and the thickness of the preparatory layers, and the properties of the mortars constituting them, vary according to the ancient use of the room where the pavements are placed and to the type of surface upon which they were built. The study contributed to the understanding of the function and the technology of the pavements' substrate and to the characterization of its constituent materials. Furthermore, the research underlined the importance of the investigation of the whole structure of the pavement, included the foundation surface, in the interpretation of the archaeological context where it is located. A series of practical applications of the results of the research, in the designing of repair mortars for pavements, in the documentation of ancient pavements in the conservation practice, and in the presentation to public *in situ* and in museums of ancient pavements, have been suggested.

Vincenzo Starinieri

Acknowledgements

The work described in this thesis has been carried out within the EU project “European PhD in Science for Conservation (EPISCON)”, contract n. MEST-CT-2005-020559.

Firstly, I wish to thank Prof. Ioanna Papayianni, who chose to be my supervisor, and gave me the opportunity to carry out my work at the Aristotle University of Thessaloniki. She always helped out whenever possible, and dispensed precious advice.

My acknowledgement goes to the staff of the Laboratory of Building Materials of the Aristotle University of Thessaloniki: to Dr. Maria Stefanidou, for operating the compression testing machine, and for answering to any kind of questions and requests about the laboratory’s facilities; to Stavroula Konopissi and Fotini Karkantelidou, for performing the analyses by means of Atomic Absorption Spectrometry and Ion Chromatography; to Vasiliki, Mixailis, Leftheris, Yannis, Alekos, Sofia, Dimitra, Dimitris, for their help in solving any kind of problem I might have had. My thanks go also to Margherita, who helped me to get into the laboratory every time I was the first one to arrive in the morning.

I am much indebted to those people who have helped me in providing case studies: to Prof. George Karadedos from the University of Thessaloniki, for the mosaics of the ancient city of Dion; to Dr. Sandra Lapenna and Prof. Silvano Agostini from the Soprintendenza Archeologica per l’Abruzzo, and to Claudio Giampaolo, for the mosaics of the Roman Villa in Tortoreto; to Prof. Rossano Fontanelli and Dr. Anna Rastrelli from the Soprintendenza Archeologica per la Toscana, for the pavements of the “Cortile Romano” in the Archaeological Museum of Florence; to Dr. Mariangela Vandini, Prof. Cesare Fiori, Prof. Rocco Mazzeo, Prof. Andrea Augenti and Dr. Enrico Cirelli from the University of Bologna, for the mosaic of the Roman Villa in Classe, Ravenna.

Special thanks go to Dr. Simona Montalbani, Prof. Daniele Fabbri and Prof. Giuseppe Chiavari from the University of Bologna, for performing the analyses by means of pyrolysis gas chromatography mass spectrometry and for fruitful discussion on the results.

Many thanks to Dr. Michele Macchiarola from the CNR-ISTEC (Institute of Science and Technology for Ceramics of Faenza), who helped in disseminating the results of my research and shared his experience and knowledge on the study of ancient pavements.

Thanks are also due to all the members of the EPISCON Steering Committee and of the International Evaluation Board, for their always constructive criticism in occasion of the annual reports on the scientific results.

Many thanks go to my EPISCON colleagues and especially to Eva, who shared from the beginning joys and worries of living and working abroad, and to my friend Marco, who stayed in touch even from distance for such a long time. Special thanks, finally, go to my mother, my father, and to my brothers Andrea and Davide, without whose support I could not have finished this thesis.

Publications

Starinieri, V.; Papayianni, I.; Stefanidou, M., 'Study of materials and technology of ancient floor mosaics' substrate', *Conservar Património* **7** (2008) 29-34.